METHANE BIOGEOCHEMICAL CYCLING OVER SEASONAL AND ANNUAL SCALES IN AN OIL SANDS TAILINGS END PIT LAKE

METHANE BIOGEOCHEMICAL CYCLING OVER SEASONAL AND ANNUAL SCALES IN AN OIL SANDS TAILINGS END PIT LAKE

BY COREY A. GOAD, B.SC.

A Thesis Submitted to the School of Graduate Studies in

Partial Fulfilment of the Requirements for the Degree

Master of Science

McMaster University

MASTER OF SCIENCE (2017) McMaster University

Earth and Environmental Sciences Hamilton, Ontario

TITLE: Methane Biogeochemical Cycling over Seasonal and Annual Scales in an Oil Sands Tailings End Pit Lake

AUTHOR: Corey A. Goad, B.Sc. (McMaster University)

SUPERVISOR: Dr. Gregory F. Slater

NUMBER OF PAGES: 103

ABSTRACT

This Master's degree study examined concentration and isotopic trends of dissolved methane, isotopic trends of phospholipid fatty acids (PLFA), and generated 1st order flux calculations to identify and assess biogeochemical cycling of dissolved methane in the first full-scale demonstration of EPL technology in the Alberta Oil Sands Region (AOSR). Base Mine Lake (BML) was commissioned by Syncrude Canada Ltd. in 2012 to facilitate the long term storage and remediation of Fluid Fine Tailings (FFT) that are generated as a result of bitumen extraction via the Clark Hot Water Extraction (CHWE) processes. The results of this project provide evidence of methane oxidation by type I methanotrophs in BML, reducing dissolved oxygen concentrations in the hypolimnion layer. The FFT layer is identified as a source zone of fermentative methanogenesis, creating saturated conditions of dissolved gases. Dissolved methane is transferred to the water column primarily by advective processes related to FFT consolidation, while diffusion is a significant secondary transfer mechanism. Dissolved methane concentrations decrease significantly across the FFT-water interface where diffusive flux rates decrease by several orders of magnitude. Concentrations decreased linearly through the hypolimnion to trace concentrations by the metalimnion, resulting in a minor enrichment of $\delta^{13}C$ of the residual dissolved methane pool. A minor enrichment of $\delta^{13}C$ in C14:0, C16:0, and C16:1 PLFA coincided across the same interval, indicating utilization of a less depleted carbon source further away from the FFT-water interface where dissolved methane concentrations were lower. PLFA $\delta^{13}C$ signatures were depleted relative to expected values of typical DOC substrates, further supporting incorporation of a depleted signature by transfer of depleted carbon from dissolved methane.

ACKNOWLEDGEMENTS

I would like to thank Dr. Greg Slater for giving me the opportunity to work on this project for the past two years, as well as the previous work experience I obtained in his lab. Greg's guidance and support have greatly assisted in the completion of this work and I am forever grateful for the experience I've received while working here at McMaster. The experience and memories I've gathered and created here will travel with me for a very long time and assist in the beginning of a long career, of which I am thankful for.

Next up is Jennie Kirby, the best lab technician that exists. Working beside her on a daily basis has been a fantastic experience, and she has taught me almost all I know about GC systems. I consider this one of the most important things I will take away from McMaster as I truly love working on and tinkering with the instrumentation. I will always cherish and miss our Monday morning Game of Thrones episode re-cap discussions. Thank you to my officemates Kelly, Sian, Mohamed, David, and Mark. These were the best people to share space with, and were always great company to grab a drink with, or to ask for help when things got a little confusing. Thank you to Dr. Allyson Brady for her advice and help throughout the project, including methane detection limit tests. Thanks to my colleagues from the Warren lab as well for going out to Fort McMurray each year to take the samples this project was based on, specifically Florent, Patrick, Danial, and Tara. Also thanks to Doug for being a staple lunch buddy throughout these two years.

Lastly moving into my personal life, I would like to thank my parents for always having an open door when I needed somewhere to crash, homemade dinners by parents seem to have an effect unparalleled to anything else when you need to relax. Thank you to Sam for being there through the writing process, sharing a coffee with someone who is also writing keeps the morale

up. Cottage weekend get aways and hiking trips made me look forward to the weekends together. Lastly, a massive thanks to my closest friends; Cris, Devin, Amir, and Alex who I can talk to about anything. A simple thing such as watching a Raptor's game in our favourite bar every Monday/Tuesday night does wonders for helping forget about everything else going on in life. Without these guys I wouldn't have made it this far in university, or life, or anything really. Here's to the next step!

TABLE OF CONTENTS

LIST OF FIGURES

LIST OF TABLES

Chapter 1: Introduction

1.1 – Alberta Oil Sands Region, Oil Sands Activity, and Landscape Reclamation

1.1.1 – Project Summary / General Intro

The Alberta Oil Sands Region (AOSR) contains the 3rd largest crude oil reserves in the world, existing in the form of a crude bitumen mixture. Extraction of bitumen from this mixture generates large volumes of tailings, a mixture consisting of unrecovered bitumen, sand, fine solids, and Oil Sand Process Water (OSPW). These tailings require a long-term management and reclamation strategy due to the toxicity of several compounds present within. End Pit Lakes (EPLs) address these issues by facilitating the de-watering of FFT below a water column, supporting biodegradation of organic compounds in the water column, and diluting salts through freshwater inflow-outflow cycling. Syncrude Canada Ltd. has commissioned the first full-scale demonstration of water-capped tailings reclamation through creation of Base Mine Lake (BML), an EPL located north of Fort McMurray, Alberta, Canada. While EPLs have been employed in other mining contexts, the unique variety of compounds present in tailings may cause oil sand EPLs to develop differently. As such, understanding the biogeochemical cycling processes active within BML has led to an intensive research initiative to monitor system development in the initial years of lake development. The goal of BML is to develop a self-sustaining ecosystem with the ability to support aquatic biota, which requires oxygenation of the water column and consistent presence of dissolved oxygen year round. This work focused on monitoring dissolved methane dynamics within the water column of BML over a two year period to assess the role of dissolved methane as an oxygen consuming constituent (OCC) through methanotrophic metabolisms.

1.1.2 – Oil Sands: Region & Tailings Generation

The AOSR contains the 3rd largest crude oil reserves in the world, containing up to 1.8 trillion barrels of bitumen spread across a total regional area of 142,200 km^2 (Figure 1.1**,** Alberta Energy Regulator (AER), 2016). Production was estimated at 2.4 million barrels per day (b/d) in 2015, with growth projections estimating 3.7 million b/d by 2030 if an additional 86,000 b/d are added per year (Canadian Association of Petroleum Producers, 2015). These oil reserves exist in the form of a crude bitumen mixture, consisting of bitumen and water surrounding sand and clay particles that are recovered through surface mining of shallow deposits and in-situ thermal extraction techniques for deeper deposits. The Clark Hot Water Extraction (CHWE) is used to extract bitumen from this crude mixture, which facilitates separation through the addition of warm water and caustic soda, followed by flotation of the bitumen with air (Masliyah, Zhou, Xu, Czarnecki, & Hamza, 2004). This process results in the generation of a tailings slurry consisting of unrecovered bitumen, fine solids, and OSPW that cannot be released into the environment due to toxicity (Bordenave et al., 2010; Holowenko, MacKinnon, & Fedorak, 2000). Tailings are deposited into settling basins where the solid components undergo settling and compaction by gravity, de-watering the slurry and causing component separation. Settling basins allow for short term water recycling, with

Figure 1.1: Geographic map of Northern Alberta displaying oil sands deposits, current mining activities, and potential future developments planned (AER, 2017)

over 85% of the water re-used in the CHWE process at Syncrude Canada Ltd. being recycled as the solids settle out of the tailings slurry (Chalaturnyk, Don Scott, & Özüm, 2002; Syncrude Canada Ltd., 2016). The partially de-watered fraction of this initial tailings slurry containing finer solids (< 44 μm) is referred to as Fluid Fine Tailings (FFT). Approximately 975.6 million m^3 of FFT were stored across the AOSR in 2013, located in settling basins spanning 220 km^2 (Government of Alberta, 2013). Managing FFT presents long-term remediation challenges due to the long dewatering times associated with the remaining fine solids, presence of organic and inorganic compounds, and large volumes. Management and remediation of existing and future FFT inventories remains a primary waste management issue, as over 262,000 m^3 of tailings slurry are generated each day in northern Alberta (Siddique, Penner, Semple, & Foght, 2011).

1.1.2 – FFT long-term remediation and landscape reclamation

Due to the concentrations of compounds present in the tailings mixture, companies operating in the AOSR are under a zero-discharge practice, which has generated a need for long-term storage solutions that will contain these large volumes of tailings. EPL technology seeks to address this issue through the deposition of FFT into decommissioned open-pit mines, followed by capping with fresh water to dilute OSPW and FFT porewater. Maintaining aerobic conditions in the water column of an EPL is of critical importance for sustaining larger aquatic biota and facilitating aerobic degradation metabolisms. This reclamation strategy aims to restore the landscape to a biologically productive state while facilitating further consolidation of FFT over several decades (Figure 1.2, Westcott & Watson, 2007). As the FFT consolidates porewater containing OSPW is constantly expelled into the water column. This releases a variety of compounds, including many reduced compounds such as methane that can be oxidized in the water column leading to reduction in dissolved oxygen concentrations via aerobic degradation

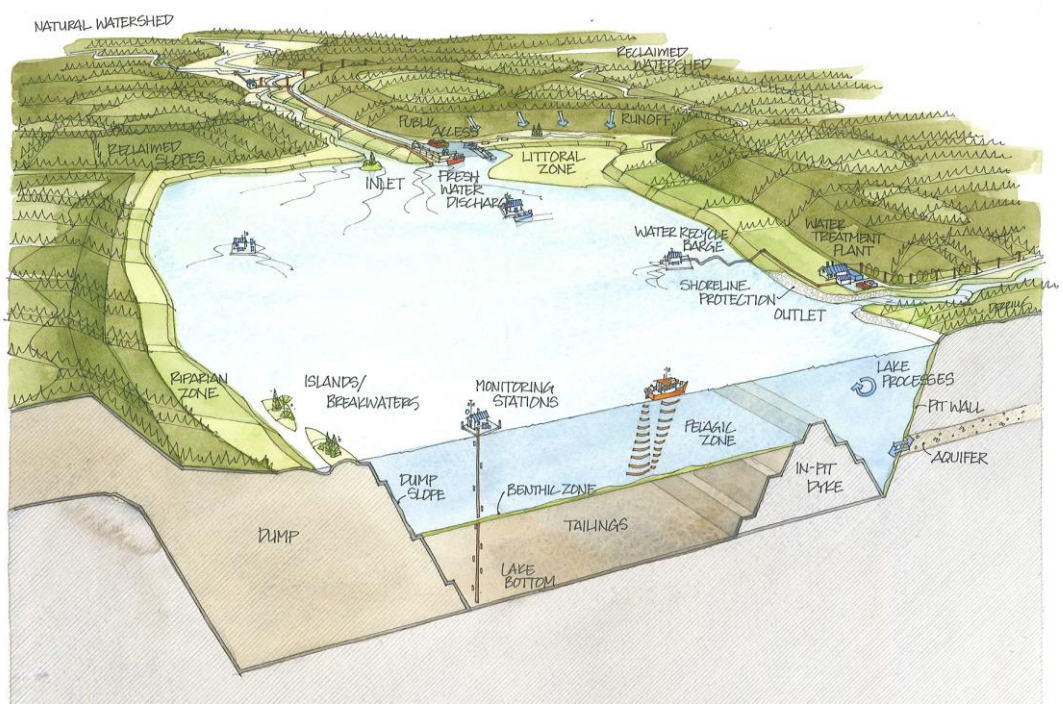

Figure 1.2: Schematic of an End Pit Lake system, labels on diagram to outline potential important features related to monitoring and development (CEMA, 2012).

pathways. Maintaining oxic conditions to facilitate microbial degradation of these compounds is crucial to the development of a biologically productive ecosystem that will support aquatic biota in the future. To achieve this goal, constant and frequent monitoring of geochemical characteristics of both the water column and FFT are required to track lake development over the lifetime of the project. The first full-scale demonstration of this wet-landscape reclamation technique is being conducted by Syncrude Canada Ltd. through the commissioning of BML north of Fort McMurray, Alberta, Canada. Deposition of FFT at the West In-Pit area of Syncrude Canada Ltd.'s lease began in 1994 and concluded in 2012 with a total depth of approximately 48m. Water capping began with 5m of OSPW after FFT placement concluded, followed by another 2.5m of OSPW addition in 2013 for a total water cap depth of approximately 7-8m over 48m of FFT (Dompierre, Lindsay, Cruz-Hernandez, & Halferdahl, 2016). Consistent FFT consolidation since then has resulted in an increased depth of the water column to an overall

depth of approximately 10m in 2017. BML exhibits dimictic turnover events occurring in the spring and fall, and is thermally stratified between these events. The FFT layer of BML has been identified as a primary source zone of dissolved methane to the water column through numerous transfer mechanisms, leading to concerns of future dissolved oxygen concentrations.

1.1.3 – Microbial Mediated Degradation & Importance of Oxygen

OSPW and FFT contain a wide variety of organic compounds that can be aerobically degraded by microbes over time. For instance, alkyl-substituted Polycyclic Aromatic Hydrocarbons (PAHs) and Naphthenic Acids (NAs) have been detected in oil sands tailings at elevated concentrations (Giesy, Anderson, & Wiseman, 2010). Degrading these compounds requires dissolved oxygen to be present in the water column, which is an issue if a significant amount is consumed by the oxidation of dissolved methane. Aside from biodegradation of these tailings compounds, oxygen plays a critical role as a Terminal Electron Acceptor (TEA) in aerobic respiration pathways of macro-organisms whose presence is required for a stable functional ecosystem to develop. Based on the observation of dissolved methane concentrations in tailings ponds and settling basins, dissolved methane transfer to the BML water column is expected to be a primary controller of dissolved oxygen via the activity of methanotrophic bacteria. Methanotrophic bacteria have been shown to have a high competitive affinity for oxygen, enabling them to effectively utilize even very low concentrations of oxygen (Knief, Kolb, Bodelier, Lipski, & Dunfield, 2006; Kolb, Knief, Dunfield, & Conrad, 2005). Further, they utilize oxygen at a 2:1 molar ratio with dissolved methane (Michael J Whiticar, 1999). If the activities of methanotrophic organisms do deplete oxygen levels in BML, this will potentially limit the development of a self-sustaining ecosystem in BML. In addition, limitations on dissolved oxygen can also have a significant impact on biodegradation of PAHs and other

petroleum hydrocarbons. Microcosm studies tested biodegradation rates of numerous monoaromatic hydrocarbons under a variety of TEA limiting conditions and treatments and found that without dissolved oxygen numerous PAHs compounds did not degrade over time (Hutchins, 1991). Another study examined petroleum hydrocarbon degradation demonstrated the importance of oxygen as a TEA in biodegradation due to the specialized oxygenase enzymes employed exclusively by aerobic degraders (Zhou & Crawford, 1995). Understanding the occurrence and extent of methanotrophy and associated oxygen depletion is thus a key component in the assessment of BML water column development.

1.2 – Methane Biogeochemical Cycling – Microbes and Metabolic Pathways

1.2.1 – Production of Methane via Fermentation & CO_2 Reduction Pathways

Biogenic methane is the product of methanogenesis, a microbial metabolism carried out by archaea present in anoxic sediments. This metabolism undertakes one of two pathways; methyl-based fermentation or CO_2 reduction, with the end product being generation of methane through the oxidation of small organic compounds produced from microbial fermentation of larger organic compounds. The FFT in tailings ponds exhibit saturated dissolved methane conditions, and have been shown to possess established archaeal communities composed of methanogens (Penner & Foght, 2010). Due to this observation methane present in tailings is thought to be biogenic in origin. Numerous studies have linked methanogenic pathways to the biodegradation of PAHs and other organic compounds present in the FFT porewater and OSPW inputs, and a study of entrapped gasses in MLSB have shown to be composed of up to 60% methane, with emissions from the surface being 60 to 80% methane (Holowenko et al., 2000; Siddique, Fedorak, & Foght, 2006; Siddique, Fedorak, Mackinnon, & Foght, 2007).

The fermentation pathways are the most energetically favourable metabolism of methanogens, generating the most biomass and CH_4 per mole of substrate utilized. This metabolism utilizes the methyl group of acetate and an H^+ from the surrounding formation water to generate methane and CO_2 as a by-product, as seen in Equation 1 (M. J. Whiticar, Faber, & Schoell, 1986).

$$CH_3COOH + H^+ \rightarrow CO_2 + CH_4 \quad (1)$$

This metabolism is the primary pathway utilized in freshwater sediments generally due to the lack of an established sulphate zone, and thus lack of Sulphate Reducing Bacteria (SRBs) competitors for acetate and H_2. BML offers a unique situation as it's constructed to model a freshwater lake, but has a very different geochemical balance as it contains significant sulphate concentrations and the FFT/OSPW inputs provide a variety of organic compounds not naturally found in these abundances.

The second metabolic pathway is CO_2 reduction (Equation 2). This metabolism is less energetically favourable but can operate in a more reducing environment than other competitors, often resulting in a methanogenic zone located below SRBs where small methyl-based compounds are generally depleted, leading to an availability of H_2.

$$CO_2 + 4\ H_2 \rightarrow 2\ H_2O + CH_4 \quad (2)$$

This pathway is commonly found in marine sediments where there is sufficient sulphate to form an SRB zone that depletes more favourable compounds for methanogenesis, or very deep in freshwater sediments. As previously stated, the unique nature of an EPL environment and its inputs may cause this metabolism to be more prevalent when compared to a normal freshwater system, potentially being present at a shallower depth.

1.2.2 – Factors Influencing Methanogenic Rates

There are a number of controls on the occurrence and extent of methanogenesis. In the case of BML, which is located in a very cold environment and is ice covered for a significant portion of the year, temperature will be an important factor that might affect methane production. Temperature has a direct correlation to methanogenesis rates in freshwater sediments and has also been demonstrated to influence the community of methanogens present, with different community structure being present in psychrophilic conditions versus thermophilic (Nozhevnikova, Holliger, Ammann, & Zehnder, 1997). Methanogenic archaea have been observed metabolizing organic matter from psychrophilic (-20°C -> 10°C) to hyperthermophilic (60°C -> 122°C) conditions. Recently five new strains of methanogenic archaea were isolated from periodically-permanently frozen tundra wetland soils and anoxic sediments of Baldegger Lake, Switzerland. These isolates were able to oxidize organic matter down to a temperature of 1°C, but displayed optimal growth ranges of 25-35°C, enforcing the unique ability of methanogenic archaea to operate in cold environments, at a lower metabolic rate (Simankova et al., 2003). These results suggest that methanogenic archaea will still be actively producing methane in EPL environments regardless of the time of year as the FFT will not reach freezing temperatures, but their metabolic rate and thus methane generation may be affected.

Another study examined the effects of both temperature and organic inputs on methanogenesis rates in two freshwater lake sediments and found that while temperature is important in determining the rate of CH_4 generation, organic matter inputs control CH_4 production in constant temperature environments as they control the potential for and/or extent of substrate limitation (Kelly & Chynoweth, 1981). Due to the large number of organic compounds present in FFT these methanogenic archaea will presumably have ample substrate to

utilize, leading to high rates of methane production in an EPL environment, potentially similar to tailings pond activity already observed at Mildred Lake Settling Basin (MLSB) (Penner & Foght, 2010). Numerous studies on the MLSB tailings pond FFT have shown the coupling of methanogenic pathways to the biodegradation of larger organic compounds present in abundance, providing the smaller organic substrates required by methanogens utilizing fermentation pathways (Siddique et al., 2006, 2007, 2011). In this case if organic inputs are present in large quantities, other external factors such as temperature and H_2 availability may have the largest impact on controlling methanogenic production rates in EPLs.

Another factor that can affect rates of methanogenesis is competition with other microorganisms for substrates. Understanding the competitive relationship between methanogens and SRBs can provide insight to the methanogenic pathway active within the FFT layer of BML, which is important when considering substrate utilization and the resulting $\delta^{13}C$ values. It is widely acknowledged through numerous studies that SRBs can outcompete methanogens for H_2 and acetate substrates, impeding but not completely inhibiting both acetate fermentation and CO_2 reduction metabolic pathways (Lovley & Klug, 1986; Oremland & Polcin, 1982; Schönheit, Kristjansson, & Thauer, 1982). Regardless of SRB competition, it has been shown that methanogenic archaea can utilize other small organic methylated compounds like methanol, methylamine, and dimethyl sulfide without requiring H_2, allowing fermentation based methanogenesis to continue in the presence of SRBs (Conrad, 2005). While fermentation pathways may still be able to operate in the presence of SRBs, overall rates may be lower due to substrate restrictions to these more specific compounds. Two previous studies, one focused on two tailings ponds, and one on BML have demonstrated consistent results of elevated dissolved sulphate levels in the water column, transitioning to low concentration zones shortly after the

FFT-water interface when compared to overall FFT depth of BML (Dompierre et al., 2016; Stasik, Loick, Knöller, Weisener, & Wendt-Potthoff, 2014). Dompierre et al. (2016) located sulphate depleted zone directly below the FFT interface at numerous sites across BML, potentially supporting less microbial competition for H_2 and small methyl-based compounds required for fermentative methanogenesis by SRBs. The generation and transfer of dissolved methane occurs through several mechanisms that are currently poorly understood in BML. Loading of dissolved methane to the water column of BML directly fuels methane oxidation and therefore oxygen consumption.

1.2.2 – Transfer Mechanics of Dissolved Methane from FFT to Water Column

The transfer of dissolved gases from FFT in an EPL system is governed by four main processes: molecular diffusion from FFT porewater, turbulent diffusion at the FFT/water interface due to stirring related to waves and/or ebullition, advection through porewater expression due to FFT consolidation, and dissolution from gas bubbles. These four processes all contribute differently, making discussion of the transfer mechanisms highly speculative without further work on BML. Diffusion is a passive transfer process governed by Fick's Law (Equation 3), relating the change in concentration over a distance relative to a compound's determined diffusion coefficient in terms of a flux rate.

$$J = - D \left(dC/dx\right) \quad (3)$$

Where:
J = Flux
D = Diffusivity
dC = change in concentration
dx = change in depth

Diffusion can be broken down into two components, molecular which tends to be slow in a liquid medium, and turbulent which is a faster process that is a function of liquid mixing.

Molecular diffusion is caused by the random movement of molecules, and is a function of the concentration of the compound and the distance of travel being observed. Turbulent diffusion is a process faster than molecular diffusion, but still slower than advective processes functioning under the same set of variables as molecular diffusion. Turbulent diffusion will transfer molecules of a compound faster than molecular diffusion when the proper requirements are met, meaning turbulence eddies are present within the liquid. These eddies randomly cycle fresh water towards the compound source zone, constantly refreshing the initial concentration gradient to drive increased diffusive movement. Diffusion processes are generally a slower transfer process than advection, but may be comparable if significant mixing is present to support rapid turbulent diffusion. As a result, understanding the contribution of turbulent diffusion is difficult to assess, and its relative contribution is a function of the advective processes currently active.

The most likely sources of dissolved methane to the surface water column are related to advection of FFT porewater into the water column due to either porewater expression during FFT consolidation or through interface mixing related to waves and/or ebullition. Expression of porewater from FFT due to consolidation causes transfer of dissolved methane in the upper porewater to the water column. The FFT layer of BML is expected to be consolidating for years, meaning these advective processes will likely provide continuous mass importing of dissolved methane. This loading can be estimated using porewater concentrations and expected water expression based on consolidation rates. Bubble release from the FFT causes advective transfer of saturated porewater through turbulent diffusion associated with bubble movement. Release of ebullition disturbs the FFT interface resulting in turbulent mixing at localized areas. MLSB and BML have exhibited significant ebullition across large portions of the lake surface, potentially providing adequate mixing to support turbulent diffusion. In addition, internal waves have the

potential to disturb the FFT water interface and result in further turbulent diffusion or methane release from porewater. Ebullition will also cause disturbances in the FFT layer, leading to increased advective release of dissolved methane, further enforcing that advective processes are expected to be the primary import mechanism governing this system. Given the short transit time of bubbles within the water column, dissolution from bubbles is not likely to be a major control on methane transfer. Dissolution of gases from bubbles during travel through the water column is governed by Henry's law, and is primarily a function of the partial pressure of the gas in the bubble, concentration of the gas in the water column, and the overall time for this exchange to occur. A larger effect may be seen during winter when the lake experiences an ice cap over the water column, trapping gas bubbles and increasing exposure time and therefore dissolution.

Both diffusion and dissolution of dissolved methane in water have been shown to be temperature dependent, with rates being retarded in lower temperature environments meaning seasonal processes will be have an impact on these transfer rates (Witherspoon & Saraf, 1966). Likewise, seasonal ice cover can reduce wave movement within BML, lowering interface mixing and therefore advective import of saturated FFT porewater. Once dissolved methane has been transferred to the water column, consumption via methanotrophic bacteria can begin due to the concurrent presence of dissolved oxygen, as this is normally depleted shortly across the interface.

1.2.3 – Biogenic Oxidation of Methane: Methanotrophic Bacteria

Microbially facilitated methane oxidation via methanotrophic bacteria is the only removal mechanism of methane in aerobic aquatic systems, with dissolved oxygen being the terminal electron acceptor for their metabolism. Due to the methanogenic source zones established in FFT, the upwards flux of dissolved methane to the BML water column will result in decreasing

dissolved oxygen concentrations if methanotrophs are present and active, raising concerns for developing and maintaining an oxic water column over time.

Methanotrophs consist of three subgroups based on their enzymatic capacity and assimilation pathways; Type I, Type II, and Type X. These three subgroups oxidize CH_4 to methanol through use of a methane monooxygenase (MMO) enzyme expressed as either soluble (sMMO) or membrane-bound particulate (pMMO), where expression is governed by environmental conditions and microbial subgroup (Hanson & Hanson, 1996). Both MMOs require two reducing equivalents to split O_2, using one oxygen to form methanol and the other to water. Methanol is then oxidized to formaldehyde, where methanotrophic metabolism branches into the two different assimilation pathways, or is continuously oxidized to CO_2, as seen in Equation 4.

$$CH_4 + O_2 \rightarrow CH_3OH \rightarrow HCHO \rightarrow HCOOH \rightarrow CO_2 \quad (4)$$

Types I methanotrophs utilize the Ribulose Monophosphate (RuMP) assimilation pathway, using formaldehyde directly for biosynthesis, whereas Type II utilize the Serine assimilation pathway, that uses a two-step reaction where formaldehyde is converted into serine, while CO_2 is fixed by another enzyme to completion. Type I methanotrophs tend to outcompete type II methanotrophs in low methane, high oxygen environments like freshwater lakes, whereas type II can outcompete type I in higher methane, lower nitrate concentration environments more representative of marine systems (Jahnke, Summons, Hope, & Des Marais, 1999). Type X methanotrophs share enzymes from both the RuMP and serine pathways found across type I and II methanotrophs, and have been demonstrated to grow at higher temperatures (Jiang et al., 2010).

Similar to methanogenesis, methanotrophy is subject to numerous variables that will influence consumption rate and therefore impact on oxygen consumption. Temperature has a similar effect on methanotrophic bacteria as it does on methanogen archaea, with an optimal temperature for growth and consumption being around 25 to 30°C for most species, while metabolism occurred down to 0°C and up to 50°C (Mohanty, Bodelier, & Conrad, 2007). Numerous studies have shown that ammonium fertilizers inhibit methanotrophic bacteria in lake environments, while the specific mechanism of inhibition is still being studied and may be species specific (Bedard & Knowles, 1989; Hanson & Hanson, 1996). Past pure culture studies have indicated that nitrite may inhibit methane oxidation of certain methanotrophic bacteria, but more recent studies have observed nitrification and denitrification occurring concurrently with methanotrophy (King & Schnell, 1994). These studies postulate that inhibition of methanotrophs by ammonia and nitrate in forest soils is dependent upon the species present, the concentration of ammonia and nitrate, as well as the duration of exposure (Nyerges & Stein, 2009). These results demonstrate that numerous factors have an influence on consumption rates across different environments, and that further research is required to fully understand environmental effects on methanotrophic bacteria.

Methanotrophy in the water column of freshwater lakes is normally a less prominent metabolism due to the low amounts of methane generated in these systems. The most active zone of methane consumption occurs at the oxic-anoxic transition zone, regularly associated around the sediment-water interface or below, depending on variables such as lake size, depth, and nutrient availability (Conrad, 2009; Lidstrom & Somers, 1984). In an EPL environment this oxic-anoxic interface may be located in the water column due to the larger number of compounds being degraded through a variety of aerobic metabolisms, including methanotrophy.

This would be more characteristic of marine or eutrophic lake systems where oxygen is depleted in the hypolimnion layer of the water column, in which case the most active zone of methanotrophy should be situated around the metalimnion where dissolved oxygen would be present and increasing in concentration with rising depth (Blumenberg, Seifert, & Michaelis, 2007; Harrits & Hanson, 1980). Use of stable carbon isotopes allows for enhanced understanding of the methanogenic pathways used to generate dissolved methane and provide evidence for microbial consumption in a water column.

1.2.4 – Stable Carbon Isotope Analysis for Methanogenic Pathway Assessment and Proof of Microbial Oxidation in a Water Column

Applying stable carbon and hydrogen isotope analysis to dissolved methane in the water column of BML can provide information on the methanogenic pathway (fermentation vs CO_2 reduction pathways) as well as provide supporting evidence if methanotrophy is actively occurring. Stable carbon isotope analysis measures the relative abundance of the ^{13}C isotope over the more abundant ^{12}C isotope. The result is a calculated $\delta^{13}C$ value reported in parts per mille (‰) units and standardized through use of the Vienna Pee Dee Belemnite (PDB) standard

$$\delta^{13}C\ (‰) = \left[\frac{\left(\frac{^{13}C}{^{12}C}\right)_{sam} - \left(\frac{^{13}C}{^{12}C}\right)_{std}}{\left(\frac{^{13}C}{^{12}C}\right)_{std}}\right] \cdot 1000 \quad (5)$$

(Equation 5).

Fermentative methanogenesis produces methane with $\delta^{13}C/\delta^{2}H$ values of -45 to -70‰ and -290 to -400‰, while CO_2 reduction generates more depleted $\delta^{13}C$ values and more enriched $\delta^{2}H$ values of -60 to -110‰ and -150 to -250‰ respectively (Michael J Whiticar, 1999). Pairing $\delta^{13}C$ values with $\delta^{2}H$ values allows for complete elucidation of methanogenic pathways as the $\delta^{2}H$

values between fermentation and CO_2 reduction don't overlap and are completely separated by a range of approximately -40 ‰.

Once the $\delta^{13}C$ value of the dissolved methane in the FFT have been determined, tracking the change in value over a depth series or concentration can provide one line of evidence of active methanotrophy. There is overwhelming proof that methanotrophic consumption of dissolved methane in aquatic environments significantly reduced the amount present before reaching the atmosphere, with most consumption occurring around the oxic-anoxic boundary (Hanson & Hanson, 1996; Trotsenko & Khmelenina, 2005). Assessing the trends over this boundary layer should display an enrichment of the $\delta^{13}C$ values if there are methanotrophic bacteria actively consuming the dissolved methane (Michael J Whiticar, 1999). This is a result of a preferential uptake of ^{12}C methane over ^{13}C methane by these bacteria due to thermodynamic favourability, resulting in a positive shift of the residual methane pool's signature as more ^{13}C methane remains relative to ^{12}C methane (Galimov, 2006). Use of isotopic trends along with concentration data offers a second supporting piece of evidence, as this should coordinate with a decrease in concentration across the boundary as well. If concentration analysis was used separately without isotope data, a decrease may be observed but could be attributed to other processes like diffusion rather than oxidation. If diffusion is driving the loss of methane across a water column then no enrichment would be seen in the $\delta^{13}C$ values across depth or concentration change as no fractionation would be occurring due to lack of bacteria preferentially selecting ^{12}C methane (Templeton, Chu, Alvarez-Cohen, & Conrad, 2006).

1.3 – Phospholipid Fatty Acids – Use as Biomarkers, $\delta^{13}C$ incorporation, and General Biomass Assessment within an EPL Water Column

1.3.1 – PLFA Definition and Notation

Phospholipid Fatty Acids (PLFAs) are structural lipids present in bacteria, eukarya, and archaea as the primary component of their cellular membranes. These compounds have been shown to degrade shortly after cell death, meaning analysis provides information based on the active and viable microbial community at the time of sampling (Harvey, Fallon, & Patton, 1986). Applying PLFA analysis to BML water column samples provides information on community structure and composition, biomarker analysis of methanotrophs, and tracing of $\delta^{13}C$ signatures to support potential methanotrophic consumption of dissolved methane. Phospholipids are composed of a polar phosphate head with two nonpolar fatty acid tails (Figure 1.3). In bacteria and eukarya, an ester linkage connects these components together, whereas in archaea an ether linkage connects them (Lodish et al., 2013). Due to this difference in linkage, methanogen lipids and methanotroph lipids require different derivatizations to allow for identification and quantification in the lab.

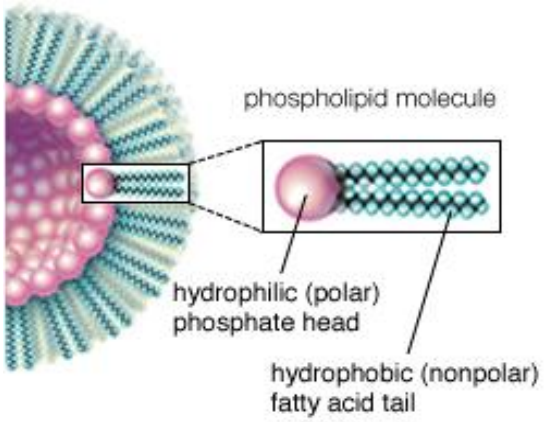

Figure 1.3: Phospholipid schematic diagram illustrating polar head and nonpolar fatty acid tail components (Encyclopedia Britannica, 2017)

PLFA can be isolated from an intact sediment or water sample allowing for direct analysis of the microbial community at one specific point in time. This allows for biomarker analysis and biomass estimations to gather detailed information regarding the microbial community composition and its changes over time. This technique can also be highly

complementary to dissolved methane concentration and isotopic analysis as it allows for tracing of depleted signature incorporation if methanotrophic bacteria are present and actively metabolising. PLFAs are named using the IUPAC-IUBMB protocol and associated short hand notation (Fahy et al., 2005). PLFA will be discussed using the ω short hand notation in the form of A:BωC(c or t), where A, B, and C represent the number of carbon atoms, number of double bonds, position of the double bonds relative to the aliphatic end of the structure, and c or t for cis or trans configuration respectively.

1.3.2 – Biomass Estimations for Overall Community Assessment

PLFA analysis provides a unique snapshot of the viable microbial community at the time of sampling, which can be modified through the use of conversion factors to obtain biomass estimates for the water column at different depths. This can be achieved through utilizing conversion factors that convert total phospholipid concentration in picomoles to biomass (cells/mL), and then normalizing this to the sample volume the PLFA was extracted from. Conversion factors vary based on environment (soil vs. water column) and are subject to variability based on cell size, species, and related variability of these within the profile (Green & Scow, 2000). Comparison of biomass estimates across depth profiles and sampling periods can allow for general assessment of microbial community abundance changes that may be occurring due to active environmental engineering decisions related to the development of BML.

1.3.3 – PLFA Use as Biomarkers for Methanotrophic Bacteria in the Water Column

PLFA structure can vary depending on the species of microbe, with different PLFA being produced in response to environmental stresses and conditions (Haack, Garchow, Odelson, Forney, & Klug, 1994). Due to diversity of available structures PLFA can be classified into saturates, unsaturates, branched, and cyclic groups, with each specific PLFA providing different

information about the microbial community. Some PLFAs are unique and distinguish them from other microbes, allowing pure culture studies to identify specific PLFAs as biomarkers that are only expressed by one microbe. Using this technique in BML can assist in assessing active pathways related to methane biogeochemical cycling. The C16:1ω8c, C16:1ω5c/t PLFA are unique to type I methanotrophs, while C18:1ω8c are unique to type II methanotrophs (Bodelier et al., 2009; Bowman, Skerratt, Nichols, & Sly, 1991). Identification of these PLFA biomarkers would indicate methanotrophs are present in a water column, and quantification of their molar percent contribution to the total PLFA profile can provide information on their relative abundance within the community. Generating this biomarker data set across a depth profile will determine if and where methanotrophy is active within the water column, the specific depths containing methanotrophic bacteria, and can correlate with dissolved methane and oxygen data to further support potential consumption trends observed.

1.3.4 – PLFA Stable Carbon Isotope Analysis – Dissolved Methane Utilization

Pairing PLFA biomarker analysis with compound specific stable carbon isotope analysis can provide further supporting evidence of methanotrophy within BML. As previously established, dissolved methane generated through methanogenic pathways will have a depleted $\delta^{13}C$ value with respect to other carbon sources in the water column. Utilization of δ13C depleted dissolved methane by methanotrophic bacteria will cause a partial transfer of this depleted signature into the PLFA signatures, with the most significant depletion observed in the C16:1ω8c, C16:1ω5c/t, and C18:1ω8c biomarker PLFA (Bodelier et al., 2009; Pancost et al., 2000). Obtaining compound specific $\delta^{13}C$ signatures for these biomarkers can require a substantial amount of mass, requiring large sample volumes and higher throughput filtering to accommodate the increased volume. Comparing the signature of the unsaturated PLFA pool with

the saturated pool that contains general bacteria biomarkers like C16:0 will show a gap if methanotrophy is incorporating the depleted methane into the pool, whereas the C16:0 will have a more enriched value due to utilization of other carbon sources for growth.

1.4 – Thesis Outline and Structure

The focus of this thesis is to examine biogeochemical cycling of dissolved methane in the water column and FFT of the first ever full-scale demonstration of EPL technology at Base Mine Lake, located and constructed on the Syncrude Canada Ltd. lease north of Fort McMurray, Alberta, Canada. The primary mechanism of interest regarding cycling is consumption of dissolved methane within the water column via methanotrophic bacteria and the resulting implications with regard to dissolved oxygen concentrations. Determining if methanotrophy is actively consuming dissolved methane and oxygen in the water column is critical as the EPL water column must stay oxic to facilitate biodegradation and generation of a stable lake environment. Chapter two is a manuscript being prepared for submission to Organic Geochemistry that presents the dissolved methane and oxygen data sampled from the BML water column over two years, and discusses the trends observed. Isotopic analysis of dissolved methane in the water column and FFT layer was also carried out to track $\delta^{13}C$ fractionation with respect to location of the methane within the water column. Chapter three is a manuscript being prepared for submission to Applied Geochemistry, presenting the data from PLFA analysis of the BML water column over two years in the form of the associated biomass estimates over different profiles, biomarker analysis with respect to methanotrophs, as well as $\delta^{13}C$ values associated with PLFA groupings. This data is then discussed and linked back to dissolved methane $\delta^{13}C$ values from chapter two to provide evidence of depleted signature incorporation into the microbial community, further supporting the hypothesis of methane consumption within the water column.

Chapter four provides conclusions for the work presented in chapters two and three, as well as a future work section.

1.5 References

Alberta Energy Regulator. (2016). Executive Summary, ST 98-2016: Alberta's Energy Reserves 2015 & Supply/Demand Outlook 2016-2025, 8. Retrieved from http://www1.aer.ca/st98/data/executive_summary/ST98-2016_Executive_Summary.pdf

Allen, E. W. (2008). Process water treatment in Canada's oil sands industry: I. Target pollutants and treatment objectives. *Journal of Environmental Engineering and Science*, *7*(2), 123–138. https://doi.org/10.1139/S07-038

Bedard, C., & Knowles, R. (1989). CO Oxidation by Methanotrophs and Nitrifiers. *Microbiology*, *53*(1), 68–84. Retrieved from http://apps.isiknowledge.com/full_record.do?product=UA&search_mode=GeneralSearch&qid=11&SID=X16536DGgEAkOn8a882&page=1&doc=1&colname=WOS

Blumenberg, M., Seifert, R., & Michaelis, W. (2007). Aerobic methanotrophy in the oxic-anoxic transition zone of the Black Sea water column. *Organic Geochemistry*, *38*(1), 84–91. https://doi.org/10.1016/j.orggeochem.2006.08.011

Bodelier, P. L. E., Gillisen, M.-J. B., Hordijk, K., Damsté, J. S. S., Rijpstra, W. I. C., Geenevasen, J. a J., & Dunfield, P. F. (2009). A reanalysis of phospholipid fatty acids as ecological biomarkers for methanotrophic bacteria. *The ISME Journal*, *3*(5), 606–617. https://doi.org/10.1038/ismej.2009.6

Bordenave, S., Kostenko, V., Dutkoski, M., Grigoryan, A., Martinuzzi, R. J., & Voordouw, G. (2010). Relation between the activity of anaerobic microbial populations in oil sands tailings ponds and the sedimentation of tailings. *Chemosphere*, *81*(5), 663–668.

https://doi.org/10.1016/j.chemosphere.2010.07.058

Boschker, H. T. S., de Brouwer, J. F. C., & Cappenberg, T. E. (1999). The contribution of macrophyte-derived organic matter to microbial biomass in salt-marsh sediments: Stable carbon isotope analysis of microbial biomarkers. *Limnology and Oceanography*, *44*(2), 309–319. https://doi.org/10.4319/lo.1999.44.2.0309

Boschker, H. T. S., & Middelburg, J. J. (2002). Stable isotopes and biomarker in microbial ecology. *FEMS Microbiology Ecology*, *40*, 85–95.

Bowman, J. P., Skerratt, J. H., Nichols, P. D., & Sly, L. I. (1991). Phospholipid fatty acid and lipopolysaccharide fatty acid signature lipids in methane-utilizing bacteria, *85*(January), 15–21. https://doi.org/10.1111/j.1574-6968.1991.tb04693.x

Canadian Association of Petroleum Producers. (2015). Crude Oil, (June), 1–9.

Chalaturnyk, R. J., Don Scott, J., & Özüm, B. (2002). Management of Oil Sands Tailings. *Petroleum Science and Technology*, *20*(9–10), 1025–1046. https://doi.org/10.1081/LFT-120003695

Chen, M., Walshe, G., Chi Fru, E., Ciborowski, J. J. H., & Weisener, C. G. (2013). Microcosm assessment of the biogeochemical development of sulfur and oxygen in oil sands fluid fine tailings. *Applied Geochemistry*, *37*, 1–11. https://doi.org/10.1016/j.apgeochem.2013.06.007

Chi Fru, E., Chen, M., Walshe, G., Penner, T., & Weisener, C. (2013). Bioreactor studies predict whole microbial population dynamics in oil sands tailings ponds. *Applied Microbiology and Biotechnology*, *97*(7), 3215–3224. https://doi.org/10.1007/s00253-012-4137-6

Conrad, R. (2005). Quantification of methanogenic pathways using stable carbon isotopic signatures: A review and a proposal. *Organic Geochemistry*, *36*(5), 739–752. https://doi.org/10.1016/j.orggeochem.2004.09.006

Conrad, R. (2009). The global methane cycle: Recent advances in understanding the microbial processes involved. *Environmental Microbiology Reports*, *1*(5), 285–292. https://doi.org/10.1111/j.1758-2229.2009.00038.x

Coveney, M. F., & Wetzel, R. G. (1995). Biomass, production, and specific growth rate of bacterioplankton and coupling to phytoplankton in an oligotrophic lake, *40*(7).

Deines, P., Bodelier, P. L. E., & Eller, G. (2007). Methane-derived carbon flows through methane-oxidizing bacteria to higher trophic levels in aquatic systems. *Environmental Microbiology*, *9*(5), 1126–1134. https://doi.org/10.1111/j.1462-2920.2006.01235.x

Dompierre, K. A., Lindsay, M. B. J., Cruz-Hernandez, P., & Halferdahl, G. M. (2016). Initial geochemical characteristics of fluid fine tailings in an oil sands end pit lake. *Science of the Total Environment*, *556*, 196–206. https://doi.org/10.1016/j.scitotenv.2016.03.002

Duan, Z., & Mao, S. (2006). A thermodynamic model for calculating methane solubility, density and gas phase composition of methane-bearing aqueous fluids from 273 to 523 K and from 1 to 2000 bar. *Geochimica et Cosmochimica Acta*, *70*(13), 3369–3386. https://doi.org/10.1016/j.gca.2006.03.018

Eby, P., Gibson, J. J., & Yi, Y. (2015). Suitability of selected free-gas and dissolved-gas sampling containers for carbon isotopic analysis. *Rapid Communications in Mass Spectrometry*, *29*(13), 1215–1226. https://doi.org/10.1002/rcm.7213

Fahy, E., Subramaniam, S., Brown, H. A., Glass, C. K., Merrill, A. H., Murphy, R. C., … Dennis, E. a. (2005). A comprehensive classification system for lipids. *Journal of Lipid Research*, *46*, 839–861. https://doi.org/10.1194/jlr.E400004-JLR200

Galimov, E. M. (2006). Isotope organic geochemistry. *Organic Geochemistry*, *37*(10), 1200–1262. https://doi.org/10.1016/j.orggeochem.2006.04.009

Giesy, J. P., Anderson, J. C., & Wiseman, S. B. (2010). Alberta oil sands development. *Pnas*, *107*(3), 951–952. https://doi.org/10.1073/pnas.0912880107

Government of Alberta. (2013). Facts and Statistics. Retrieved February 7, 2017, from http://www.energy.alberta.ca/OilSands/791.asp

Green, C. T., & Scow, K. M. (2000). Analysis of phospholipid fatty acids (PLFA) to characterize microbial communities in aquifers. *Hydrogeology Journal*, *8*(1), 126–141. https://doi.org/10.1007/s100400050013

Haack, S. K., Garchow, H., Odelson, D. A., Forney, L. J., & Klug, M. J. (1994). Accuracy, Reproducibility, and Interpretation of Fatty Acid Methyl Ester Profiles of Model Bacterial Communities. *Appl. Envir. Microbiol.*, *60*(7), 2483–2493. Retrieved from http://aem.asm.org/content/60/7/2483.short

Hanson, R. S., & Hanson, T. E. (1996). Methanotrophic Bacteria. *Microbiological Reviews*, *60*(2), 439–471. https://doi.org/

Harrits, S. M., & Hanson, R. S. (1980). Stratification of aerobic methane-oxidizing organisms in Lake Mendota, Madison, Wisconsin. *Limnology and Oceanography*, *25*(3), 412–421. https://doi.org/10.4319/lo.1980.25.3.0412

Harvey, H. R., Fallon, R. D., & Patton, J. S. (1986). The effect of organic matter and oxygen on the degradation of bacterial membrane lipids in marine sediments, *50*, 795–804.

Hayes, J. M. (2001). Fractionation of the Isotopes of Carbon and Hydrogen in Biosynthetic Processes. *Reviews in Mineralogy and Geochemistry*, *43*(March), 225–277. https://doi.org/10.2138/gsrmg.43.1.225

Hessen, O. (1985). The relation between bacterial carbon and dissolved humic compounds in oligotrophic lakes, *31*, 215–223.

Holowenko, F. M., MacKinnon, M. D., & Fedorak, P. M. (2000). Methanogens and sulfate-reducing bacteria in oil sands fine tailings waste. *Canadian Journal of Microbiology*, *46*(10), 927–937. https://doi.org/10.1139/w00-081

Hutchins, S. R. (1991). Biodegradation of Monoaromatic Hydrocarbons by Aquifer Microorganisms Using Oxygen, Nitrate, or Nitrous-Oxide as the Terminal Electron-Acceptor. *Applied and Environmental Microbiology*, *57*(8), 2403–2407.

Jahnke, L. L., Summons, R. E., Hope, J. M., & Des Marais, D. J. (1999). Carbon isotopic fractionation in lipids from methanotrophic bacteria II: The effects of physiology and environmental parameters on the biosynthesis and isotopic signatures of biomarkers. *Geochimica et Cosmochimica Acta*, *63*(1), 79–93. https://doi.org/10.1016/S0016-7037(98)00270-1

Jiang, H., Chen, Y., Jiang, P., Zhang, C., Smith, T. J., Murrell, J. C., & Xing, X.-H. (2010). Methanotrophs: Multifunctional bacteria with promising applications in environmental bioengineering. *Biochemical Engineering Journal*, *49*(3), 277–288. https://doi.org/10.1016/j.bej.2010.01.003

Jordan, M. J., & Likens, G. E. (1980). Measurement of planktonic bacterial production in an oligotrophic lake. *Limnology and Oceanography*, *25*(4), 719–732. https://doi.org/10.4319/lo.1980.25.4.0719

Kelly, C. A., & Chynoweth, P. (1981). Carol A. Kelly2 and David P. Chynoweth3, *26*, 891–897.

King, G. M., & Schnell, S. (1994). Ammonium and nitrite inhibition of methane oxidation by Methylobacter albus BG8 and Methylosinus trichosporium OB3b at low methane concentrations. *Applied and Environmental Microbiology*, *60*(10), 3508–3513.

Knief, C., Kolb, S., Bodelier, P. L. E., Lipski, A., & Dunfield, P. F. (2006). The active

methanotrophic community in hydromorphic soils changes in response to changing methane concentration. *Environmental Microbiology*, *8*(2), 321–333. https://doi.org/10.1111/j.1462-2920.2005.00898.x

Kolb, S., Knief, C., Dunfield, P. F., & Conrad, R. (2005). Abundance and activity of uncultured methanotrophic bacteria involved in the consumption of atmospheric methane in two forest soils. *Environmental Microbiology*, *7*(8), 1150–1161. https://doi.org/10.1111/j.1462-2920.2005.00791.x

Lidstrom, M. E., & Somers, L. (1984). Seasonal study of methane oxidation in lake washington. *Applied and Environmental Microbiology*, *47*(6), 1255–1260.

Lodish, H., Berk, A., Kaiser, C. A., Krieger, M., Bretscher, A., Ploegh, H., & Amon, A. (2013). *Molecular Cell Biology* (7th ed.). W.H. Freeman and Company.

Lovley, D. R., & Klug, M. J. (1986). Model for the distribution of sulfate reduction and methanogenesis in freshwater sediments. *Geochimica et Cosmochimica Acta*, *50*(1), 11–18. https://doi.org/10.1016/0016-7037(86)90043-8

Masliyah, J., Zhou, Z. J., Xu, Z., Czarnecki, J., & Hamza, H. (2004). Understanding Water-Based Bitumen Extraction from Athabasca Oil Sands. *The Canadian Journal of Chemical Engineering*, *82*(4), 628–654. https://doi.org/10.1002/cjce.5450820403

Mohanty, S. R., Bodelier, P. L. E., & Conrad, R. (2007). Effect of temperature on composition of the methanotrophic community in rice field and forest soil. *FEMS Microbiology Ecology*, *62*(1), 24–31. https://doi.org/10.1111/j.1574-6941.2007.00370.x

Nozhevnikova, A. N., Holliger, C., Ammann, A., & Zehnder, A. J. B. (1997). Methanogenesis in Sediments from Deep Lakes at Different temperatures (2-70C).

Nyerges, G., & Stein, L. Y. (2009). Ammonia cometabolism and product inhibition vary

considerably among species of methanotrophic bacteria. *FEMS Microbiology Letters*, *297*(1), 131–136. https://doi.org/10.1111/j.1574-6968.2009.01674.x

Oremland, R. S., & Polcin, S. (1982). Methanogenesis and Sulfate Reduction: Competitive and Noncompetitive Substrates in Estuarine Sediments. *Applied and Environmental Microbiology*, *44*(6), 1270–1276. https://doi.org/10.1016/0198-0254(83)90262-5

Pancost, R. D., Damsté, J., Sinninghe, S., Lint, S. De, Maarel, M. J. E. C. Van Der, & Gottschal, J. C. (2000). Biomarker Evidence for Widespread Anaerobic Methane Oxidation in Mediterranean Sediments by a Consortium of Methaogenic Archaea and Bacteria. *Applied and Environmental Microbiology*, *66*(3), 1126–1132. https://doi.org/10.1128/AEM.66.3.1126-1132.2000.Updated

Pancost, R. D., & Sinninghe Damste, J. S. (2003). Carbon isotopic compositions of prokaryotic lipids as tracers of carbon cycling in diverse settings. *Chemical Geology*, *195*(1–4), 29–58. https://doi.org/10.1016/S0009-2541(02)00387-X

Penner, T. J., & Foght, J. M. (2010). Mature fine tailings from oil sands processing harbour diverse methanogenic communities. *Canadian Journal of Microbiology*, *56*(6), 459–70. https://doi.org/10.1139/w10-029

Schonheit, P., Keweloh, H., & Thauer, R. K. (1991). Factor F420 degradation in Methanobacterium thermoautotrophicum during exposure to oxygen. *Biochemistry*, *266*(2), 14151–14154. Retrieved from http://www.jbc.org/content/266/22/14151.short

Schönheit, P., Kristjansson, J. K., & Thauer, R. K. (1982). Kinetic mechanism for the ability of sulfate reducers to out-compete methanogens for acetate. *Archives of Microbiology*, *132*(3), 285–288. https://doi.org/10.1007/BF00407967

Semrau, J. D. (2011). Bioremediation via methanotrophy: Overview of recent findings and

suggestions for future research. *Frontiers in Microbiology*, *2*(OCT), 1–7. https://doi.org/10.3389/fmicb.2011.00209

Siddique, T., Fedorak, P. M., & Foght, J. M. (2006). Biodegradation of Short-Chain n -Alkanes in Oil Sands Tailings under Methanogenic Conditions. *Environmental Science & Technology*, *40*(17), 5459–5464. https://doi.org/10.1021/es060993m

Siddique, T., Fedorak, P. M., Mackinnon, M. D., & Foght, J. M. (2007). Metabolism of BTEX and naphtha compounds to methane in oil sands tailings. *Environmental Science and Technology*, *41*(7), 2350–2356. https://doi.org/10.1021/es062852q

Siddique, T., Penner, T., Semple, K., & Foght, J. M. (2011). Anaerobic biodegradation of longer-chain n-alkanes coupled to methane production in oil sands tailings. *Environmental Science and Technology*, *45*(13), 5892–5899. https://doi.org/10.1021/es200649t

Simankova, M. V, Kotsyurbenko, O. R., Lueders, T., Nozhevnikova, A. N., Wagner, B., Conrad, R., & Friedrich, M. W. (2003). Isolation and characterization of new strains of methanogens from cold terrestrial habitats. *Systematic and Applied Microbiology*, *26*(2), 312–318. https://doi.org/10.1078/072320203322346173

Stasik, S., Loick, N., Knöller, K., Weisener, C., & Wendt-Potthoff, K. (2014). Understanding biogeochemical gradients of sulfur, iron and carbon in an oil sands tailings pond. *Chemical Geology*, *382*, 44–53. https://doi.org/10.1016/j.chemgeo.2014.05.026

Syncrude Canada Ltd. (2016). *Sustainability Report*.

Templeton, A. S., Chu, K. H., Alvarez-Cohen, L., & Conrad, M. E. (2006). Variable carbon isotope fractionation expressed by aerobic CH4-oxidizing bacteria. *Geochimica et Cosmochimica Acta*, *70*(7), 1739–1752. https://doi.org/10.1016/j.gca.2005.12.002

Trotsenko, Y. A., & Khmelenina, V. N. (2005). Aerobic methanotrophic bacteria of cold

ecosystems. *FEMS Microbiology Ecology*, *53*(1), 15–26. https://doi.org/10.1016/j.femsec.2005.02.010

Westcott, F., & Watson, L. (2007). End Pit Lakes Technical Guidance Document. Prepared by Clearwater Environmental Consultants Inc. for the Cumulative Environmental Management Association (CEMA) End Pit Lakes Subgroup., 51.

Whiticar, M. J. (1999). Carbon and hydrogen isotope systematics of bacterial formation and oxidation of methane. *Chem. Geol.*, *161*(1–3), 291–314. https://doi.org/10.1016/S0009-2541(99)00092-3

Whiticar, M. J., Faber, E., & Schoell, M. (1986). Biogenic methane formation in marine and freshwater environments: CO2 reduction vs. acetate fermentation-Isotope evidence. *Geochimica et Cosmochimica Acta*, *50*(5), 693–709. https://doi.org/10.1016/0016-7037(86)90346-7

Witherspoon, P. a., & Saraf, D. N. (1966). Diffusion of Methane, Ethane, Propane, and n-Butane. *Journal of Physical Chemistry*, *510*(6), 3752–3755. https://doi.org/10.1021/j100895a017

Zhou, E., & Crawford, R. L. (1995). Effects of oxygen, nitrogen, and temperature on gasoline biodegradation in soil. *Biodegradation*, *6*(2), 127–140. https://doi.org/10.1007/BF00695343

Chapter 2

BIOGEOCHEMICAL CYCLING OF DISSOLVED METHANE IN BASE MINE LAKE: FERMENTATIVE METHANOGENESIS AND OXIDATION BY METHANOTROPHIC BACTERIA

Manuscript in preparation for submission to Organic Geochemistry

Goad, C.[1], Slater G.F[1], Risacher, F. [1], Morris, P. [1], Arriaga, D.[1], Lindsay, M.[2], Warren, L.A.[3]

[1]School of Geography and Earth Sciences, McMaster University, Hamilton, Ontario, Canada

[2]Department of Geological Sciences, University of Saskatchewan, Saskatoon, Saskatchewan, Canada

[3]Department of Civil Engineering, University of Toronto, Toronto, Ontario, Canada

Abstract

Bitumen extraction in the Alberta Oil Sand Region (AOSR) produces large volumes of tailings that are being managed as part of land reclamation activities. Syncrude Canada Ltd. has undertaken the first full scale demonstration of water-capped Fluid Fine Tailings (FFT) via the development of Base Mine Lake, an end pit lake. This study investigated biogeochemical cycling of microbial methane produced within the FFT and released to surface waters during the initial stages of lake development via concentration and isotopic analysis. Dissolved methane concentrations in the epilimnion were very low ranging from 0.1 to 0.5 μM. Below this, dissolved methane increased from 1.3-2.0 μM in the metalimnion (5 to 6m depth), to 25-75 μM at 8 m depth in the upper hypolimnion and further to 75-150 μM directly above the sediment water interface (9-10m depth). This trend was opposite to that observed for oxygen which decreased from 75% saturation in the epilimnion to 1-2% in the hypolimnion. Dissolved methane concentrations within the FFT reached saturation within ~0.5m of the FFT-water interface. Stable carbon and hydrogen isotope analyses ($\delta^{13}C$, $\delta^{2}H$) of dissolved methane within the FFT ranged from -60 to -70 ‰ and -298 to -349 ‰ respectively, indicating production via fermentation pathways. A 5‰ minor isotopic enrichment in methane $\delta^{13}C$ with concurrent decreasing concentrations was consistent with methane oxidation in the water column. Preliminary diffusive flux calculations support removal of dissolved methane across the FFT-water and metalimnion-hypolimnion interfaces as well. Ongoing research is focussed on trends in these parameters as lake development continues in order to assess the potential for continued influence of methane production and oxidation on the oxygen levels within this system.

2.1 – Introduction

2.1.1 – Introduction to the Alberta Oil Sands Region (AOSR) and Bitumen Extraction

The Alberta Oil Sands Region (AOSR) hosts the 3rd largest oil reserves globally, spanning across three local geographic areas; encompassing a total regional area of 142,200 km^2 and containing up to 1.8 trillion barrels of bitumen (Alberta Energy Regulator (AER), 2016). In 2015, production reached 2.4 million barrels/day (bbl/d) solely from oil sands sources, with growth projecting an increase of ~86,000 b/d year over year totaling 3.7 million b/d by 2030 (Canadian Association of Petroleum Producers, 2015). Bitumen is extracted from the crude oil sands mixture via the Clark Hot Water Extraction (CHWE) process that generates a tailings slurry composed of Oil Sands Process Water (OSPW), un-recovered bitumen, sand, and fine solids (Bordenave et al., 2010; Holowenko, MacKinnon, & Fedorak, 2000). As of 2013, 975.6 million m^3 of tailings are stored in ~220 km^2 of settling basins across the oil sands region (Government of Alberta, 2013). The partially de-watered fraction of the original tailings mixture continuously undergoing densification in settlings basins are referred to as Fluid Fine Tailings (FFT). Management of FFT as a component of site reclamation activities faces challenges due to the long compaction times associated with very fine solids present within FFT. Development of effective reclamation approaches for FFT remains a primary waste management issue as over 262,000 m^3 of tailings slurry are generated each day in northern Alberta (Siddique, Penner, Semple, & Foght, 2011).

2.1.2 – Land Reclamation, End Pit Lake (EPL) Technology, and Base Mine Lake Introduction

Regulations set by the AER during the application process for oil sands land development state the land must be reclaimed to "equivalent capability", or a similar biologically productive state after development has ceased. (Giesy, Anderson, & Wiseman, 2010; Syncrude Canada Ltd.,

2016). This requirement has led to the development of both wet and dry reclamation strategies that include the design and testing of End Pit Lake (EPL) technology by Syncrude Canada Ltd. The EPL technology aims to resolve both the long term storage and settlement issue of FFT while remediating the disturbed landscapes across the AOSR (Westcott & Watson, 2007).

Base Mine Lake is the first full scale demonstration of wet reclamation of FFT through the development of an EPL by Syncrude Canada Ltd. Placement of FFT into the mined out pit began in 1994 and concluding in 2012 with a total FFT depth of circa 48m. Initial water capping of the FFT occurring with 5m of OSPW after FFT placement concluded in 2012, with another 2.5m of OSPW being added in 2013 for a total water cap depth of approximately 7.5m (Dompierre, Lindsay, Cruz-Hernandez, & Halferdahl, 2016). Constant FFT consolidation since 2012 has led to an increased water column depth, with an overall depth of 10m in 2017. BML receives freshwater inputs from the neighboring Beaver Creek Reservoir (BCR), and has water removed for further bitumen extraction creating an input-output cycling of the water cap. This constant input of freshwater alongside microbial-mediated degradation of OSPW compounds is designed to improve water quality of BML as FFT continues to dewater and expel porewater.

2.1.3. Influence and Importance of Methane in Development of EPL Environments

Biogeochemical cycling of methane has been identified as a primary water quality concern in the development of EPLs due to potential consumption of oxygen via methanotrophic metabolisms, leading to decreased availability for aerobic processes required in the formation of a biologically productive lake (Westcott & Watson, 2007). EPLs are designed to be self-sustaining ecosystems that remediate OSPW pumped into the lake by facilitating the natural breakdown of toxic compounds via microbial degradation, requiring significant oxygen saturation in order to maximize degradation rates (Allen, 2008). Numerous studies have

identified methanogenesis by archaeal microbes as a dominant microbial metabolism occurring in mature oil sands tailings, due to depletion of oxygen and other terminal electron acceptors throughout the FFT layer (Chi Fru, Chen, Walshe, Penner, & Weisener, 2013; Penner & Foght, 2010; Siddique, Fedorak, & Foght, 2006; Stasik, Loick, Knöller, Weisener, & Wendt-Potthoff, 2014). Microbial methanogenesis can proceed by either fermentative or CO_2 reduction pathways and can utilize a variety of organic compounds present in FFT including carbon dioxide, acetate, and methanol (Hanson & Hanson, 1996). These metabolic pathways are carried out by microbes that are obligate anaerobes as a result of a critical hydrogenase complex's instability when dissolved oxygen is present (Schonheit, Keweloh, & Thauer, 1991; Whiticar, 1999). Stable isotope analysis of carbon and hydrogen can be used to examine production in the FFT. Stable carbon and hydrogen isotopes of dissolved methane in the FFT porewater can allow differentiation of the source carbon between carbon dioxide and acetate or methanol, and thus if the pathway is fermentative or CO_2 reduction. Fermentative methanogenesis produces methane with $\delta^{13}C/\delta^{2}H$ values of -45 to -70‰ and -290 to -400‰, while CO_2 reduction generates more depleted $\delta^{13}C$ values and more enriched $\delta^{2}H$ values of -60 to -110‰ and -150 to -250‰ respectively (Figure 2.1).

Dissolved methane may be oxidized by methanotrophic bacteria in aerobic conditions, being the sole removal mechanism in lake environments other than export from the system. Methanotrophs are classified into three subgroups by taxonomic distinctions; Type I, Type II, and Type X. These three subgroups oxidize CH_4 to methanol through use of a methane monooxygenase (MMO) enzyme expressed in two forms; either soluble (sMMO) or membrane-bound particulate (pMMO). Expression is determined by environmental conditions and microbial genetics (Hanson & Hanson, 1996). Both MMOs require two reducing equivalents to split O_2,

using one oxygen to form methanol and the other to water. Methanol is then oxidized to formaldehyde where assimilation to a biosynthetic pathway occurs, or is further oxidized to CO_2 (Equation 1**)**.

$$CH_4 + O_2 \rightarrow CH_3OH \rightarrow HCHO \rightarrow HCOOH \rightarrow CO_2 \quad (1)$$

The complete oxidation of CH_4 to CO_2 consumes oxygen in a 2:1 molar ratio to methane, demonstrating methanotrophic activity can impact dissolved oxygen concentrations of the BML water cap significantly as a result of production and transfer from the FFT layer. Isotopic analyses on dissolved methane in the water column can confirm aerobic methane oxidation, as methanotrophic bacteria prioritize uptake of the ^{12}C methane, causing an enrichment in the ^{13}C of the residual methane pool throughout the water column towards the surface with decreasing concentration (Whiticar, 1999). Biogenic methane is exported from the FFT methanogenic zone into the water column by diffusive processes, advection of porewater via water expression linked to FFT compaction, and ebullition. Ebullition is the main vector of methane emission from the surface of an EPL and contributes dissolved methane to the water column through dissolution.

This study is focussed on understanding trends in dissolved methane and oxygen concentrations in the water column and FFT throughout development of the first full scale test of EPL technology by Syncrude Canada Ltd. The production mechanisms of dissolved methane in the FFT are first addressed, followed by processes controlling dissolved methane concentrations in the water column above. These results will aid in the understanding of biogeochemical cycling of dissolved methane through the development of the first full-scale EPL site in northern Alberta, Canada.

2.2 - Materials & Methods

2.2.1 – Sampling Locations & Schedule

Sample collection occurred between May 2015 to September 2015, July 2016 to September 2016, and February 2017. Sample collection was delayed from May to July in 2016 due to active wildfires in the region. Sample collection was conducted across three floating platforms (P1, P2, P3) along a diagonal transect, with P1 being positioned at the center of the lake (Figure 2.2**)**. Sample collection in 2016 focussed primarily on P1 due to consistent results across the three platforms in the previous year, and has increased sampling frequency.

2.2.2 - CH_4 Sample Collection and Preservation

Dissolved methane samples were collected in 60mL Wheaton serum bottles treated with ~3.7mg of saturated mercuric chloride solution, plugged with 13mm blue butyl septum stoppers and sealed with an aluminum crimped ring prior to evacuation by vacuum pump (Eby, Gibson, & Yi, 2015). Methane water column samples were collected in an air-tight Van Dorn water sampler. Immediately upon retrieval of the Van Dorn, water samples were withdrawn into air-tight 60mL syringes, and transferred into treated sample bottles. A subset of methane water column samples and FFT were collected using a Fixed Interval Sampler (FIS), a steel device with collection chambers every 10cm totalling 2m in length, filled via suction created by withdrawing a plunger. The sample chambers were sealed at depth prior to re-surfacing the device. Nalgene bottles were fixed to the sides of the sample chambers once re-surfaced, then the water was removed from the sample chamber, and methane sampling via sealed syringe took place immediately, minimizing exposure time of sample water to the atmosphere. This sampling device allowed for increased accuracy and resolution of sample collection down to intervals of 10cm and was used for both water column and FFT sampling. All sample bottles were stored

inverted at all times to prevent any gas exchange or sample loss through the septum stoppers. Bottles were filled with 30mL of sample water for dissolved methane concentration analysis and 50mL for methane $\delta^{13}C$ analysis. FFT methane samples were collected in untreated evacuated 120mL amber serum bottles, sealed with 13mm blue butyl septum stoppers and a crimped aluminum ring. Samples were frozen after sampling, and thawed then refrigerated a week prior to analysis. After analysis select FFT bottles were opened and dried out, to correct for different water content per bottle and correct measured concentrations accordingly. Air blanks were collected on the sample boat through piercing a septum with an open needle once every two weeks, removing the needle when pressure had equilibrated. These air blanks were taken to determine methane concentrations above the lake, and to simulate a worst case scenario blank if a sample bottle was exposed to the atmosphere.

2.2.3 – Dissolved Methane Concentration Analysis

Sample bottles under residual vacuum were brought to atmospheric pressure through addition of high purity helium (AlphaGaz 99.999%) prior to analysis. Dissolved methane concentrations in water column samples were quantified by injection of 1000 μL of sample bottle headspace on a SRI 8610C Gas-Chromatograph (GC) (silica gel column 0.91 m x 2.1 mm) coupled to a Thermal Conductivity Detector (TCD) and Flame Ionization Detector (FID) with an oven temperature hold at 40°C. The TCD was used to monitor N_2/O_2 (not quantified) between air blanks and water column samples, allowing for verification of sample bottle integrity as exposure to air would be observed through elevated values for N_2/O_2. Dissolved methane concentrations in FFT samples were quantified by injection of 100uL of sample headspace due to elevated concentrations. All samples were injected in triplicate (RSD $\leq$ 10%) and quantified on methane calibration curves created and maintained directly from gas tanks with pre-characterized

methane concentrations. Peak integration and quantification was conducted using PeakSimple software v3.29 (©SRI Instruments). Aqueous methane concentrations were determined by calculating the total mass of methane in the bottle headspace based on concentration and headspace volume and allocating this to the water volume added.

2.2.4 – Dissolved Methane $\delta^{13}C$, $\delta^{2}H$ Analysis

Stable carbon isotope analysis of methane was quantified by 300uL headspace injections (triplicate, RSD ≤ 10%) on an Agilent 6890 GC (GSQ; 30m × 0.32 mm) coupled to a Thermo Delta Plus XP Isotope Ratio Mass Spectrometer via a Conflo III interface (GC-IRMS) with a continuous oven temperature hold at 30°C. GC-IRMS data was processed with Isodat NT 2.0 Software (©Thermo Electron Company). Carbon isotope ratios were normalized to the Vienna Pee Dee Belmenite (VPDB) standard. All samples were injected in triplicate, with $\delta^{13}C$ standard deviation of approximately +/- 0.5 ‰ based on standard reproducibility and instrument accuracy. In order to get accurate and reproducible results, sample concentrations must be greater than 20 μM, limiting this to hypolimnion and FFT samples.

Deuterium analysis of CH_4 was carried out at Memorial University of Newfoundland (MUN) on an Agilent 6890N GC coupled to a Delta V Plus IRMS via a GC Combustion III interface (30m x 0.32mm x 15 μm, Carboxen 1010 column) with a oven temperature program of 110 °C for 5.5 min; to 180 °C @ 35 °C/min and a final hold for 2 min. The temperature conversion reactor was held at 1450°C. Hydrogen isotope ratios were normalized to the Vienna Pee Dee Belemnite (VPDB) standard. Based on standard reproducibility and instrument accuracy, $\delta^{2}H$ measurement error is approximately +/- 5.0 ‰.

2.3 – Results

2.3.1 – Base Mine Lake – Site State - O_2 Saturation & Thermal Stratification

Base Mine Lake is a dimictic EPL, turning over and mixing the water column completely in late April to early May and late August to early September. Between these turnover events thermal stratification of the water column creates three distinct geochemical zones that influence oxygen saturation. Temperature profiles show the epilimnion layer occurring between 0 to 5m depth, followed by the metalimnion between 5 to 6m, and the hypolimnion from 6m to the interface located approximately at 9.5m, as seen in Figures 2.3 & 2.4**.** The lake turnover event in August both years caused the temperature to become equal throughout the lake.

YSI multi-sensor oxygen profiles were mostly consistent across both 2015 and 2016, with maximum O_2 saturations of 75 to 80% occurring in the upper epilimnion, followed by a sharp decline through the metalimnion to ~30%, and a continued rapid decline to ~1 to 2% in the hypolimnion by a depth of ~6 to 7m as shown by Figures 2.5 & 2.6**.** Oxygen saturation profiles in 2016 show epilimnion oxygen values at 80% and metalimnion values 10 to 15% higher than 2015 values, delaying sub-anoxic oxygen conditions for an additional 0.5-1m in the hypolimnion when compared to the 2015 profiles. The lake turnover event that occurred in August both years caused thermal stratification to be lost and increased O_2 saturation of up to 30% to reach previously established hypolimnetic depths of 8.5m (Risacher et al., in preparation).

2.3.2 – Dissolved Methane Concentrations & $\delta^{13}C$ Values – Summer Water Columns

Dissolved methane in the water column followed similar distribution and concentration patterns across all platforms sampled in both the 2015 and 2016 sample sets (Figure 2.7**)**. Dissolved concentrations in the epilimnion ranged between 0.1 to 0.8 μM across all months and years, with higher range numbers of 0.3 to 0.4 μM occurring in August as overall concentrations

increase in the lake (n = 77, range = 0.11 to 0.81 μM, mean = 0.38 +/- 0.21 μM). These values were above the level of laboratory air blanks that were consistently below detection and field air blanks that yielded concentrations of ≤0.1 μM. The trace amounts of methane in the field air blanks were likely related to methane ebullition from the lake surface around the sampling barge. As every effort was made to exclude this air during sample collection these field air blanks represent a worst case scenario and it is more likely that field samples received negligible contributions of methane as shown by laboratory blanks. Metalimnion samples collected by both Van Dorn and FIS procedures yielded methane concentrations that were generally slightly higher than the epilimnion ranging from 0.11 to 4.6 μM (n = 76, range = 0.11 to 4.60 μM, mean = 0.59 +/-0.76 μM). Hypolimnion samples collected by both sampling protocols yielded a notably higher methane concentration range of 25 to 150 μM increasing steeply with depth (Figure 2.7**)** (n = 120, range = 2.86 to 149.6 μM, mean = 48.46 +/- 39.3 μM). Comparison of samples collected by Van Dorn and FIS methods showed excellent agreement (Figure 2.8). This demonstrated that the FIS sampling technique was not losing any significant concentration of methane during sampling and therefore enables high resolution methane concentration profiling. In addition the FIS methane concentrations in the hypolimnion show that the trends in methane concentrations observed by the more widely spaced Van Dorn samples are representative of the high resolution trends. This shows that the methane concentrations profiles are highly consistently structured through depth changes in the hypolimnion. Dissolved methane concentrations in the hypolimnion increased over time, with mean concentrations reaching the higher end of the observed concentration range as the months progressed. Fall turnover resulted in a sharp decline in methane concentration during September both years (Figure 2.9**).** Observed methane concentrations in the water cap were far below saturation which was estimated to be

3010 μM (+/- 10%) at 8 m depth using the model created by Duan & Mao (2006) using temperature, pressure, and salt inputs (T = 281K, P = 1.51325bar, mNaCl = 0.0285 mol/L).

Stable carbon isotope analysis of dissolved methane in hypolimnion samples yielded depleted $\delta^{13}C$ values ranging between -61 to -64 ‰. These $\delta^{13}C$ values showed no direct trend with depth in the hypolimnion (Figure 2.10**)**. The most isotopically depleted value was observed at the deepest depth (excluding one outlier) and the most isotopically enriched value was at the top of the sample range (excluding one outlier)**.** However, these samples did display an enrichment of 3‰ as dissolved methane concentration decreased from 150 μM to 20 μM (Figure 2.11).

2.3.3 – Dissolved Methane Concentrations, $\delta^{13}C$, $\delta^{2}H$ Values – Fluid Fine Tailings

Dissolved methane concentration in porewater samples from the FFT taken by FIS sampling ranged between 1000 - 5000 μM (n = 20, range = 1580 - 4885 μM, mean = 3121 +/- 1103 μM). These values were comparable with the solubility of methane in the FFT which was estimated to be 3770 μM (+/- 10%) by the same model as above, using conditions expected at the surface of the FFT (T = 284K, P = 2.0265bar, mNaCl = 0.010 mol/L) (Duan & Mao, 2006). Porewater methane concentrations in the upper FFT were circa 20 times higher than the deepest hypolimnion samples with a decrease of approximately 2000 μM occurring over the upper 0.5 m towards the interface. Porewater dissolved methane concentrations increased with increasing depth in the FFT (Figure 2.12). While there were insufficient data to quantitatively assess it, this trend was consistent with an expected increasing trend in methane solubility due to increasing pressure. The $\delta^{13}C$ values of dissolved methane in the FFT samples were generally more depleted than the water column ranging between -61 to -75 ‰, with no trend pertaining to depth (Figure 2.13**)**. Stable hydrogen isotope analysis returned depleted values ranging from -289 to -

343 ‰, with no trend pertaining to depth similar to the $\delta^{13}C$ values, as shown in Figure 2.14. A cross plot of the $\delta^{13}C$ / $\delta^{2}H$ values (Figure 2.15) shows both isotopes enriching together, and when overlain on Figure 2.1 show biogenic origin via fermentation type pathways.

2.3.4 – O_2 Saturation and Temperature Profile – February 2017 Water Column

The February 2017 O_2 and temperature profiles differ as the water column was covered with ice. The temperature profile was relatively constant, with an overall temperature change of 3°C across the entire depth profile. The epilimnion layer below the ice cap was ~0°C, increasing to 1°C at depth 7m, then increasing to 3°C by 9m. The O_2 saturation decreased from ~67% at surface waters to 50% at depth 7.5m, decreasing steeply to 14% at 9m, and then sub-anoxic conditions below.

2.3.5 – Dissolved Methane Concentrations & $\delta^{13}C$ Values – Winter Water Column

Dissolved methane concentration profiles sampled in February 2017 displayed elevated levels across all depths with respect to summer water column samples of 2015 and 2016. The surface epilimnion concentrations below the ice were ~170 μM, decreasing down to 140 μM at 6.5m depth then sharply increasing to ~250 μM at 9m (Figure 2.16). Stable carbon isotope analysis of dissolved methane yielded $\delta^{13}C$ values ranging from -57 to - 61‰. The isotopic composition of methane from surface to 6.5 m was constant (n = 4, range = -60.6 to -61.1 ‰, mean = 60.9 +/- 0.2 ‰) and became enriched to values outside of the range observed in the FFT with increasing depth and increasing concentration toward the FFT (Figure 2.17). A cross plot of $\delta^{13}C$ versus respective dissolved methane concentrations show an inverse enrichment trend to summer months, with greatest enrichment pertaining to highest concentration samples (Figure 2.18).

2.4 – Discussion

2.4.1 - FFT as a source zone of methanogenesis via fermentation pathways

Dissolved methane concentrations and isotopic compositions demonstrate biogenic production of methane via fermentative pathways within the FFT layer. Dissolved concentrations in the FFT began at ~1000 μM around the interface and increased to saturated conditions predicted by the Duan and Mao (2006) model within 1 to 2m of the interface. The release of significant numbers of bubbles from the sediments throughout the lake supports the observation that methane production is exceeding saturation throughout the sampled FFT depths (Figure 2.12). A previous study of BML FFT porewater characteristics observed ORP values averaging -250 to -100mV across numerous locations and depths, further supporting reductive conditions conducive to methanogenic pathways (Dompierre et al., 2016). Bioreactor studies using BML FFT have shown microbial communities shifting from primarily bacterial fingerprints to archaeal dominant fingerprints over time as redox zones are established, suggesting a similar community has been established in the FFT layer of BML. These experiments showed anaerobic FFT layers hosting an increased number of methanogenic archaeal signatures compared to FFT layers under aerobic conditions, suggesting the BML FFT layer will shift towards an increasingly methanogenic archaeal dominated community as oxygen is further depleted with depth (Chi Fru et al., 2013). The observed concentration increases seen with depth and subsequent bubble release due to saturated concentrations are consistent with these bioreactors studies, ORP values, and biogeochemical processes observed in MLSB, indicating the BML FFT layer is a source zone of biogenic methane via methanogenic activity (Penner & Foght, 2010).

The depleted $\delta^{13}C$ and $\delta^{2}H$ values of -61 to -75 ‰ and -289 to -343 ‰ respectively of the dissolved methane in the FFT indicate that biogenic production is a result of fermentation

pathways, rather than CO_2 reduction pathways (Figure 2.1). This indicates that methanogens are utilizing short-chain fatty acids released by biodegradation of larger organic compounds present in the FFT. Short-chain fatty acids are competitive substrates, regularly depleted in the sulphate reducing zone by Sulphate Reducing Bacteria (SRBs) located above the methanogenic zone. Previous studies of porewater characteristics in BML FFT indicates SRB activity is normally restricted to a narrow depth window below the interface where SO_4^{2-} is the major porewater TEA (Chen, Walshe, Chi Fru, Ciborowski, & Weisener, 2013; Stasik et al., 2014). Numerous laboratory studies conducted using MLSB FFT have shown the degradation of short-chain and long-chain n-alkanes, as well as BTEX compounds are coupled to methanogenic pathways (Siddique et al., 2006; Siddique, Fedorak, Mackinnon, & Foght, 2007; Siddique et al., 2011), providing a wide range of degradable substrates to fuel fermentative methanogenesis.

Plots of $\delta^{13}C$ and $\delta^{2}H$ values versus depth (Figure 2.13 & 2.14) yielded no correlation across platforms, as well as plots of $\delta^{13}C$ and $\delta^{2}H$ values versus concentration (not shown), suggesting that methanotrophy is not occurring within the FFT layer between the interface at 10m and the 17m depth mark. This further supports the FFT as a primary production zone for dissolved methane in the BML system. This is further reinforced by the scattering of concentration data in the saturated FFT layer, exhibiting no correlation with depth that would be indicative of methanotrophy. Concentration losses around the interface zone are likely attributed to variable transfer mechanics such as; diffusive processes, advection via porewater expression driven by continuous FFT settling, and advection via column mixing around the interface layer.

2.4.2 – Dissolved Methane Trends & Transfer across the Interface

While saturated methane conditions exist in the FFT below the interface, the highest concentration samples in the deep hypolimnion of ~150 μM are 20 times below estimated

dissolved methane solubility values of 3010 μM (+/- 10%). From this point methane concentrations decrease circa linearly to the bottom of the metalimnion where concentrations reach 1 to 2 μM, then decrease to trace concentrations through the epilimnion to the lake surface. The primary source of dissolved methane to the water column is transfer from the FFT. While ongoing methane release via ebullition is occurring, it's assumed the residence time of these bubbles within the water column is insufficient for substantial dissolution to occur. However, the trace concentrations within the epilimnion and metalimnion may be due to dissolution during bubble travel, which is currently under investigation.

Diffusive transport of dissolved methane can be assessed by comparing flux rates calculated at different points in the profile, specifically around the FFT-water and hypolimnion-metalimnion interfaces to further understand transfer mechanisms. Figure 2.19 shows the fluxes of dissolved methane calculated using Fick's law and the high resolution FIS data, with several data points to constrain CH_4 concentrations in the upper FFT. These calculations result in a flux rate into the bottom water that is on the order of $1.4x10^{-3}$ nM $cm^{-2}s^{-1}$. Since the concentration of methane in the bottom water is the outcome of both molecular diffusion and advection from water expression, it is interesting to assess which of these processes may dominate this flux. Based on the diffusive flux estimated using Fick's law and the FFT surface area (6,313,636 m^2), a first order estimation of mass flux of methane from the FFT yielded a value of $2.8x10^6$ moles/year. This can be compared to an estimate of the advective flux through water expression. Assuming 1 m water expression over a year, an FFT surface area of 6,313,636 m^2, and a mean dissolved methane concentration of circa 2305 μM in the upper 1 m of FFT porewater, the advective mass loading would be $1.5x10^7$ nM/year. Based on these 1st order estimates it appears

that advective loading via water expression should dominate as the primary dissolved methane flux to the water column.

Regardless of the mechanism, the fluxes of methane upward in the water column decrease drastically away from the FFT (Figure 2.19). The diffusive fluxes in the hypolimnion are in the range of 10^{-6} nM $cm^{-2}s^{-1}$ and vary by an order of magnitude, and fluxes calculated from the hypolimnion into the metalimnion decrease by another order of magnitude to 10^{-7} nM $cm^{-2}s^{-1}$ and vary to 10^{-8} nM $cm^{-2}s^{-1}$. Comparing the flux rates over the FFT-water interface to the flux rates at the hypolimnion-metalimnion interface, there is a four order of magnitude decrease. This implies that there is a significant removal mechanism active affecting dissolved methane concentrations in the hypolimnion. The variability of fluxes across the hypolimnion suggests that this removal is variably distributed though the water column. The only plausible removal mechanism for methane in this system is consumption by aerobic methane oxidation. The calculated fluxes indicate that this oxidation is occurring both at the interfaces (FFT-water cap, and hypolimnion to metalimnion) but also to varying extents throughout the water column.

2.4.3 – Aerobic Methanotrophy as a Consumption Mechanism in the Water Column

The trends in dissolved methane concentrations and stable isotopic compositions are most consistent with ongoing aerobic methanotrophy occurring in the hypolimnion of BML being responsible for the observed fluxes. The presence of oxygen at 1-2 % saturation precludes further methane production via methanogens in the water column. However, the oxygen present is sufficient to support methane consumption by methanotrophs as they have a very high oxygen affinity and are capable of functioning in a wide range of environments, including very low oxygen (Knief, Kolb, Bodelier, Lipski, & Dunfield, 2006; Kolb, Knief, Dunfield, & Conrad, 2005). The steep decrease observed in dissolved methane concentrations through the

hypolimnion towards the metalimnion coincides with a sharp increase in oxygen saturation, consistent with oxygen consumption at the deepest depths being driven by methane oxidation.

Notably, the trends of methane concentrations with depth observed at the majority of sampling times, and in particular in the high resolution FIS data taken between 7.6 and 9.4m in August 2016, are linear. The linearity of these trends would be consistent with an equilibrium diffusive profile for methane where inputs at the base of hypolimnion are equal to fluxes out at the top. Given the lack of observed methane in the metalimnion, this would imply that methanotrophy at the hypolimnion/metalimnion transition is consuming the methane being released from the FFT. However, there are several factors that challenge this interpretation, first being the assumption of equilibrium conditions. This assumption requires that the rate of diffusion through the bottom 3 meters of the hypolimnion is rapid relative to changes in the input from the FFT. Further, given the temporal variations in the dissolved methane profile observed in the hypolimnion, this equilibration must respond to changes in methane concentrations relatively rapidly. Molecular diffusion is thought to be insufficiently rapid to support this. However, turbulent diffusion could provide such a mechanism. Ebullition of methane from the FFT could provide a mechanism to create turbulent diffusion effects throughout the water column and as such could potentially encourage increased diffusion rates. However, if such mixing were very fast across the whole water column, the methane profile should become well mixed and constant throughout that section. Since this is not the case, the turbulent diffusion has to be occurring on smaller scales that allows preservation of the vertical concentration profile observed. Unfortunately at this point the extent and rate of this process is not currently well constrained in BML. A second challenge is that oxygen consumption experiments at different depths in the water column indicate increasing rates of oxygen consumption moving away from the

metalimnion toward the hypolimnion (Arriaga et al., in preparation). These results indicate that methane removal is occurring throughout the hypolimnion, not only at the top of the hypolimnion. An ongoing, variable rate of oxygen consumption throughout the hypolimnion water column would be expected to divert the concentration profile away from linearity. The fact that this is not observed implies a complex relationship between oxygen consumption and methane concentrations. One potential explanation is that the methane concentration profile is not in fact at equilibrium, but that varying oxygen consumption rates along the profile and making what would be a concave, diffusive profile resemble a linear profile. While these trends support methane oxidation as a primary consumption mechanism, it is clear that numerous factors are influencing profile behaviour, with both consumption and diffusive processes contributing.

Results of stable carbon isotopic analysis of dissolved methane in the hypolimnion were consistent with the occurrence of methanotrophy. The $\delta^{13}C$ of the dissolved methane ranged from -64 to -61‰. The majority of these values were within range of values observed within the FFT with some values becoming more enriched than those observed in the FFT (Figure 2.10). While there was variability in the values a trend of minor isotopic enrichment with decreasing concentrations was observed, consistent with methane oxidation. It must be noted that the shift in isotopic compositions is not large at only ~5‰. However, while larger fractionation of the methane pool has been observed during methane oxidation in many systems, it has been demonstrated that fractionation factor varies with cell density and thus that isotopic fractionation can often not be used to estimate the extent of methanotrophy (Templeton, Chu, Alvarez-Cohen, & Conrad, 2006). The results reported by Templeton et al. (2006) demonstrated that as cell abundances of methanotrophs increased isotopic fractionation of the residual methane pool

decreased. This was proposed to be due to smaller fractionations during methane transport to the site of reaction dominating the expression of the larger fractionation during reaction. Given the relative low cell densities determined for the water column in BML (Chapter 3), it would be expected that the isotopic fractionation associated with methanotrophy would be at the larger scales with alpha values of ~30‰. However, if the transport of the methane to the reaction site of the methanotrophs is limiting this would supress such fractionation. Such transport limited fractionation of methane would be consistent with the isotopic data observed in BML.

2.4.4 – Temporal Variations of Dissolved Methane

Dissolved methane concentration trends over the summer show an increasing build-up in the hypolimnion both years, indicating that oxidative and diffusive export processes in the water column are being outpaced by import processes from the FFT layer. These trends indicate that the import rate from the FFT increases over time, or that the consumption rate in the water column is fixed lower than the FFT import rate and is constantly outpaced once thermal stratification has been established. As a result of the increasing dissolved methane concentrations and constant presence of dissolved oxygen in the hypolimnion through the summer both years, substrate availability is unlikely to be a limiting factor for oxidative processes. This may suggest a fixed rate of methanotrophy, lower than the import rate associated with diffusion and advective loading via porewater expression of settling FFT. The increase in concentration was consistent across both 2015 and 2016, demonstrating similar behavior in build-up suggesting a constant rate of methanotrophy or increasing import from the FFT over the summer months (Figure 2.9).

2.4.5 – Dissolved Methane Concentration & $\delta^{13}C$ Trends – February 2017

Dissolved methane concentrations and isotopic trends observed during the winter indicated similar processes were occurring in the hypolimnion, while an increased source of

dissolved methane to the epilimnion was occurring due to methane bubbles trapped under the ice. Winter epilimnion dissolved methane concentrations exceeded summer observations by three orders of magnitude (165 +/- 10 μM) and were relatively stable through the epilimnion. (Figure 2.16). We proposed that these elevated methane concentrations are the result of dissolution of methane from bubbles trapped under the ice. Ebullition from the FFT of BML was not analyzed during this study, a previous study of MLSB FFT ebullition indicated composition of ~20-60% methane (Holowenko et al., 2000). The consistent concentrations of methane in the surface water imply that diffusive fluxes are low. Methane fluxes downward are negligible when taking error of the methane concentrations into account. The lack of consumption in the winter epilimnion data is noteworthy because the high epilimnion concentrations are concurrent with abundant dissolved oxygen (65% Saturation, 9.6 mg/L). This indicates that despite both reactants being present, aerobic methanotrophy is not occurring in the epilimnion during the winter. This is further supported by the consistent $\delta^{13}C$ values of ~61‰ through the epilimnion (Figure 2.17). The explanation for this lack of aerobic methanotrophy is unknown at this time. One possible explanation is that the methanotrophic bacteria may not be present in the epilimnion. It may be that the methanotrophic microbial communities do not exist in the upper water column of the lake. Though it is possible that the removal of suspended particles via the addition of alum in the fall of 2016 also removed that were attached to the particles and thus they were absent in surface waters over the winter. Ongoing genetic analysis will test this hypothesis. An alternative hypothesis is that the colder temperatures in winter have decreased the rates of methanotrophy. If methanotrophic rates were decreased in the epilimnion due to colder temperatures, even if they were ongoing, it might be that the extent of degradation is very small and insufficient to be recognized based on the concentration or isotopic profiles. However, as

described below, there is evidence of aerobic methanotrophy ongoing in the hypolimnion at similar temperatures in the winter.

The hypolimnion winter concentration profile exhibited a linear decrease upwards from the FFT interface to the metalimnion, decreasing from ~250 μM at 9m to ~140 μM at 6.5m depth (Linear Regression (r^2) = 0.91). This linear decrease observed through the hypolimnion is consistent with decreasing summer trends observed, indicating continued methanotrophic consumption in this layer during winter. This observation is also supported by 1st order diffusive flux calculations (Figure 2.19). Diffusive fluxes across the FFT/water interface were comparable to summer values at 10^{-3} nM $cm^{-2}s^{-1}$. Methane fluxes within the hypolimnion were likewise comparable with summer data (10^{-6} nM $cm^{-2}s^{-1}$), decreasing with increasing distance from the FFT-Water interface. The maximum dissolved methane concentrations were higher for the winter samples than the summer, potentially indicating slower rates of methane oxidation. However, this might also be the result of longer time elapsing between fall turnover and sampling, enabling greater buildup of methane concentrations to occur. The $\delta^{13}C$ values further support active methanotrophy within the hypolimnion layer, displaying similar enrichment trends as seen in the summer. The $\delta^{13}C$ values display a minor enrichment of ~5‰ occurring from the interface to the 6.5m depth (Figure 2.17). Notably, the $\delta^{13}C$ values relationship to concentration is inverse to the observed trends in summer, which showed dissolved methane at the top of the hypolimnion being the most enriched. The winter samples show increased enrichment coinciding with the highest concentration samples closest to the FFT-water interface (Figure 2.18). This trend is unexpected as it would be expected that the greatest isotopic enrichment would be observed for the most degraded samples. One potential explanation for this observation is that the majority of methane oxidation is taking place at the FFT-Water interface (consistent with the

greatest decrease in fluxes) and that these samples are capturing the remnant methane from this degradation. The methane observed higher in the water column may be either due to variations in isotopic fractionation due to variations in cell densities and/or reaction rates as previously suggested for the summer data. It may also represent inputs of methane due to dissolution from bubbles or another mechanism where methane bypasses the zone of oxidation. Further work will be required in order to explain these observations more fully.

2.5 - Conclusions

The results presented from this study strongly suggest methanotrophic bacteria are present and actively consuming dissolved methane and oxygen in the water column of BML, most actively in the hypolimnion. The FFT layer has been identified as a saturated source zone of dissolved methane via fermentative methanogenesis. Transfer of this dissolved methane to the water column is dominated by advection via FFT porewater expression, over molecular diffusion, though contributions from advection by interface mixing and dissolution from bubbles may also be occurring. Dissolved methane was primarily restricted to the hypolimnion which maintained sub-oxic conditions throughout the year, with methane still being detected around trace concentrations in the metalimnion and epilimnion. Dissolved methane concentrations decreased linearly from ~150 μM at the interface to trace concentrations at the metalimnion over a steeply increasing dissolved oxygen gradient. Methane fluxes also decreased by four orders of magnitude over this interval, implying aerobic methanotrophy occurring as a significant methane sink. This decrease in concentration and fluxes was accompanied by a minor enrichment in associated $\delta^{13}C$ values of ~3‰. A larger fractionation should be observed if methanotrophy was the sole mechanism removing dissolved methane, leading to the conclusion other factors are influencing the profile. The same decreasing concentration trends were observed in the

hypolimnion during ice cover and winter stratification, accompanied by a similar minor enrichment of ~5‰ that was observed at the FWI. This implied that the greatest consumption is occurring at this point, despite concentrations being the highest. Elevated concentrations of methane in the epilimnion in the winter were attributed to dissolution from gas bubbles trapped under the ice. The lack of consumption of dissolved methane in the upper water column may be a result of the removal of bacteria due to alum addition in the fall of 2016, or to differentiate distributions of methanotrophic organisms, or to slower rates of methanotrophy due to lower temperatures being outpaced by influx due to bubble dissolution. This study provides evidence suggesting that methanotrophic bacteria are actively metabolizing in the hypolimnion of this unique reclamation system, actively reduced oxygen availability. Accompanying OCR experiments further support methanotrophic consumption linked to decreasing dissolved oxygen concentrations over time. As dissolved oxygen is critical for biodegradation of various compounds present in OSPW and FFT, understanding active biogeochemical cycling of dissolved methane through this study's results helps understand oxygen consumption in the first full-scale end pit lake related to oil sands reclamation.

2.6 – References

Alberta Energy Regulator. (2016). Executive Summary, ST 98-2016: Alberta's Energy Reserves 2015 & Supply/Demand Outlook 2016-2025, 8. Retrieved from http://www1.aer.ca/st98/data/executive_summary/ST98-2016_Executive_Summary.pdf

Allen, E. W. (2008). Process water treatment in Canada's oil sands industry: I. Target pollutants and treatment objectives. *Journal of Environmental Engineering and Science*, *7*(2), 123–138. https://doi.org/10.1139/S07-038

Bordenave, S., Kostenko, V., Dutkoski, M., Grigoryan, A., Martinuzzi, R. J., & Voordouw, G.

(2010). Relation between the activity of anaerobic microbial populations in oil sands tailings ponds and the sedimentation of tailings. *Chemosphere, 81*(5), 663–668. https://doi.org/10.1016/j.chemosphere.2010.07.058

Canadian Association of Petroleum Producers. (2015). Crude Oil, (June), 1–9.

Chen, M., Walshe, G., Chi Fru, E., Ciborowski, J. J. H., & Weisener, C. G. (2013). Microcosm assessment of the biogeochemical development of sulfur and oxygen in oil sands fluid fine tailings. *Applied Geochemistry, 37*, 1–11. https://doi.org/10.1016/j.apgeochem.2013.06.007

Chi Fru, E., Chen, M., Walshe, G., Penner, T., & Weisener, C. (2013). Bioreactor studies predict whole microbial population dynamics in oil sands tailings ponds. *Applied Microbiology and Biotechnology, 97*(7), 3215–3224. https://doi.org/10.1007/s00253-012-4137-6

Dompierre, K. A., Lindsay, M. B. J., Cruz-Hernandez, P., & Halferdahl, G. M. (2016). Initial geochemical characteristics of fluid fine tailings in an oil sands end pit lake. *Science of the Total Environment, 556*, 196–206. https://doi.org/10.1016/j.scitotenv.2016.03.002

Duan, Z., & Mao, S. (2006). A thermodynamic model for calculating methane solubility, density and gas phase composition of methane-bearing aqueous fluids from 273 to 523 K and from 1 to 2000 bar. *Geochimica et Cosmochimica Acta, 70*(13), 3369–3386. https://doi.org/10.1016/j.gca.2006.03.018

Eby, P., Gibson, J. J., & Yi, Y. (2015). Suitability of selected free-gas and dissolved-gas sampling containers for carbon isotopic analysis. *Rapid Communications in Mass Spectrometry, 29*(13), 1215–1226. https://doi.org/10.1002/rcm.7213

Giesy, J. P., Anderson, J. C., & Wiseman, S. B. (2010). Alberta oil sands development. *Pnas, 107*(3), 951–952. https://doi.org/10.1073/pnas.0912880107

Government of Alberta. (2013). Facts and Statistics. Retrieved February 7, 2017, from

http://www.energy.alberta.ca/OilSands/791.asp

Hanson, R. S., & Hanson, T. E. (1996). Methanotrophic Bacteria. *Microbiological Reviews*, *60*(2), 439–471. https://doi.org/

Holowenko, F. M., MacKinnon, M. D., & Fedorak, P. M. (2000). Methanogens and sulfate-reducing bacteria in oil sands fine tailings waste. *Canadian Journal of Microbiology*, *46*(10), 927–937. https://doi.org/10.1139/w00-081

Knief, C., Kolb, S., Bodelier, P. L. E., Lipski, A., & Dunfield, P. F. (2006). The active methanotrophic community in hydromorphic soils changes in response to changing methane concentration. *Environmental Microbiology*, *8*(2), 321–333. https://doi.org/10.1111/j.1462-2920.2005.00898.x

Kolb, S., Knief, C., Dunfield, P. F., & Conrad, R. (2005). Abundance and activity of uncultured methanotrophic bacteria involved in the consumption of atmospheric methane in two forest soils. *Environmental Microbiology*, *7*(8), 1150–1161. https://doi.org/10.1111/j.1462-2920.2005.00791.x

Penner, T. J., & Foght, J. M. (2010). Mature fine tailings from oil sands processing harbour diverse methanogenic communities. *Canadian Journal of Microbiology*, *56*(6), 459–70. https://doi.org/10.1139/w10-029

Schonheit, P., Keweloh, H., & Thauer, R. K. (1991). Factor F420 degradation in Methanobacterium thermoautotrophicum during exposure to oxygen. *Biochemistry*, *266*(2), 14151–14154. Retrieved from http://www.jbc.org/content/266/22/14151.short

Siddique, T., Fedorak, P. M., & Foght, J. M. (2006). Biodegradation of Short-Chain n -Alkanes in Oil Sands Tailings under Methanogenic Conditions. *Environmental Science & Technology*, *40*(17), 5459–5464. https://doi.org/10.1021/es060993m

Siddique, T., Fedorak, P. M., Mackinnon, M. D., & Foght, J. M. (2007). Metabolism of BTEX and naphtha compounds to methane in oil sands tailings. *Environmental Science and Technology*, *41*(7), 2350–2356. https://doi.org/10.1021/es062852q

Siddique, T., Penner, T., Semple, K., & Foght, J. M. (2011). Anaerobic biodegradation of longer-chain n-alkanes coupled to methane production in oil sands tailings. *Environmental Science and Technology*, *45*(13), 5892–5899. https://doi.org/10.1021/es200649t

Stasik, S., Loick, N., Knöller, K., Weisener, C., & Wendt-Potthoff, K. (2014). Understanding biogeochemical gradients of sulfur, iron and carbon in an oil sands tailings pond. *Chemical Geology*, *382*, 44–53. https://doi.org/10.1016/j.chemgeo.2014.05.026

Syncrude Canada Ltd. (2016). *Sustainability Report*.

Templeton, A. S., Chu, K. H., Alvarez-Cohen, L., & Conrad, M. E. (2006). Variable carbon isotope fractionation expressed by aerobic CH4-oxidizing bacteria. *Geochimica et Cosmochimica Acta*, *70*(7), 1739–1752. https://doi.org/10.1016/j.gca.2005.12.002

Westcott, F., & Watson, L. (2007). End Pit Lakes Technical Guidance Document. Prepared by Clearwater Environmental Consultants Inc. for the Cumulative Environmental Management Association (CEMA) End Pit Lakes Subgroup., 51.

Whiticar, M. J. (1999). Carbon and hydrogen isotope systematics of bacterial formation and oxidation of methane. *Chem. Geol.*, *161*(1–3), 291–314. https://doi.org/10.1016/S0009-2541(99)00092-3

2.7 – Figures

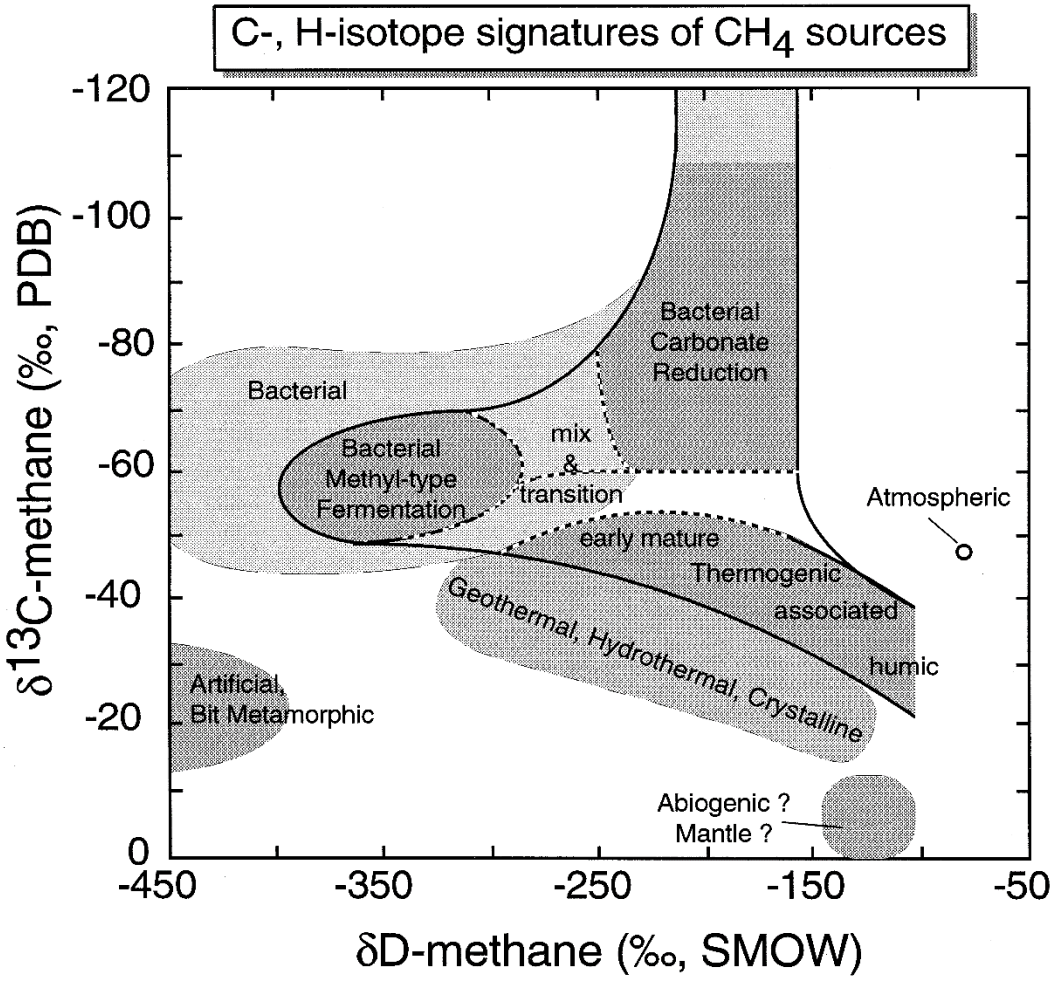

Figure 2.1: Determination of methane source pathway by stable carbon and hydrogen isotope cross-plotting (Whiticar, 1999).

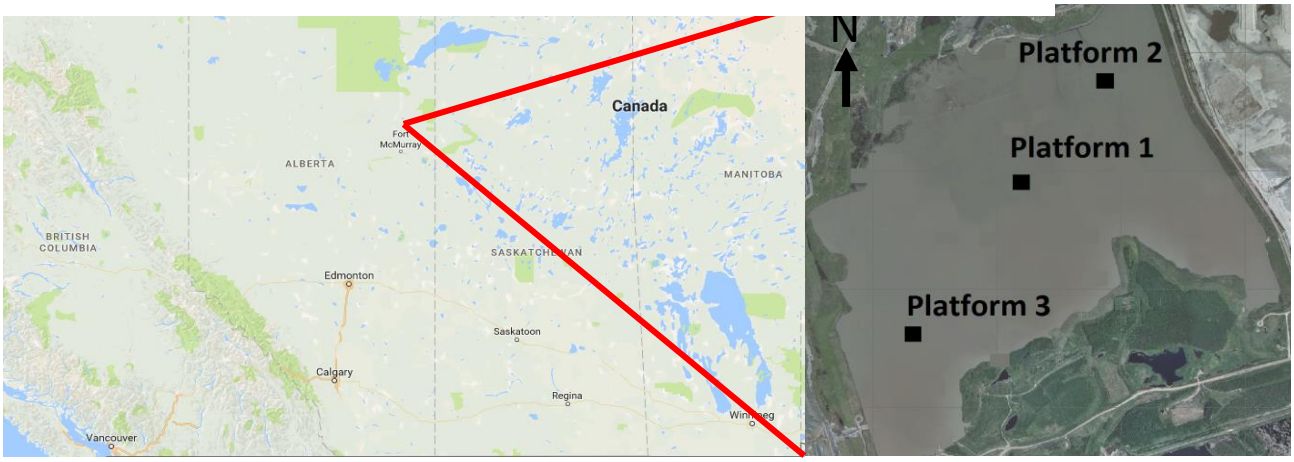

Figure 2.2: Location of BML in northern Alberta, Canada on the left. Satellite image of BML on the right, with sampling platforms labelled.

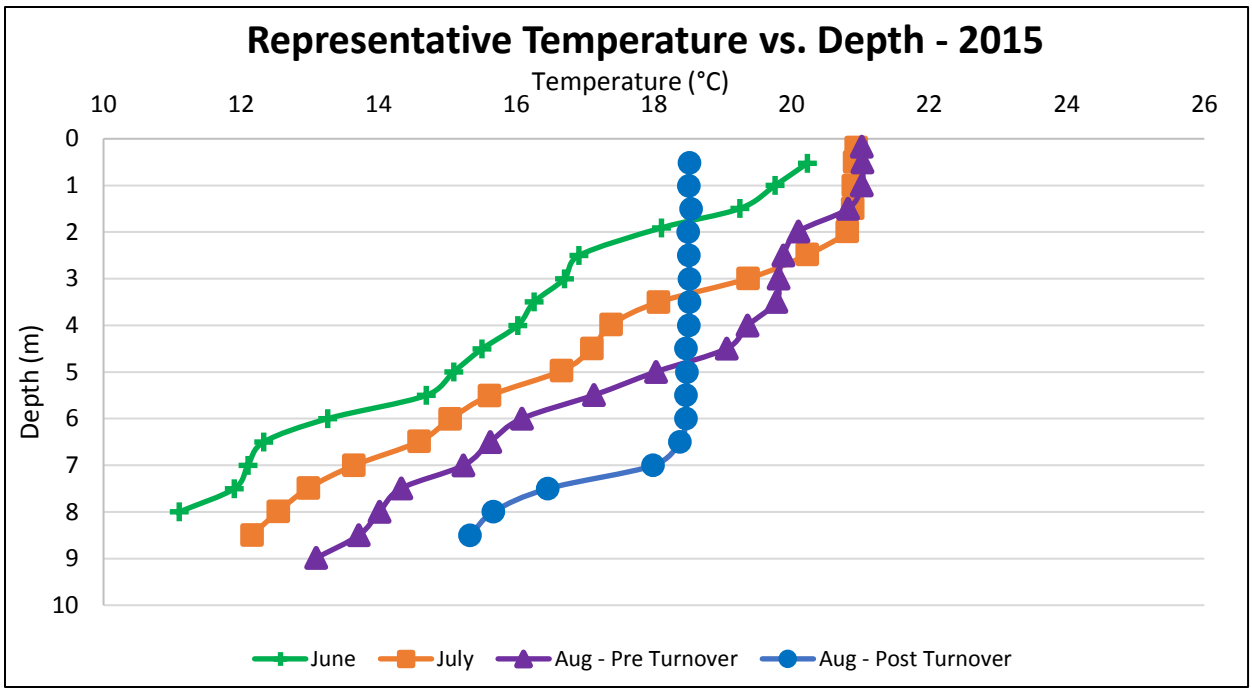

Figure 2.3: Representative temperature profiles versus depth over 2015 sample months.

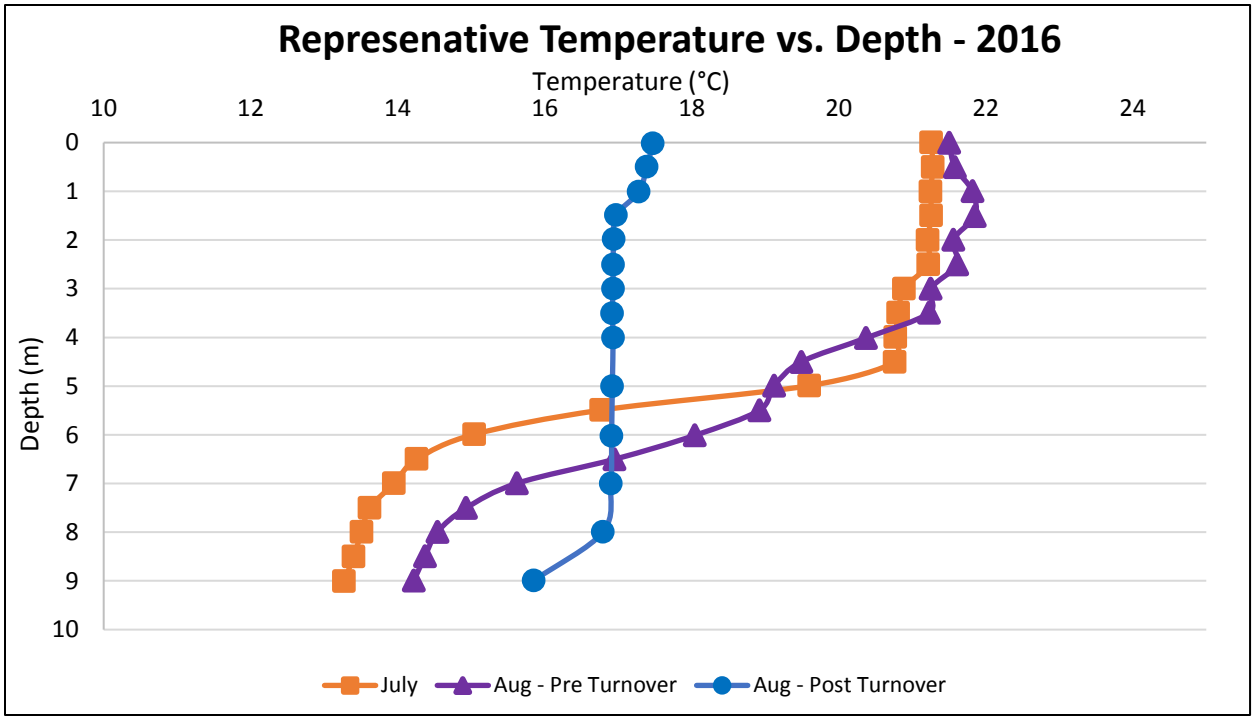

Figure 2.4: Representative temperature profiles versus depth over 2016 sample months.

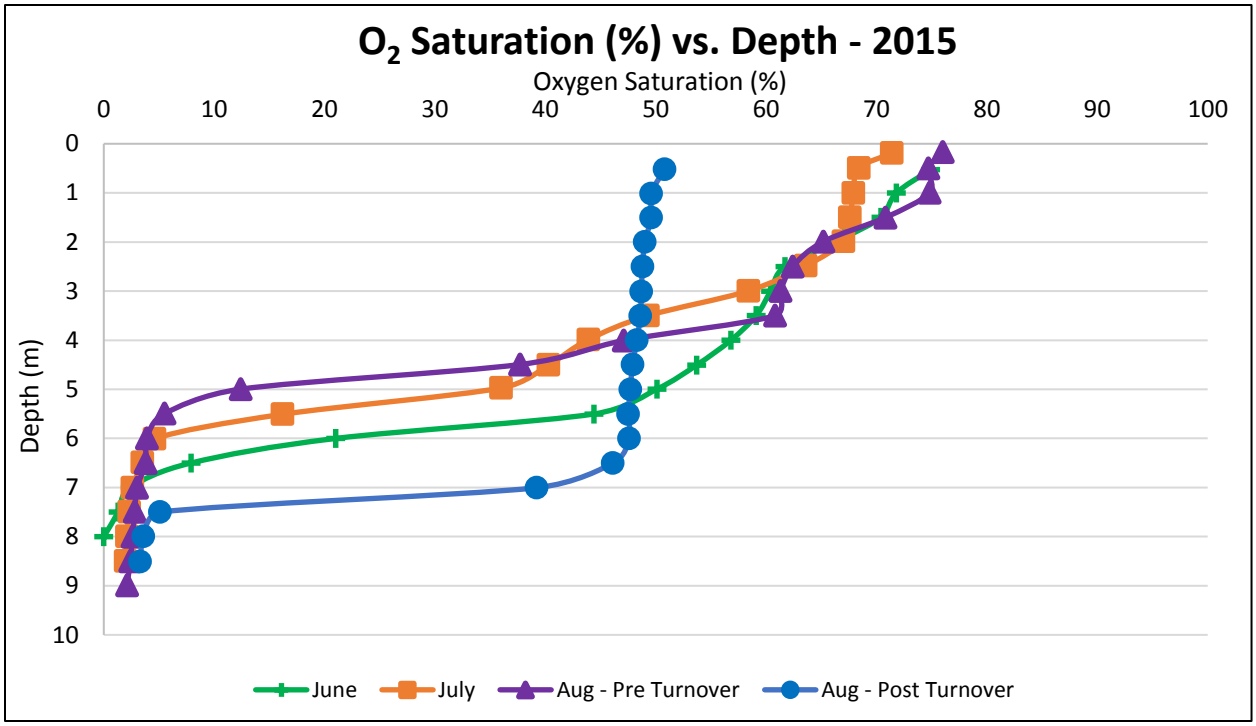

Figure 2.5: Representative O_2 saturation (%) profiles versus depth occurring over 2015.

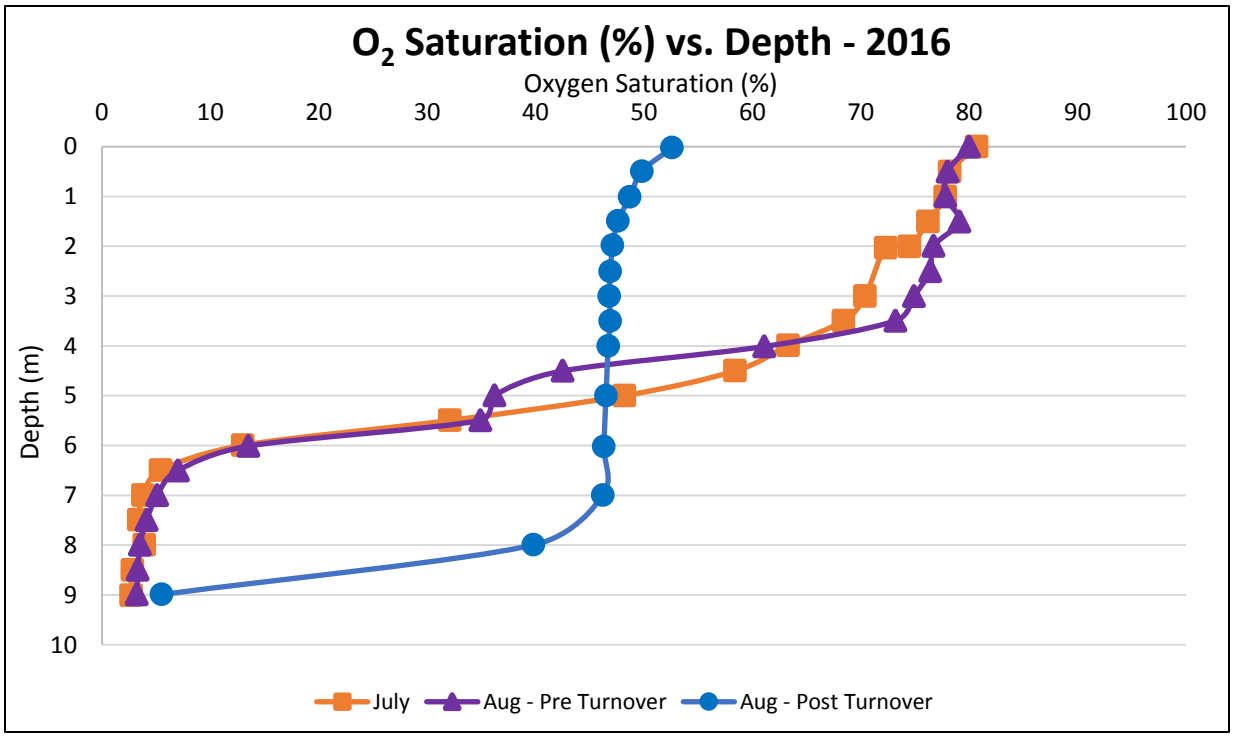

Figure 2.6: Representative O_2 saturation (%) versus depth trends occurring over 2016.

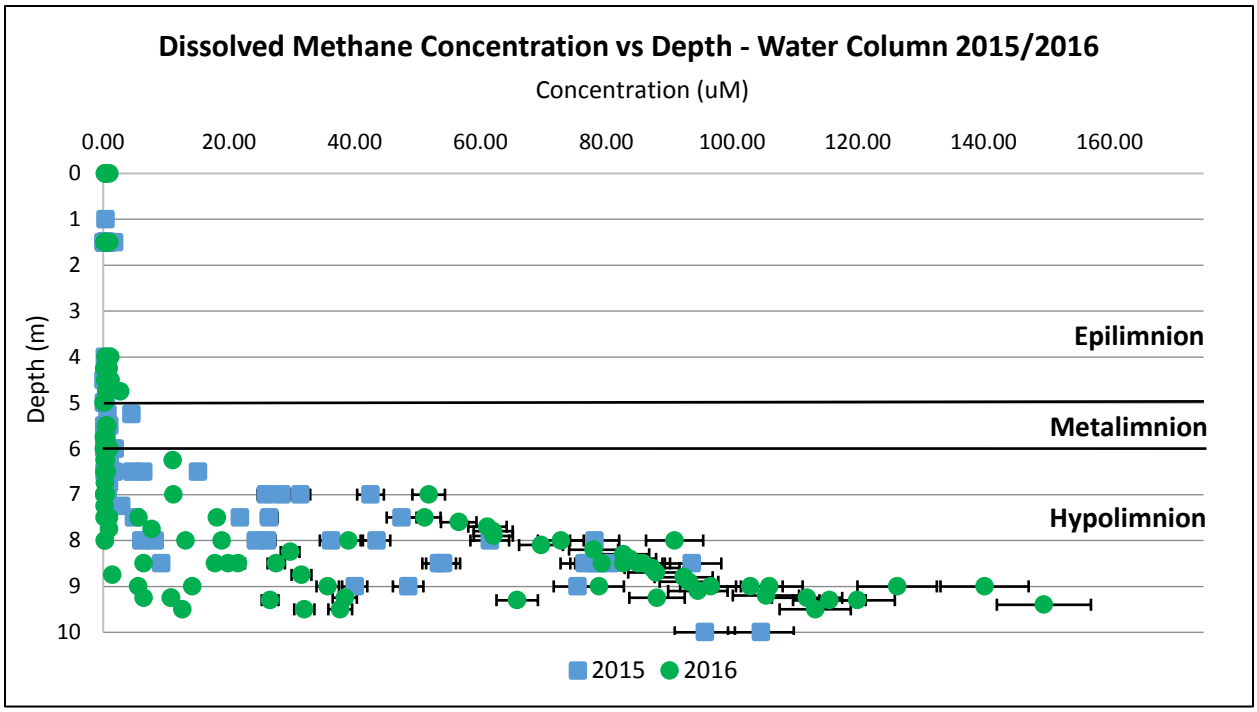

Figure 2.7: Dissolved methane concentrations across all depths from 2015 and 2016, showing a steep linear concentration increase with increasing depth in the hypolimnion.

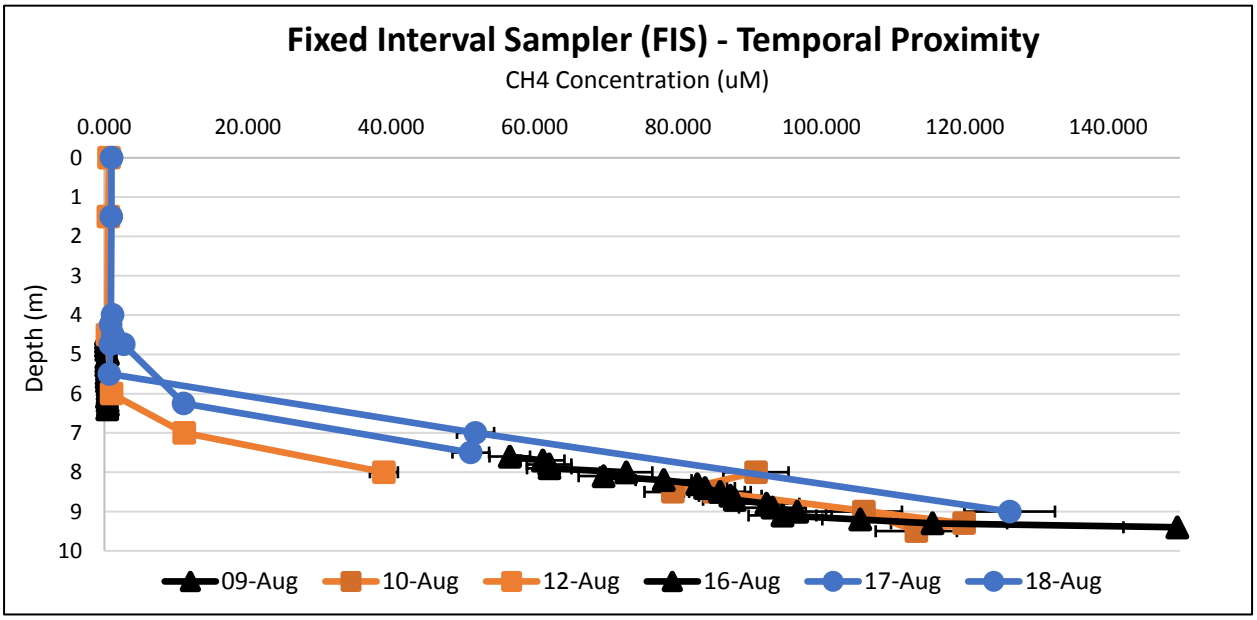

Figure 2.8: Dissolved methane concentrations versus depth. Regular methane bottles (blue circles, orange squares) sampled temporally around the FIS hypolimnetic samples (black triangles) plotted to validate FIS sampling method and demonstrate consistency between methods.

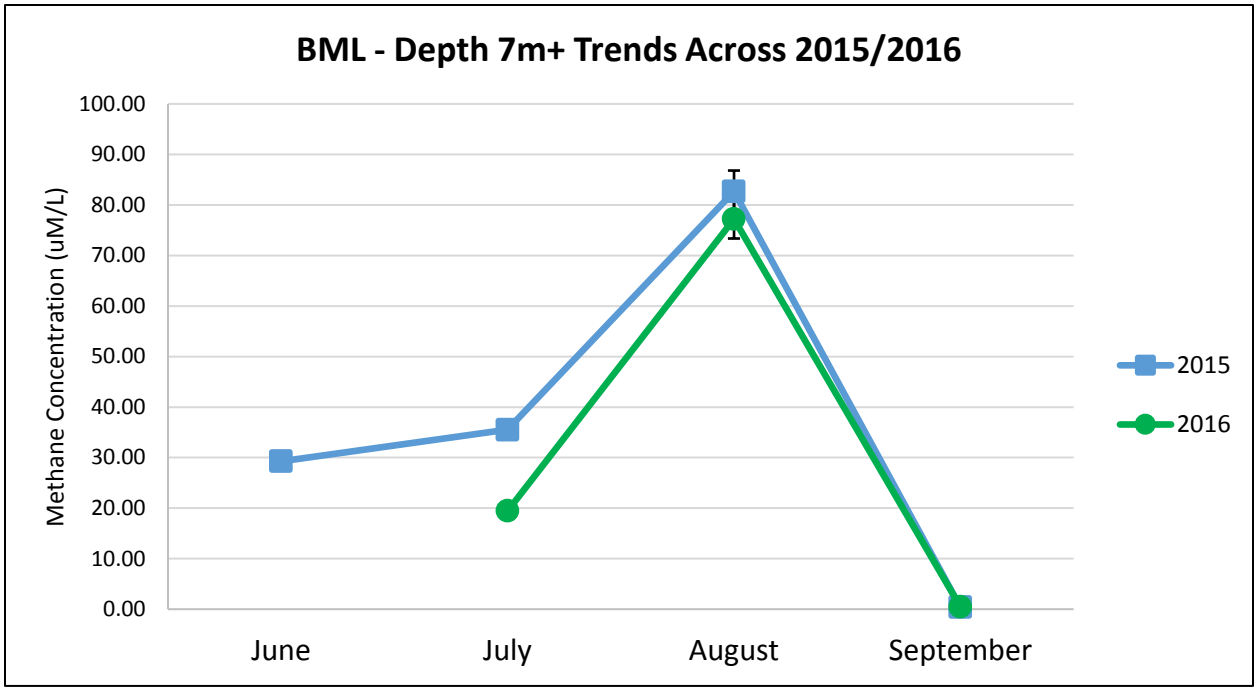

Figure 2.9: Average dissolved methane concentrations of hypolimnetic samples (7m+ depth) across 2015 and 2016.

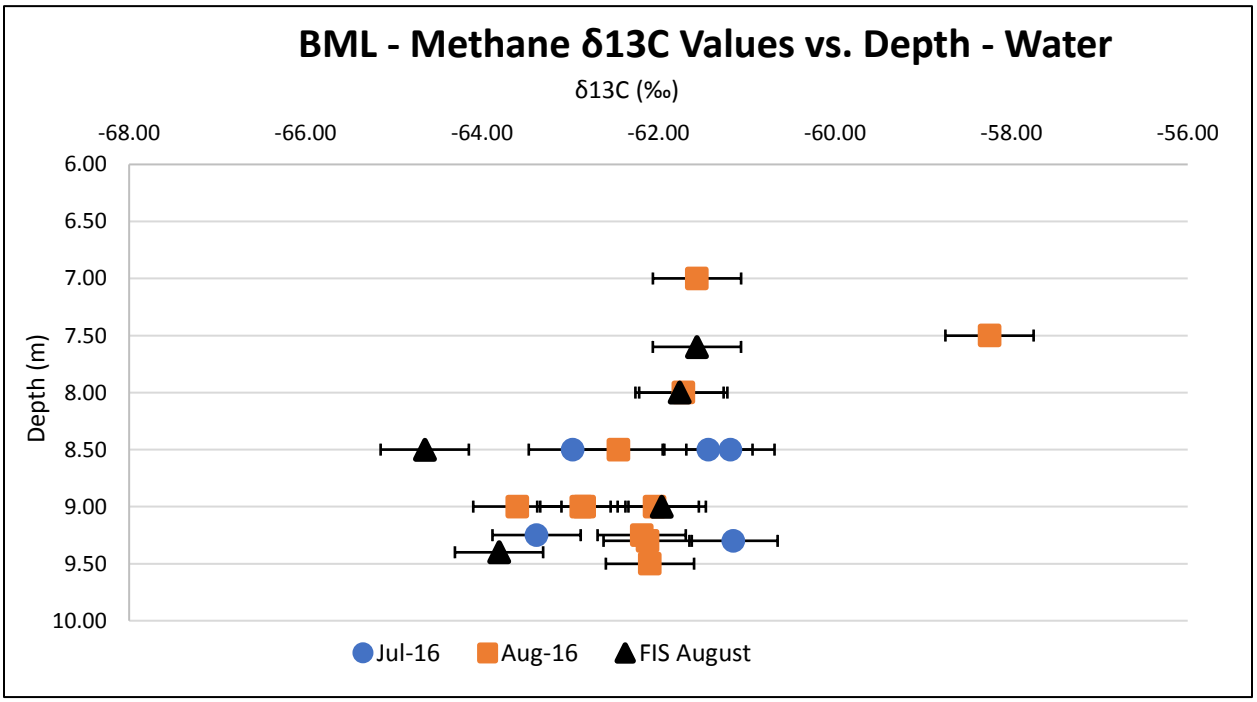

Figure 2.10: Dissolved methane $\delta^{13}C$ values showing no correlation with depth between months. Multiple samples of same depth vary over weekly samples.

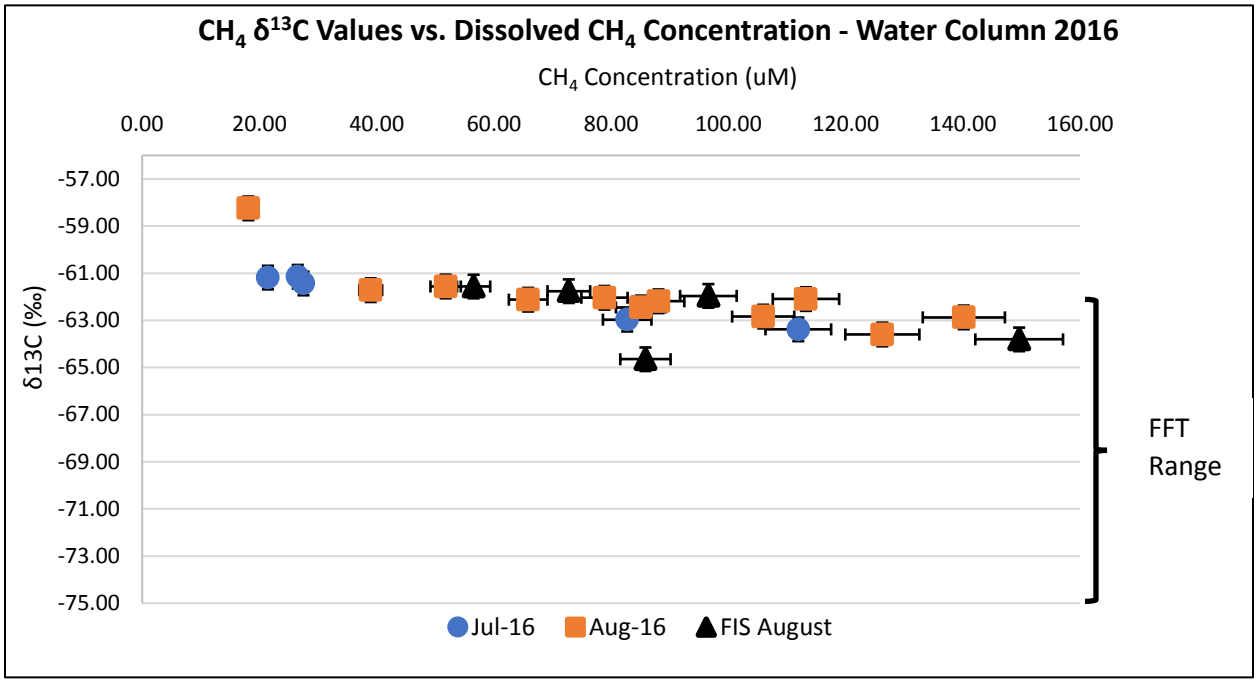

Figure 2.11: Dissolved methane concentrations versus δ13C values in hypolimnetic samples with concentration above 20 µM. FFT range of isotope values indicated on the side.

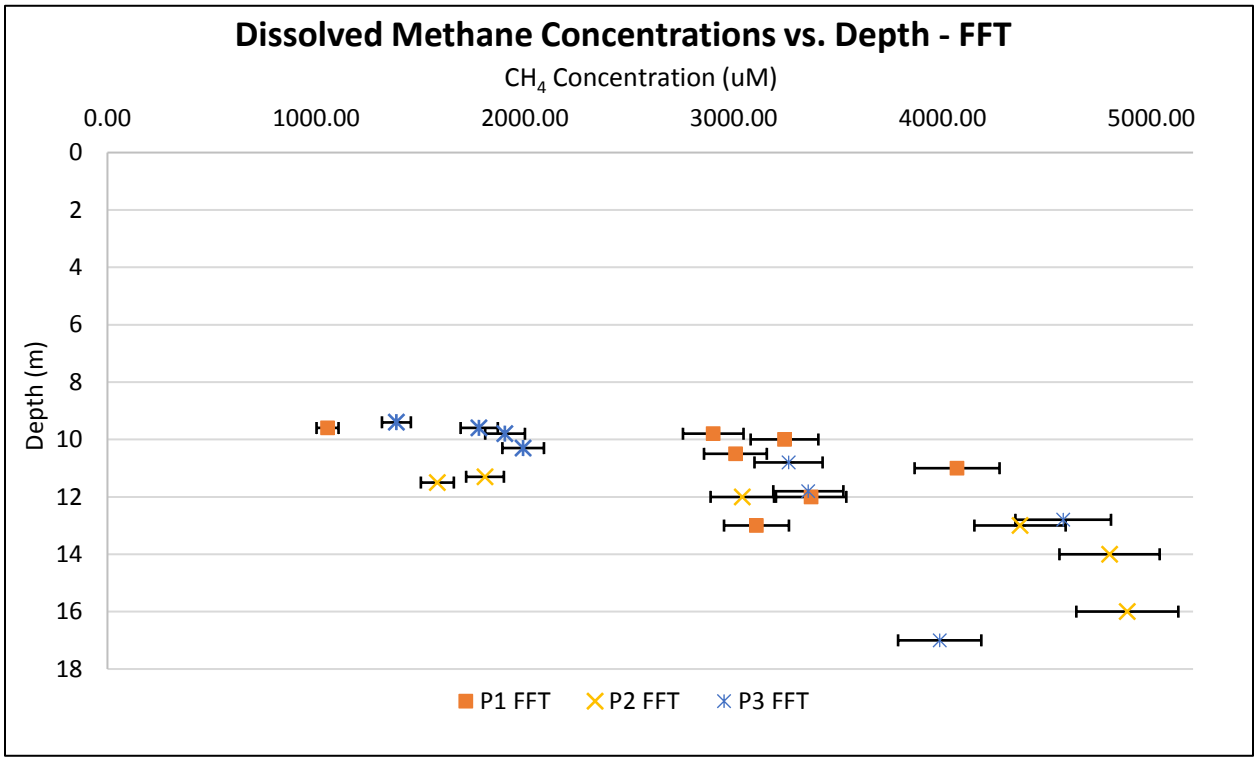

Figure 2.12: Dissolved methane concentrations of FFT samples versus depth. FFT-Water interface at 9.5m depth where shallowest samples occur.

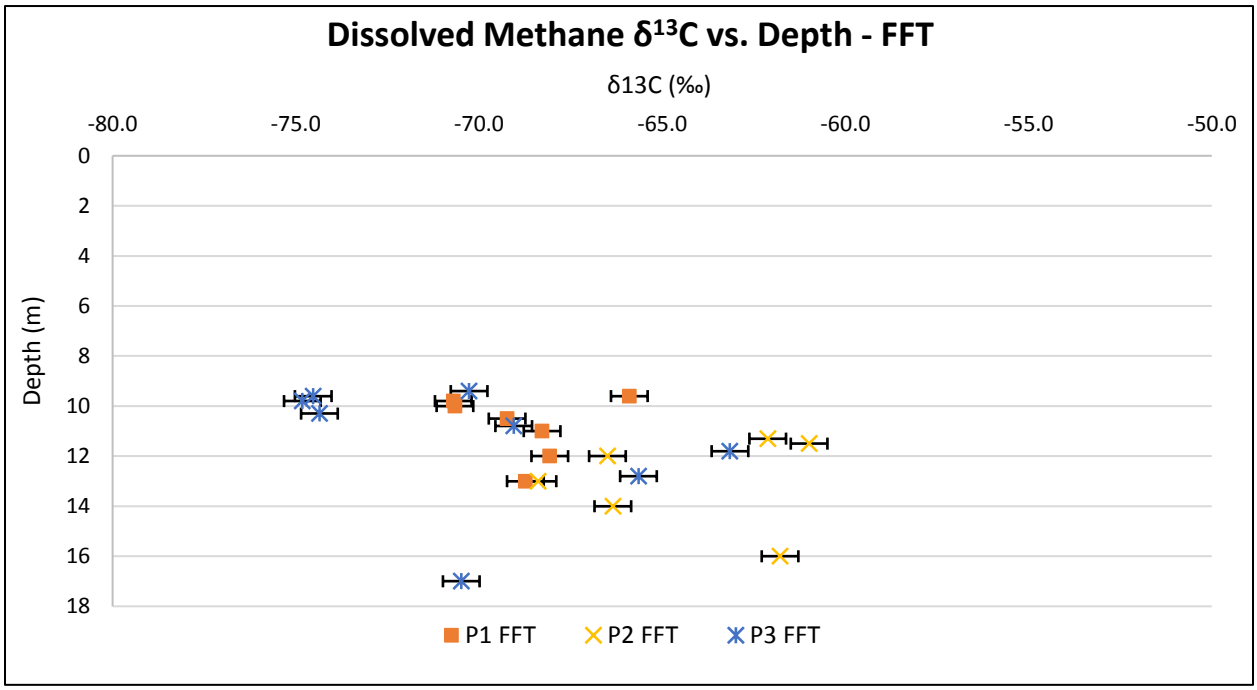

Figure 2.13: $\delta^{13}C$ values of FFT samples versus depth. FFT-Water interface at 9.5m depth where shallowest samples occur.

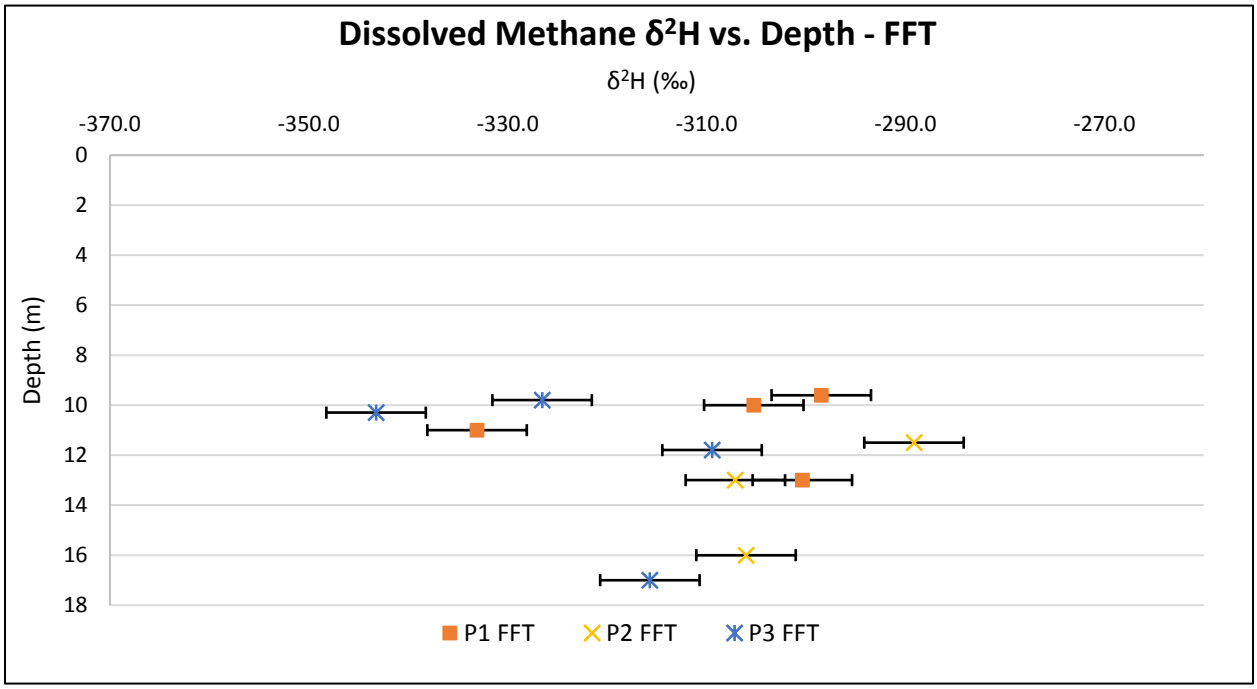

Figure 2.14: $\delta^{2}H$ values of FFT samples versus depth. FFT-Water interface at 9.5m depth where shallowest samples occur.

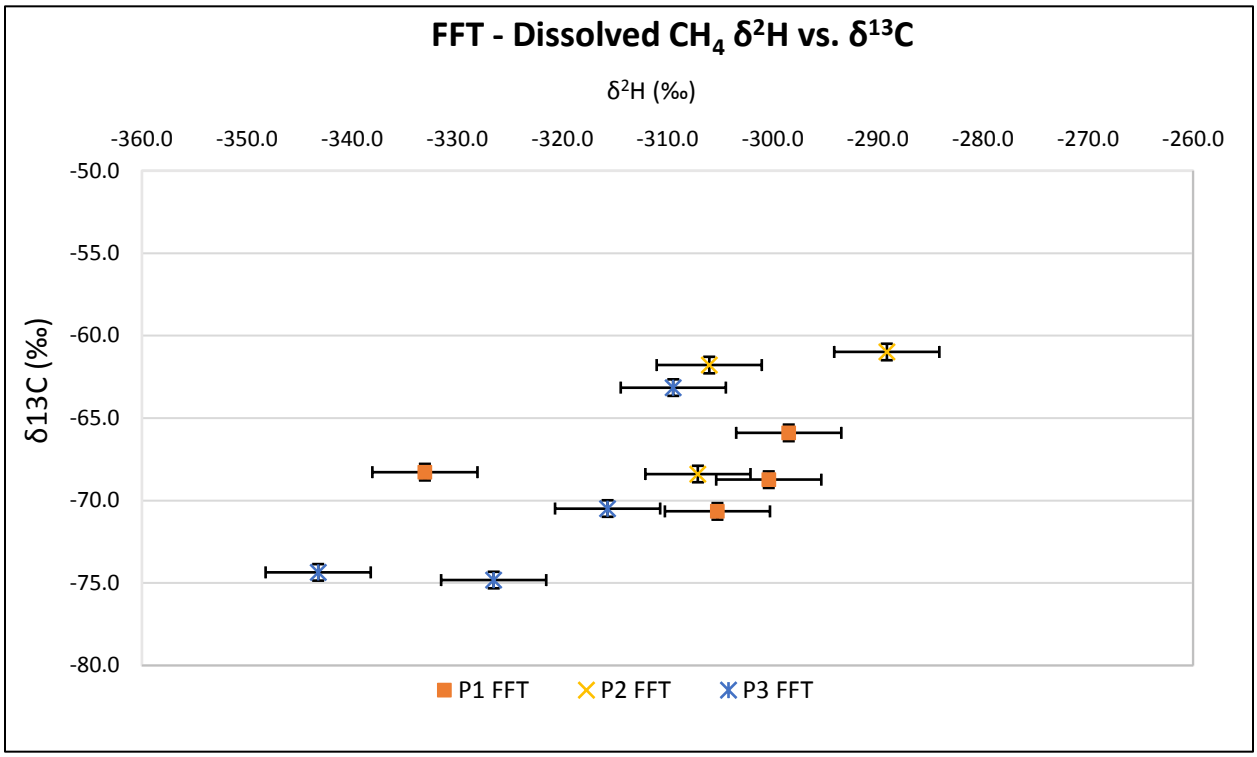

Figure 2.15: Cross plot of $\delta^{13}C$ / $\delta^{2}H$ values of dissolved methane in the FFT, showing enrichment trends across both parameters.

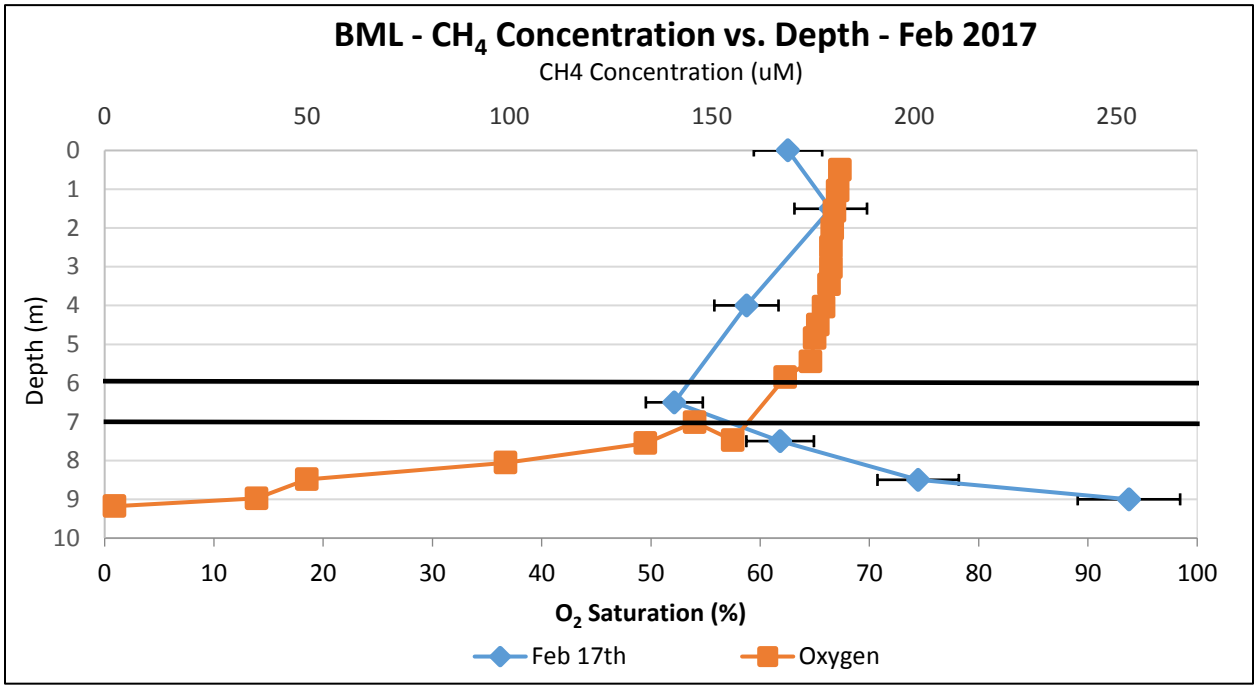

Figure 2.16: Dissolved methane and corresponding oxygen profiles for February 2017 sampling, conducted on BML months after full lake ice cover established.

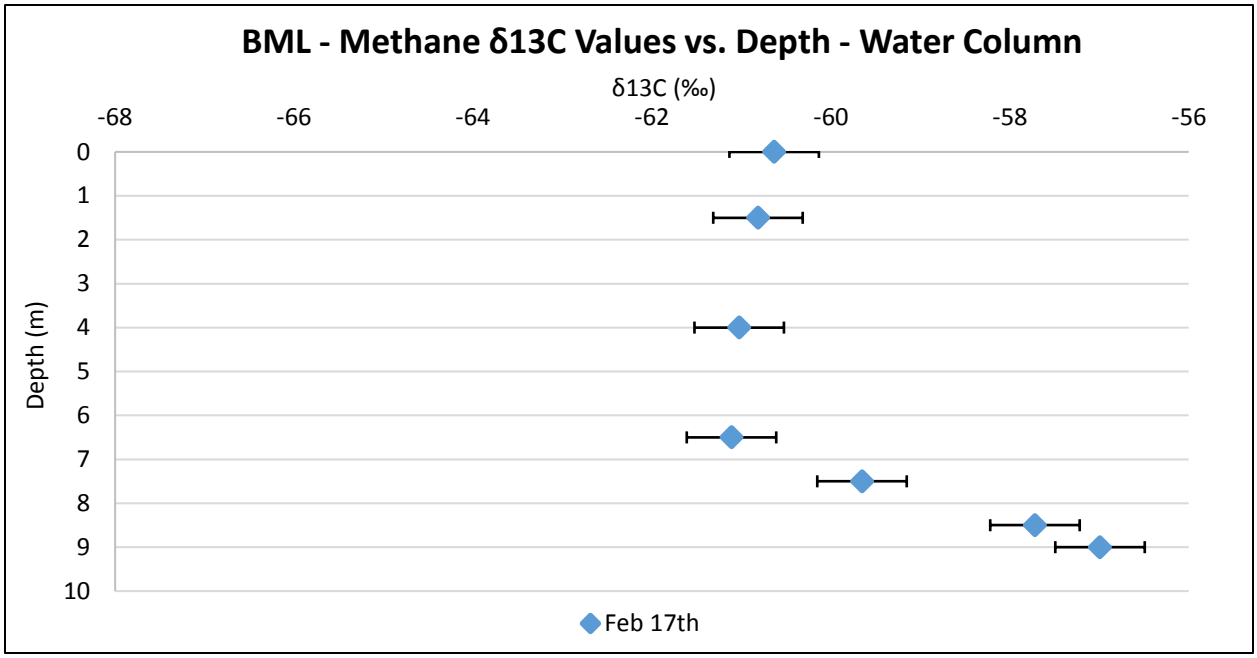

Figure 2.17: $\delta^{13}C$ values of February 2017 samples versus depth, displaying an enrichment of $\delta^{13}C$ with increasing depth.

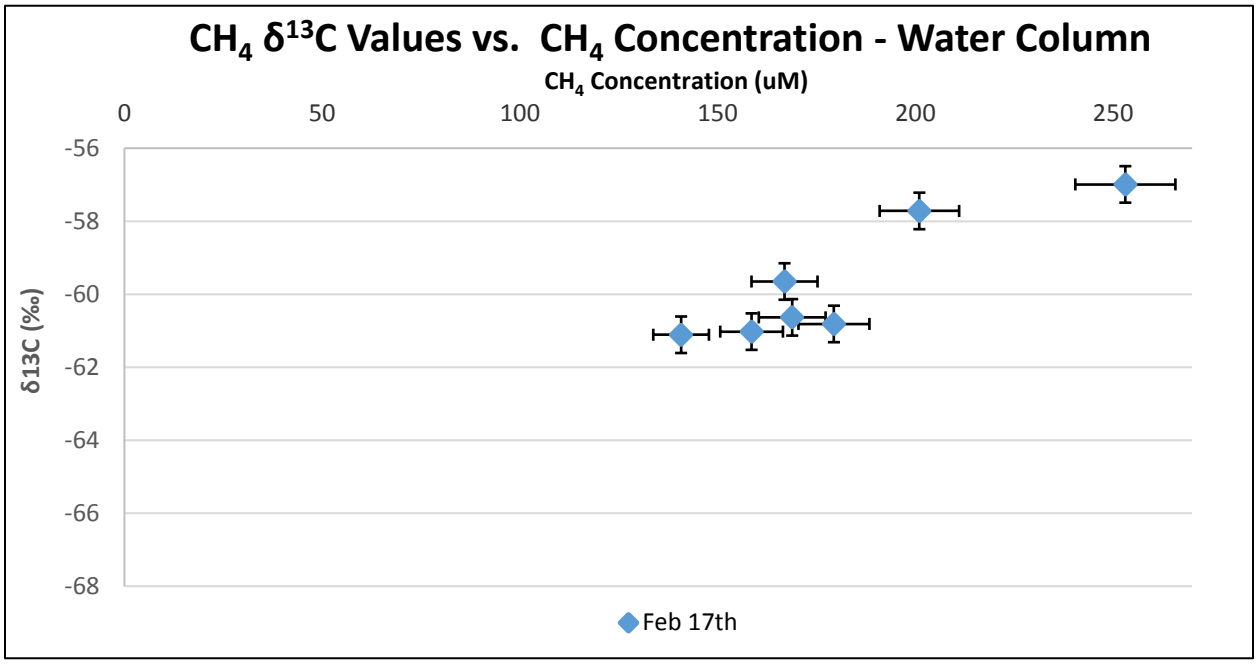

Figure 2.18: Dissolved methane concentration vs $\delta^{13}C$ values of February 2017 samples. Enrichment of $\delta^{13}C$ with increasing concentration.

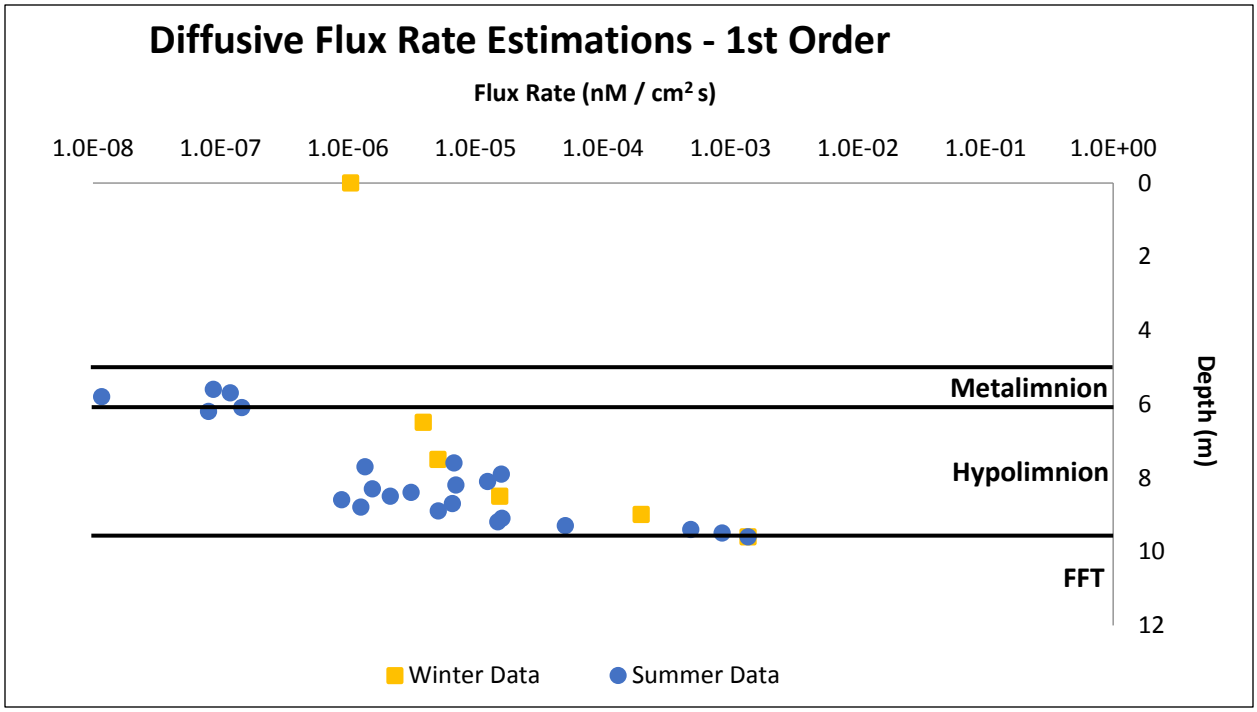

Figure 2.19: Preliminary diffusive flux calculations using dissolved methane profiles. Notable order of magnitude drops over interface zones for summer data, magnitude drop across hypolimnion in the winter data.

Chapter 3

TRANSFER OF DEPLETED DISSOLVED METHANE $\delta^{13}C$ SIGNATURES INTO PLFA SUPPORTING ACTIVE METHANOTROPHY IN BASE MINE LAKE

Manuscript in preparation for submission to Applied Geochemistry

Goad, C.[1], Slater G.F[1], Risacher, F. [1], Morris, P. [1], Arriaga, D.[1], Warren, L.A.[2]

[1]School of Geography and Earth Sciences, McMaster University, Hamilton, Ontario, Canada

[2]Department of Civil Engineering, University of Toronto, Toronto, Ontario, Canada

Abstract

Base Mine Lake (BML) is the first full scale demonstration of water-capped Fluid Fine Tailings (FFT) reclamation. Over two field seasons in 2015 and 2016 the water column of BML had dissolved methane concentrations ranging between trace (~1μM) concentrations in the surface waters, to ~140μM towards the FFT-water interface. This study investigated the microbial community present in the water column of BML over these two years via phospholipid fatty acid (PLFA) biomarker and stable carbon isotope analysis to determine if methanotrophic bacteria are present and actively metabolizing microbial methane released from the methanogenic FFT source zone. In 2015 cellular biomass estimates based on PLFA concentrations were 6 to 7 $x10^5$ cells/mL in June and July and increased to 2 x 10^6 cells/mL in August/Sept. In 2016, cellular biomass estimates in July 2016 were consistent as the previous year (5 $x10^5$ cells/mL) but decreased to 3.8 $x10^5$ in August/September. Epilimnion C18:1s and C16:0 $\delta^{13}C$ values of -32 +/- 0.5‰ and -35 +/- 0.5 ‰ were comparable with expectation for metabolism of DOC carbon sources with values of circa -30‰. The $\delta^{13}C$ of pooled C16:1 PLFA which would include the methanotroph biomarker C16:1ω8c were highly depleted (-60 to -40 ‰) in the hypolimnion, and somewhat depleted in the epilimnion (-46 to -40 ‰), indicating of utilization of methane derived carbon. The C16:0 PLFA was likewise depleted in the hypolimnion (-45 to -35 ‰) indicating that methanotrophs either comprised a greater proportion of the microbial community or that there was transfer of methane derived carbon to the rest of the microbial community. The observation of increased late summer PLFA abundances in the hypolimnion, concurrent with increased proportions of methanotroph biomarker PLFA (C16:1, C14:0) and depleted isotopic compositions directly demonstrates methanotrophy is a fundamental driver of microbial carbon cycling in the hypolimnion of BML. The $\delta^{13}C$ values of

PLFA in the epilimnion indicate that other carbon sources, such as DOC that may include petroleum hydrocarbons become more important in the epilimnion. Continuing research is focussed on monitoring microbial community development and corresponding $\delta^{13}C$ values for potential methanotroph presence in the water column as lake development continues.

3.1 – Introduction

3.1.1 – FFT Reclamation and Methane Biogeochemical Cycling

The northern AOSR contains up to 1.8 trillion barrels of bitumen, making it the 3rd largest oil reserves globally, encompassing a total area of 142,200 km^2 (Alberta Energy Regulator (AER), 2016). In 2015, production reached 2.4 million barrels/day (b/d), with projections aiming for 3.7 million b/d by 2030 (Canadian Association of Petroleum Producers, 2015). Extracting bitumen from the crude oil sands mixture generates a tailings slurry composed of Oil Sands Process Water (OSPW), sand, un-recovered bitumen, and fine solids which settles and de-waters over time to form Fluid Fine Tailings (FFT) (Bordenave et al., 2010; Holowenko, MacKinnon, & Fedorak, 2000). The first full-scale demonstration involving the wet-reclamation of FFT has been created through use of End Pit Lake (EPL) technology. Base Mine Lake (BML) was commissioned to allow densification of the FFT, biodegradation of organic compounds in OSPW compounds expelled through FFT densification, and reclaim the landscape to a biologically productive lake environment. FFT deposition began in 1994 and concluded in 2012 with a total FFT depth of 48m. A 7m water cap was placed on top of the FFT by the end of 2013 (Dompierre, Lindsay, Cruz-Hernandez, & Halferdahl, 2016). Over time, the FFT has dewatered and the bottom of the lake has become deeper, resulting in an approximate 10m water cap by the end of 2016.

Previous studies using BML FFT have shown a shift in microbial community composition from bacterial dominance towards archaeal dominance as redox zonation occurs after FFT deposition has concluded (Chi Fru et al., 2013). These archaeal dominated microbial communities have been demonstrated to be predominantly composed of methanogens. Methanogens are obligate anaerobes that can metabolize either CO_2 (carbonate reduction) or small methyl-based compounds (fermentation) to methane, with previous work on the BML water column and FFT porewater indicating that production in BML is via fermentation pathways (Previous thesis chapter). Due to the residual organic compounds present in the OSPW of the FFT porewater, constant biodegradation is thought to create substrates required for methanogenic archaea to utilize, resulting in a large production of methane to occur in the FFT layer underneath the water column (Siddique et al., 2006, 2011). In the Mildred Lake Settling Basin (MLSB) these conditions lead to the saturation of dissolved gasses in the FFT and the formation of gas bubbles consisting of ~20 to 60% methane which are transported into the water column via ebullition, contributing to the dissolved methane concentrations alongside advection of saturated porewater from FFT settling and diffusion (Holowenko et al., 2000). The release and transport of this methane has a large influence on the dissolved oxygen (DO) profile of the water column, as methanotrophic bacteria consume oxygen at a rate of 2 mols per 1 mol of methane to sustain their cellular growth (Hanson & Hanson, 1996; Previous thesis chapter). Consumption of oxygen through methanotrophic pathways results in a decrease in oxygen concentration and adversely affects other biological activities occurring in the water column. Biodegradation processes associated with toxic organic compounds expelled through FFT compaction and continued development of the water column microbial community are two primary examples of oxygen dependant processes of interest in this reclamation system (Semrau, 2011). The three

primary goals of this study are to use phospholipid fatty acid (PLFA) biomarker profiling to 1) assess the abundances of the microbial community in the water column of BML, 2) look for changes in the microbial community composition via PLFA distribution changes, and 3) to assess the occurrence and importance of methanotrophy as a fundamental component of biogeochemical cycling in BML.

PLFA analysis enables assessment of the viable biomass abundance of the microbial community of the BML water column, including the relative proportion of methanotrophic bacteria (Boschker & Middelburg, 2002). PLFAs are structural lipids that are an integral component of cellular membranes that degrade rapidly after cell death (Harvey et al., 1986). PLFA concentrations can be converted to cell abundance estimates via conversion factors (Green & Scow, 2000). PLFAs are identified using the IUPAC-IUBMB naming scheme and related short hand notation (Fahy et al., 2005). The short hand notation used is in the form of A:BωC, where A, B, and C represent the number of carbon atoms, number of double bonds, and position of the double bonds relative to the aliphatic end of the structure, respectively. Certain specific PLFA can represent specific biomarkers of certain groups of microbes, such as type I and type II methanotrophs, which are taxonomically distinct. The PLFA C16:1ω8c and C16:1ω5c/t are novel biomarkers for type I methanotrophs, while the PLFA C18:1ω8 is a novel biomarker for type II methanotrophs (Bodelier et al., 2009; Hanson & Hanson, 1996). Type I methanotrophs also demonstrate significant expression of C14:0. While not a novel PLFA biomarker for type I methanotrophs, monitoring it for coinciding concentration and isotopic trends with pooled C16:1 PLFA lends credibility to the presence of active type I methanotrophs (Deines, Bodelier, & Eller, 2007).

Stable carbon isotope analysis of PLFA provides another potential signature of methanotrophy as it has been demonstrated that incorporation of $\delta^{13}C$ depleted methane carbon results in a commensurate depletion in the $\delta^{13}C$ of methanotroph PLFA (Pancost & Sinninghe Damste, 2003). This depletion will be expressed most strongly in PLFA unique to methanotrophs, such as C16:1ω8c, C16:1ω5t and C18:1ω8 biomarkers. However, since it is often difficult to separate these biomarker PLFA from other unsaturated PLFA sufficiently to get compound specific signatures, this study looked for the depletion in the respective pooled unsaturated PLFA $\delta^{13}C$. If methane derived carbon is the primary carbon source for the microbial community then this depletion may be expected to be transferred to the rest of the community. Comparison to the $\delta^{13}C$ of the C16:0 PLFA, which are produced by all members of the community to varying extents, can enable assessment of the extent of recycling of methane derived carbon by heterotrophic metabolisms.

3.2 – Materials and Methods

3.2.1 – Sampling locations, schedule, and handling

Samples were taken across three platforms (P1, P2, P3) located diagonally across BML (Figure 3.1). June, July, and August samples were taken from all three depth zones (epilimnion, metalimnion, hypolimnion), with September profiles taken from the metalimnion and hypolimnion. Summer PLFA profiles for 2015 were created through sampling across all platforms between June and August, as well as P2 and P3 in September to capture post-turnover changes. Sampling in 2016 focused on P1 profiles sampled in July and August pre-lake turnover. The beginning of sample collection in 2016 was postponed from June to July due to active wildfires in the immediate area. Samples were collected using an air-tight Van Dorn water sampler. Upon retrieval of the Van Dorn from depth, 1L of sample water was withdrawn into a

1L Nalgene bottle pre-rinsed with methanol (MeOH). Sample bottles were frozen upon completion of day sampling and stored at -20 °C on site until transport. Samples were thawed at 4 °C prior to gravity filtration through pre-combusted 0.7 μm glass fibre filters, followed by 0.45 μm Polyvinylidene fluoride (PVDF) filters. Filters were freeze-dried for 48–72 hours prior to solvent extraction.

3.2.2 – PLFA Extraction and Conversion to Fatty Acid Methyl Esters (FAMEs)

Biomass estimates and biomarker analysis were conducted through the extraction and isolation of phospholipids from the sample filters using a modified Bligh and Dyer procedure, utilizing a dual solvent extraction consisting of 2:1:0.8 MeOH, Dichloromethane (DCM), and a phosphate buffer. Extractions were sonicated and spun overnight at room temperature before undergoing phase separation, isolating the organic fraction containing solvent from the remaining aqueous phase. Phospholipids were separated from the Total Lipid Extract (TLE) via silica gel chromatography using three fractions (F1=DCM, F2=Acetone, F3=MeOH). The phospholipids isolated in F3 were evaporated to dryness, re-dissolved using isotopically characterized KOH ($\delta^{13}C$) and a 1:1 toluene: methanol mixture, then heated to 37 °C for an hour to facilitate conversion of phospholipids to FAMEs for analysis by Gas Chromatography-Mass Spectrometry (GC-MS). A secondary silica gel chromatography was conducted (F1= 4:1 Hexane: DCM, F2= DCM, F3= MeOH) to remove additional compounds that may have interfered with FAME detection.

3.2.3 – Identification, Naming, and Quantification of FAMEs via GC-MS

All PLFA samples were identified and quantified through mass analysis on an Agilent 6890 GC (Column: DB-5MS, 0.25 μm film thickness, 30m length, 0.32mm ID) attached to an Agilent 5973 quadrupole mass spectrometer. The oven ramp temperature program was as

follows: beginning at 50°C for 1 minute, increasing by 20°C/min up to 130°C, then 4°C/min to 160°C, and 8°C/min to 300°C for 5 minutes. MSD Chemstation was used to identify FAMEs through database matching of spectra and overlaid spectra comparisons to two reference standards (Matreya PLFA mix and Supelco 37 FAME mix**)**. Quantification of FAMEs was conducted via generation of a 6-point calibration curve using four different FAMEs (14:0, 16:0, 18:0, 20:0) (R^2>0.99), back calculating using instrument areas & integration tools within MSD Chemstation.

3.2.5 – Stable Carbon Isotope Analysis ($\delta^{13}C$) of FAMEs via GC-C-IRMS

The 2016 PLFA profile samples were analyzed for stable carbon isotopes using an Agilent 6890 GC (Column: Agilent: DB-5, 0.25 μm film thickness, 30m length, 0.32mm ID) attached to a Conflo III Combustion Interface, followed by a Thermo Delta Plus XP Isotope Ratio Mass Spectrometer (IRMS). Isodat NT 2.0 Software (©Thermo Electron Company) was used to analyze GC-C-IRMS results. Carbon isotope ratios were normalized to the Vienna Pee Dee Belemnite (VPDB) standard. A $\delta^{13}C$ value correction as applied to account for the methyl group addition from the isotopically characterized KOH during FAME derivatization. All samples were injected in triplicate, with $\delta^{13}C$ standard deviation of approximately +/- 0.5 ‰ based on standard reproducibility and instrument accuracy.

3.3 – Results & Discussion

3.3.1 – Variations in PLFA Concentrations & Biomass Estimates

PLFA concentration depth profiles showed consistent values in June 2015 at both P2 and P3 across all depths. Mean PLFA concentrations were $3.5x10^1$ +/- $6.8x10^0$ pmols/mL (n = 6, range = $2.7x10^1$ to $4.6x10^1$ pmols) (Figure 3.2). August profiles exhibited increasing PLFA concentration with increasing depth, with the largest values present in the hypolimnion. August

2015 P1 PLFA concentrations in the epilimnion were $5.0x10^1$ pmols/mL, increasing to $6.5x10^1$ in the metalimnion and further to $1.2x10^2$ pmols/mL in the hypolimnion. September 2015 P2 and P3 PLFA concentrations were generally consistent with values $7.1x10^1$ and $8.7x10^1$ pmols/mL in the metalimnion, and $9.0x10^1$ and $8.9x10^1$ in the hypolimnion (Figure 3.2). PLFA concentration profiles in 2016 were taken at P1 due to the consistency of trends observed across platforms in 2015. July 2016 PLFA concentrations had a mean of $2.8x10^1$ +/- $9.3x10^{-1}$ pmols/mL, exhibiting consistent values across all depth zones similar to the June 2015 profile (n = 3, range = $2.7x10^1$ to $2.8x10^1$ pmols/mL). August 2016 PLFA concentrations displayed an increasing trend with depth similar to August 2015. However, in this case, PLFA concentrations in August 2016 were $1.3x10^1$ pmols/mL in the epilimnion and only increased to $3.3x10^1$ pmols/mL in the hypolimnion (n = 4, range = $9.9x10^0$ to $3.3x10^1$ pmols/mL, mean = $1.4x10^1$ +/- $1.0x10^1$ pmols/mL) (Figure 3.2).

Biomass estimates of water column microbial communities were generated through a conversion factor calculation applied to total mass of extracted PLFAs. A conversion factor of $2.0x10^4$ cells/pmol of PLFA (Green & Scow, 2000) was applied to all PLFA samples, with resulting biomass estimate numbers indicated on Figure 3.2's secondary y-axis. The 2015 June PLFA profiles average biomass estimate for P2 and P3 was $7.0x10^5$ +/- $1.4x10^5$ cells/mL (n = 6, range = $5.4x10^5$ to $9.3x10^5$ cells/mL). The August 2015 P1 biomass estimates were $1.0x10^6$ cells/mL, reaching $1.3x10^6$ cells/mL in the metalimnion and further increasing to $2.4x10^6$ cells/mL in the hypolimnion. September 2015 P2 and P3 biomass estimates were consistent with August at $1.4x10^6$ and $1.7x10^6$ cells/mL in the metalimnion and $1.8x10^6$ and $1.8x10^6$ cells/mL in the hypolimnion, respectively. The July 2016 average biomass estimate was $5.5x10^5$ +/- $1.9x10^4$ cells/mL (n = 3, range = $5.3x10^5$ to $5.6x10^5$ cells/mL). PLFA biomass estimates in August 2016

were $2.5x10^5$ cells/mL in the epilimnion and increased to $6.6x10^5$ cells/mL in the hypolimnion (n = 4, range = $2.0x10^5$ to $6.6x10^5$ cells/mL, mean = $3.8x10^5$ +/- $2.1x10^5$ cells/mL).

Early season (June/July) biomass estimates were consistent for both years and across all depths sampled with a mean of $6.5x10^5$ +/- $9.3x10^4$cells/mL (n = 9, range = $5.3x10^5$ to $9.27x10^5$ cells/mL) (Figure 3.2). This implies that variations in geochemical conditions with depth or between years are not sufficient to alter the abundance of the overall microbial community in June and July. In contrast, changes in biomass estimates were observed in August/September. In 2015 while epilimnion biomass estimates remained the same circa $8.2x10^5$ cells/mL (+/- $2.5x10^5$ cells/mL), hypolimnion biomass estimates increased to circa $2.0x10^6$ cells/mL (+/- $3.5x10^5$ cells/mL) through August and September. In 2016 a similar trend of increasing biomass with depth was observed. However, in this case, epilimnion average biomass estimates dropped to $4.1x10^5$ cells/mL (+/- $2.2x10^5$ cells/mL) and hypolimnion biomass estimates reached maximum values of $5.3x10^5$ cells/mL (+/- $1.2x10^5$ cells/mL), comparable to early 2015 values. The repetition of an increasing trend of biomass with depth intriguingly points to a similar control over the two years, despite the differences in overall biomass.

The observed PLFA concentrations and biomass estimates for BML were generally consistent around $5.2x10^1$ pmols/mL and $1.0x10^6$ cells/mL which is in the lower range of what is normally observed in stratified oligotrophic lakes, with multiple studies reporting average biomass estimates between $0.3x10^6$ to $8.4x10^6$ cells/mL (Coveney & Wetzel, 1995; Hessen, 1985; Jordan & Likens, 1980). While observing a relatively consistent biomass estimate across all depths in June and July, an increase is seen with depth in August of both years. This increase in biomass established over longer stratification time in the hypolimnion suggests a change in metabolism and cycling processes or increased growth of the community at depth over time. This

could be a result of an increased prominence of methanotrophy, as dissolved methane concentrations increase over the summer months with this increase in biomass. This implies that the potential presence of methanotrophs in a certain depth zone of the lake may be having an observable influence on the total viable microbial community's biomass over time as the community matures through summer stratification.

3.3.2 – Variations in Specific PLFA Distributions

The PLFA profiles are composed of 16 PLFA that were quantified and identified through standard pairing or fragmentation pattern matching (C12:0-br, C14:0, i-C15:0, a-C15:0, C15:0, i-C16:0, C16:1, C16:1^{x}, C16:0, C17:0$^{\Delta}$, C17:0, C18:2^{x,y}, C18:1^{x}, C18:0, C19:0$^{\Delta}$, C20:0). This study analyzed the PLFA profiles by structure and separated them into groups of saturates (all single bonds), mono-unsaturates (1 double bond), poly-unsaturates (2+ double bonds), cyclic, and branched. In general, the most abundant PLFA group were the mono-unsaturates (47 +/- 10 %), followed by saturates (34 +/- 8 %), branched (10 +/- 4 %), cyclic (7 +/- 5 %) and poly-unsaturates (2 +/- 1 %). There were some notable variations in these fractions and the PLFA that comprised them (Figure 3.3 & 3.4).

The mono-unsaturated PLFAs were the most abundant across the majority of the profiles, where C16:1 comprised 70 +/- 9 % of the total mono-unsaturated PLFA, while the C18:1 PLFAs comprised the remaining 30 +/- 9%. The pooled 18:1 PLFAs molar composition % were variable across 2015 and 2016, with no specific trends related to depth or sample month, with values ranging between 6.2 to 18.6 % (n = 20, range = 6.2 to 18.6 %, mean = 13.3 +/- 2.8%). The pooled C16:1 PLFAs made up the largest component of the total PLFA profiles in all 2015 samples ranging between 26 to 35% in the epilimnion (n = 3, range = 26 to 35%, mean = 30 +/- 4.1%) up to 26 to 51% in the hypolimnion (n = 5, range = 26 to 51%, mean = 41 +/- 12%)(Figure

3.3). The pooled C16:1 PLFA in 2016 made up considerably less molar % of the profiles ranging between 17 to 24% in the epilimnion (n = 4, range = 17 to 24%, mean = 21 +/- 3%). However, molar % increased with depth similar to 2015, making up 25 to 45% of the profile (n = 3, range = 25 to 45%, mean = 37 +/- 10%) (Figure 3.4). Notably, the pooled C16:1 PLFAs exhibited clearly increasing trends with depth across both 2015 and 2016 samples. This suggests a shift in microbial community structure to organisms that express more un-saturated PLFAs than other types, specifically C16:1s.

The saturated PLFAs were the second most abundant overall, where C16:0 represented most of the saturate pool comprising 58 +/- 11 % while C14:0 was the next most abundant comprising 17 +/- 4%. The C16:0 PLFA exhibit consistent molar composition % values in 2015 profiles, ranging between 18 to 22% (n = 13, range = 17 to 22%, mean = 18 +/- 4.7%). The C14:0 PLFA made up a relatively consistent molar composition % of the total profile throughout the 2015 profiles, ranging between 3.5 to 5.5 % (n = 13, range = 3.5 to 5.5%, mean = 4.4 +/- 0.7 %). There is a notable increase in presence both saturated PLFA in the 2016 profiles with C16:0 increasing to a range of 20 to 27% (n = 7, range = 20 to 27%, mean = 24 +/- 3.4%), and C14:0 to between 5.5 to 9.6 % (n = 7, range = 5.5 to 9.6 %, mean = 8.3 +/- 1.3 %) (Figure 3.5). The observed increased values in 2016 also appear consistent across all depths, similar to the 2015 profiles.

The branched, cyclic, and poly-unsaturated PLFA groups exhibit similar trends both in 2015 and 2016 profiles. These PLFA represent a consistent percentage of the profile across the three sample depths, displaying no trends within a specific profile except for June P2 2015. A decreasing trend is seen across summer months both years, with lower representation occurring towards the fall. In June and July, these PLFA classes compose 26 +/- 5 % of the profile,

decreasing to 12 +/- 3 % in August and September. The observed decrease is concurrent with the increase in mono-unsaturated PLFA within the later summer month profiles. Based on these trends, the following discussion focusses on C16:0 due to its representation of the general bacterial community and C14:0, C16:1, and C18:1 for potential representation of methanotroph populations.

The trends in PLFA distribution, particularly in the saturated and mono-unsaturated PLFA indicate changes in the microbial community are occurring. The trend of primary interest is the increasing distribution of C16:1 PLFAs with depth over the summer months. The pooled C16:1 PLFAs may include the novel biomarkers for type I methanotrophs, so theses increasing trends are consistent with increasing proportions of these organisms. This may indicate a shift in community structure of which type I methanotrophs are present in higher abundance and make up a larger percentage of the aerobic bacteria present. The C14:0 is expressed by the general community as well as by most type I methanotrophs and exhibits relatively stable proportions through all PLFA profiles across both years. The C18:1 PLFAs that would include the novel biomarkers for type II methanotrophs show no signs of increasing depths trends like the C16:1 PLFAs, and are a relatively minor component of the profiles. This suggests that type II methanotrophs are a very small proportion or absent in the system. Pairing these data trends with stable carbon isotope data can reveal trends in carbon source utilization, specifically regarding incorporation of a depleted signature into the PLFA of the microbial community that may indicate methane consumption.

3.3.3 – Distribution and Trends in $\delta^{13}C$ Values of C14:0, C16:0, pooled C16:1 and C18:1 PLFAs

The $\delta^{13}C$ values of C14:0 and C16:0 were measured directly and C16:1s / C18:1s were measured as pooled signatures for P1 July and August 2016 profiles. Examination of the $\delta^{13}C$ values of these PLFA biomarkers show two different ranges for the epilimnion and hypolimnion.

The $\delta^{13}C$ values seen in the epilimnion for the C16:0 and pooled C18:1 PLFAs were consistent at -35 +/- 0.5‰ (n = 4) and -32 +/- 0.5 ‰ (n = 2) respectively (Figure 3.6). Since PLFA are expected to be 4-6 ‰ depleted relative to the carbon sources being utilized by bacteria (Boschker, de Brouwer, & Cappenberg, 1999), this implies that these organisms are using a carbon source with a $\delta^{13}C$ of -31 to -28 ‰ in the case of 16:0 and -28 to -20 ‰ in the case of C18:1s. These $\delta^{13}C$ values are consistent with the ranges expected for organic carbon produced via C3 photosynthetic pathways (range = -22 to -30 ‰) (Hayes, 2001). Sources of this type of C3 $\delta^{13}C$ dissolved organic carbon (DOC) in BML could include photosynthesis in the water column, fluvial or aeolian inputs of organic matter from the surrounding area, or residual petroleum hydrocarbons (including naphthenic acids). All of these organic carbon sources are known to be present and could potentially be heterotrophically metabolized in BML resulting in the observed $\delta^{13}C$ signatures for C16:1s and C:18:1s. It is notable that the C16:0 PLFA are more $\delta^{13}C$ depleted than the C18:1s. This relative depletion may be the result of variations in the $\delta^{13}C$ of the carbon sources being utilized by organisms producing the C16:0 PLFA. Since the C16:0 is produced by most bacteria, including methanotrophs, the proposed occurrence of methanotrophy provides a potential explanation for the generation of more depleted $\delta^{13}C$ values for C16:0 as compared to the general microbial population. However, given the potential ranges in $\delta^{13}C$ of the DOC, the magnitude of the shift is too small to be considered definitive.

In the hypolimnion, the $\delta^{13}C$ values of the pooled C18:1 PLFAs remain the same at -33 +/- 0.5 ‰ (n = 2), implying microbes that are producing this PLFA are not changing the carbon source or metabolism they are using relative to what is occurring in the epilimnion. As this pool of PLFA would contain the novel C18:1ω8 biomarker of type II methanotrophs, this suggests methane oxidation by type II methanotrophs is absent in the hypolimnion. In contrast, the $\delta^{13}C$ values for C16:0 decrease to -43 +/- 3.6 ‰ in the hypolimnion (n = 3, range = -47 to -40‰) (Figure 3.6). This negative offset is much larger than that observed in the epilimnion and much more strongly indicates that the microbes in the hypolimnion are utilizing a second, more isotopically depleted carbon source. The transfer of a more depleted $\delta^{13}C$ signature into the PLFA of the bacterial community can be explained by the incorporation of the depleted dissolved methane signature present in the hypolimnion into the C16:0 synthesized by type I methanotrophs (Bowman et al., 1991). The presence and influence of type I methanotrophs is directly indicated by the trends in the C14:0 and C16:1s PLFA signatures. These PLFA exhibited the most depleted $\delta^{13}C$ signatures observed in this study. The C14:0 PLFA displayed signatures of -52 +/- 3.9 ‰ in the hypolimnion (n = 3, range = -55 to -47 ‰), while the pooled C16:1 PLFAs were the most depleted at -54 +/- 5.9 ‰ (n = 3, range = -59 to -47 ‰) (Figure 3.6). These depleted values are approaching the $\delta^{13}C$ of the methane present in the hypolimnion, strongly suggesting utilization of the depleted dissolved methane via methanotrophy (Figure 3.6, -62 +/- 0.5 ‰). Notably, the C14:0 and C16:1 PLFAs are also the most isotopically depleted in the epilimnion, ranging from -40 +/- 0.5‰ (n = 2) and -46 to -40 ‰ (n = 3, mean = -42 +/- 3‰) respectively. While they are much less depleted than those observed in the hypolimnion (Figure 3.6), the observed values indicate that inputs via methanotrophy are still influencing the $\delta^{13}C$ of these PLFA. However, the reduction in the extent of the depletion suggests that other carbon

sources may also be influencing the $\delta^{13}C$ of these PLFA. Since we are combining the C16:1 PLFA with C16:1s produced by all organisms, and since C14:0 is not unique to methanotrophs, this may indicate greater inputs of these PLFA from non-methanotrophic sources. This would be consistent with a reduced proportion of methanotrophs being present and active in the epilimnion relative to other heterotrophic organisms. These observations support the contention from the previous chapter that the observed trends in oxygen and methane in the BML water column are being driven by methanotrophy (Figure 3.7).

3.4 - Conclusions

The increasing $CH_{4(aq)}$ concentrations concurrent with the presence of DO indicates a favourable environment for methanotrophic bacteria, which have been proposed to be responsible for the decreasing DO concentrations in BML with increasing depth. The activities of such bacteria could explain the four order of magnitude decrease in methane fluxes observed in the hypolimnion of BML (previous chapter). The trends in PLFA abundances, distributions and $\delta^{13}C$ values observed in this study confirm that type I methanotrophy is a major metabolism supporting the BML microbial community in the hypolimnion and a less significant, but still present, metabolism in the epilimnion. The observation of highly depleted δ13C values of biomarker PLFA in the hypolimnion in August both years directly indicates the occurrence of methanotrophy in the hypolimnion. The fact that depletion is only observed for C16:1 and not C18:1 indicates that type I methanotrophs are present and driving this process. The isotopic depletion of the general biomarker C16:0 in the hypolimnion indicates that this metabolism is sufficiently prevalent to affect the general microbial community indicators, either by direct production of C16:0 PLFA by methanotrophs, or by transfer of $\delta^{13}C$ depleted carbon from methanotrophs to other organisms by heterotrophy. The increases in hypolimnetic PLFA

abundances later in the summer are consistent with the previously reported observation of increased methane concentrations. This is consistent with increased methane supply enabling increased growth of methanotrophic organisms and thus increased PLFA abundances. The fact that C16:1 PLFA produced by type I methanotrophs also increase in the hypolimnion later in the summer further supports this trend.

Ongoing research will investigate how the role of methanotrophic organisms changes in BML as the system develops. In particular it will assess whether methanotrophy becomes sufficiently established to consume all dissolved methane in the water cap within the very upper sediments preventing further influxes, and associated oxygen demand, in the BML water column. This commonly occurs in freshwater and marine sediments, and if established in BML would enable the development of a functioning freshwater ecosystem in the surface waters, which is the ultimate goal of EPL design.

3.5 – References

Alberta Energy Regulator. (2016). Executive Summary, ST 98-2016: Alberta's Energy Reserves 2015 & Supply/Demand Outlook 2016-2025, 8. Retrieved from http://www1.aer.ca/st98/data/executive_summary/ST98-2016_Executive_Summary.pdf

Allen, E. W. (2008). Process water treatment in Canada's oil sands industry: I. Target pollutants and treatment objectives. *Journal of Environmental Engineering and Science*, *7*(2), 123–138. https://doi.org/10.1139/S07-038

Bedard, C., & Knowles, R. (1989). CO Oxidation by Methanotrophs and Nitrifiers. *Microbiology*, *53*(1), 68–84. Retrieved from http://apps.isiknowledge.com/full_record.do?product=UA&search_mode=GeneralSearch&qid=11&SID=X16536DGgEAkOn8a882&page=1&doc=1&colname=WOS

Blumenberg, M., Seifert, R., & Michaelis, W. (2007). Aerobic methanotrophy in the oxic-anoxic transition zone of the Black Sea water column. *Organic Geochemistry*, *38*(1), 84–91. https://doi.org/10.1016/j.orggeochem.2006.08.011

Bodelier, P. L. E., Gillisen, M.-J. B., Hordijk, K., Damsté, J. S. S., Rijpstra, W. I. C., Geenevasen, J. a J., & Dunfield, P. F. (2009). A reanalysis of phospholipid fatty acids as ecological biomarkers for methanotrophic bacteria. *The ISME Journal*, *3*(5), 606–617. https://doi.org/10.1038/ismej.2009.6

Bordenave, S., Kostenko, V., Dutkoski, M., Grigoryan, A., Martinuzzi, R. J., & Voordouw, G. (2010). Relation between the activity of anaerobic microbial populations in oil sands tailings ponds and the sedimentation of tailings. *Chemosphere*, *81*(5), 663–668. https://doi.org/10.1016/j.chemosphere.2010.07.058

Boschker, H. T. S., de Brouwer, J. F. C., & Cappenberg, T. E. (1999). The contribution of macrophyte-derived organic matter to microbial biomass in salt-marsh sediments: Stable carbon isotope analysis of microbial biomarkers. *Limnology and Oceanography*, *44*(2), 309–319. https://doi.org/10.4319/lo.1999.44.2.0309

Boschker, H. T. S., & Middelburg, J. J. (2002). Stable isotopes and biomarker in microbial ecology. *FEMS Microbiology Ecology*, *40*, 85–95.

Bowman, J. P., Skerratt, J. H., Nichols, P. D., & Sly, L. I. (1991). Phospholipid fatty acid and lipopolysaccharide fatty acid signature lipids in methane-utilizing bacteria, *85*(January), 15–21. https://doi.org/10.1111/j.1574-6968.1991.tb04693.x

Canadian Association of Petroleum Producers. (2015). Crude Oil, (June), 1–9.

Chalaturnyk, R. J., Don Scott, J., & Özüm, B. (2002). Management of Oil Sands Tailings. *Petroleum Science and Technology*, *20*(9–10), 1025–1046. https://doi.org/10.1081/LFT-

120003695

Chen, M., Walshe, G., Chi Fru, E., Ciborowski, J. J. H., & Weisener, C. G. (2013). Microcosm assessment of the biogeochemical development of sulfur and oxygen in oil sands fluid fine tailings. *Applied Geochemistry*, *37*, 1–11. https://doi.org/10.1016/j.apgeochem.2013.06.007

Chi Fru, E., Chen, M., Walshe, G., Penner, T., & Weisener, C. (2013). Bioreactor studies predict whole microbial population dynamics in oil sands tailings ponds. *Applied Microbiology and Biotechnology*, *97*(7), 3215–3224. https://doi.org/10.1007/s00253-012-4137-6

Conrad, R. (2005). Quantification of methanogenic pathways using stable carbon isotopic signatures: A review and a proposal. *Organic Geochemistry*, *36*(5), 739–752. https://doi.org/10.1016/j.orggeochem.2004.09.006

Conrad, R. (2009). The global methane cycle: Recent advances in understanding the microbial processes involved. *Environmental Microbiology Reports*, *1*(5), 285–292. https://doi.org/10.1111/j.1758-2229.2009.00038.x

Coveney, M. F., & Wetzel, R. G. (1995). Biomass, production, and specific growth rate of bacterioplankton and coupling to phytoplankton in an oligotrophic lake, *40*(7).

Deines, P., Bodelier, P. L. E., & Eller, G. (2007). Methane-derived carbon flows through methane-oxidizing bacteria to higher trophic levels in aquatic systems. *Environmental Microbiology*, *9*(5), 1126–1134. https://doi.org/10.1111/j.1462-2920.2006.01235.x

Dompierre, K. A., Lindsay, M. B. J., Cruz-Hernandez, P., & Halferdahl, G. M. (2016). Initial geochemical characteristics of fluid fine tailings in an oil sands end pit lake. *Science of the Total Environment*, *556*, 196–206. https://doi.org/10.1016/j.scitotenv.2016.03.002

Duan, Z., & Mao, S. (2006). A thermodynamic model for calculating methane solubility, density and gas phase composition of methane-bearing aqueous fluids from 273 to 523 K and from

1 to 2000 bar. *Geochimica et Cosmochimica Acta*, *70*(13), 3369–3386. https://doi.org/10.1016/j.gca.2006.03.018

Eby, P., Gibson, J. J., & Yi, Y. (2015). Suitability of selected free-gas and dissolved-gas sampling containers for carbon isotopic analysis. *Rapid Communications in Mass Spectrometry*, *29*(13), 1215–1226. https://doi.org/10.1002/rcm.7213

Fahy, E., Subramaniam, S., Brown, H. A., Glass, C. K., Merrill, A. H., Murphy, R. C., … Dennis, E. a. (2005). A comprehensive classification system for lipids. *Journal of Lipid Research*, *46*, 839–861. https://doi.org/10.1194/jlr.E400004-JLR200

Galimov, E. M. (2006). Isotope organic geochemistry. *Organic Geochemistry*, *37*(10), 1200–1262. https://doi.org/10.1016/j.orggeochem.2006.04.009

Giesy, J. P., Anderson, J. C., & Wiseman, S. B. (2010). Alberta oil sands development. *Pnas*, *107*(3), 951–952. https://doi.org/10.1073/pnas.0912880107

Government of Alberta. (2013). Facts and Statistics. Retrieved February 7, 2017, from http://www.energy.alberta.ca/OilSands/791.asp

Green, C. T., & Scow, K. M. (2000). Analysis of phospholipid fatty acids (PLFA) to characterize microbial communities in aquifers. *Hydrogeology Journal*, *8*(1), 126–141. https://doi.org/10.1007/s100400050013

Haack, S. K., Garchow, H., Odelson, D. A., Forney, L. J., & Klug, M. J. (1994). Accuracy, Reproducibility, and Interpretation of Fatty Acid Methyl Ester Profiles of Model Bacterial Communities. *Appl. Envir. Microbiol.*, *60*(7), 2483–2493. Retrieved from http://aem.asm.org/content/60/7/2483.short

Hanson, R. S., & Hanson, T. E. (1996). Methanotrophic Bacteria. *Microbiological Reviews*, *60*(2), 439–471. https://doi.org/

Harrits, S. M., & Hanson, R. S. (1980). Stratification of aerobic methane-oxidizing organisms in Lake Mendota, Madison, Wisconsin. *Limnology and Oceanography*, *25*(3), 412–421. https://doi.org/10.4319/lo.1980.25.3.0412

Harvey, H. R., Fallon, R. D., & Patton, J. S. (1986). The effect of organic matter and oxygen on the degradation of bacterial membrane lipids in marine sediments, *50*, 795–804.

Hayes, J. M. (2001). Fractionation of the Isotopes of Carbon and Hydrogen in Biosynthetic Processes. *Reviews in Mineralogy and Geochemistry*, *43*(March), 225–277. https://doi.org/10.2138/gsrmg.43.1.225

Hessen, O. (1985). The relation between bacterial carbon and dissolved humic compounds in oligotrophic lakes, *31*, 215–223.

Holowenko, F. M., MacKinnon, M. D., & Fedorak, P. M. (2000). Methanogens and sulfate-reducing bacteria in oil sands fine tailings waste. *Canadian Journal of Microbiology*, *46*(10), 927–937. https://doi.org/10.1139/w00-081

Hutchins, S. R. (1991). Biodegradation of Monoaromatic Hydrocarbons by Aquifer Microorganisms Using Oxygen, Nitrate, or Nitrous-Oxide as the Terminal Electron-Acceptor. *Applied and Environmental Microbiology*, *57*(8), 2403–2407.

Jahnke, L. L., Summons, R. E., Hope, J. M., & Des Marais, D. J. (1999). Carbon isotopic fractionation in lipids from methanotrophic bacteria II: The effects of physiology and environmental parameters on the biosynthesis and isotopic signatures of biomarkers. *Geochimica et Cosmochimica Acta*, *63*(1), 79–93. https://doi.org/10.1016/S0016-7037(98)00270-1

Jiang, H., Chen, Y., Jiang, P., Zhang, C., Smith, T. J., Murrell, J. C., & Xing, X.-H. (2010). Methanotrophs: Multifunctional bacteria with promising applications in environmental

bioengineering. *Biochemical Engineering Journal*, *49*(3), 277–288. https://doi.org/10.1016/j.bej.2010.01.003

Jordan, M. J., & Likens, G. E. (1980). Measurement of planktonic bacterial production in an oligotrophic lake. *Limnology and Oceanography*, *25*(4), 719–732. https://doi.org/10.4319/lo.1980.25.4.0719

Kelly, C. A., & Chynoweth, P. (1981). Carol A. Kelly2 and David P. Chynoweth3, *26*, 891–897.

King, G. M., & Schnell, S. (1994). Ammonium and nitrite inhibition of methane oxidation by Methylobacter albus BG8 and Methylosinus trichosporium OB3b at low methane concentrations. *Applied and Environmental Microbiology*, *60*(10), 3508–3513.

Knief, C., Kolb, S., Bodelier, P. L. E., Lipski, A., & Dunfield, P. F. (2006). The active methanotrophic community in hydromorphic soils changes in response to changing methane concentration. *Environmental Microbiology*, *8*(2), 321–333. https://doi.org/10.1111/j.1462-2920.2005.00898.x

Kolb, S., Knief, C., Dunfield, P. F., & Conrad, R. (2005). Abundance and activity of uncultured methanotrophic bacteria involved in the consumption of atmospheric methane in two forest soils. *Environmental Microbiology*, *7*(8), 1150–1161. https://doi.org/10.1111/j.1462-2920.2005.00791.x

Lidstrom, M. E., & Somers, L. (1984). Seasonal study of methane oxidation in lake washington. *Applied and Environmental Microbiology*, *47*(6), 1255–1260.

Lodish, H., Berk, A., Kaiser, C. A., Krieger, M., Bretscher, A., Ploegh, H., & Amon, A. (2013). *Molecular Cell Biology* (7th ed.). W.H. Freeman and Company.

Lovley, D. R., & Klug, M. J. (1986). Model for the distribution of sulfate reduction and methanogenesis in freshwater sediments. *Geochimica et Cosmochimica Acta*, *50*(1), 11–18.

https://doi.org/10.1016/0016-7037(86)90043-8

Masliyah, J., Zhou, Z. J., Xu, Z., Czarnecki, J., & Hamza, H. (2004). Understanding Water-Based Bitumen Extraction from Athabasca Oil Sands. *The Canadian Journal of Chemical Engineering*, *82*(4), 628–654. https://doi.org/10.1002/cjce.5450820403

Mohanty, S. R., Bodelier, P. L. E., & Conrad, R. (2007). Effect of temperature on composition of the methanotrophic community in rice field and forest soil. *FEMS Microbiology Ecology*, *62*(1), 24–31. https://doi.org/10.1111/j.1574-6941.2007.00370.x

Nozhevnikova, A. N., Holliger, C., Ammann, A., & Zehnder, A. J. B. (1997). Methanogenesis in Sediments from Deep Lakes at Different temperatures (2-70C).

Nyerges, G., & Stein, L. Y. (2009). Ammonia cometabolism and product inhibition vary considerably among species of methanotrophic bacteria. *FEMS Microbiology Letters*, *297*(1), 131–136. https://doi.org/10.1111/j.1574-6968.2009.01674.x

Oremland, R. S., & Polcin, S. (1982). Methanogenesis and Sulfate Reduction: Competitive and Noncompetitive Substrates in Estuarine Sediments. *Applied and Environmental Microbiology*, *44*(6), 1270–1276. https://doi.org/10.1016/0198-0254(83)90262-5

Pancost, R. D., Damsté, J., Sinninghe, S., Lint, S. De, Maarel, M. J. E. C. Van Der, & Gottschal, J. C. (2000). Biomarker Evidence for Widespread Anaerobic Methane Oxidation in Mediterranean Sediments by a Consortium of Methaogenic Archaea and Bacteria. *Applied and Environmental Microbiology*, *66*(3), 1126–1132. https://doi.org/10.1128/AEM.66.3.1126-1132.2000.Updated

Pancost, R. D., & Sinninghe Damste, J. S. (2003). Carbon isotopic compositions of prokaryotic lipids as tracers of carbon cycling in diverse settings. *Chemical Geology*, *195*(1–4), 29–58. https://doi.org/10.1016/S0009-2541(02)00387-X

Penner, T. J., & Foght, J. M. (2010). Mature fine tailings from oil sands processing harbour diverse methanogenic communities. *Canadian Journal of Microbiology*, *56*(6), 459–70. https://doi.org/10.1139/w10-029

Schonheit, P., Keweloh, H., & Thauer, R. K. (1991). Factor F420 degradation in Methanobacterium thermoautotrophicum during exposure to oxygen. *Biochemistry*, *266*(2), 14151–14154. Retrieved from http://www.jbc.org/content/266/22/14151.short

Schönheit, P., Kristjansson, J. K., & Thauer, R. K. (1982). Kinetic mechanism for the ability of sulfate reducers to out-compete methanogens for acetate. *Archives of Microbiology*, *132*(3), 285–288. https://doi.org/10.1007/BF00407967

Semrau, J. D. (2011). Bioremediation via methanotrophy: Overview of recent findings and suggestions for future research. *Frontiers in Microbiology*, *2*(OCT), 1–7. https://doi.org/10.3389/fmicb.2011.00209

Siddique, T., Fedorak, P. M., & Foght, J. M. (2006). Biodegradation of Short-Chain n -Alkanes in Oil Sands Tailings under Methanogenic Conditions. *Environmental Science & Technology*, *40*(17), 5459–5464. https://doi.org/10.1021/es060993m

Siddique, T., Fedorak, P. M., Mackinnon, M. D., & Foght, J. M. (2007). Metabolism of BTEX and naphtha compounds to methane in oil sands tailings. *Environmental Science and Technology*, *41*(7), 2350–2356. https://doi.org/10.1021/es062852q

Siddique, T., Penner, T., Semple, K., & Foght, J. M. (2011). Anaerobic biodegradation of longer-chain n-alkanes coupled to methane production in oil sands tailings. *Environmental Science and Technology*, *45*(13), 5892–5899. https://doi.org/10.1021/es200649t

Simankova, M. V, Kotsyurbenko, O. R., Lueders, T., Nozhevnikova, A. N., Wagner, B., Conrad, R., & Friedrich, M. W. (2003). Isolation and characterization of new strains of methanogens

from cold terrestrial habitats. *Systematic and Applied Microbiology*, *26*(2), 312–318. https://doi.org/10.1078/072320203322346173

Stasik, S., Loick, N., Knöller, K., Weisener, C., & Wendt-Potthoff, K. (2014). Understanding biogeochemical gradients of sulfur, iron and carbon in an oil sands tailings pond. *Chemical Geology*, *382*, 44–53. https://doi.org/10.1016/j.chemgeo.2014.05.026

Syncrude Canada Ltd. (2016). *Sustainability Report*.

Templeton, A. S., Chu, K. H., Alvarez-Cohen, L., & Conrad, M. E. (2006). Variable carbon isotope fractionation expressed by aerobic CH4-oxidizing bacteria. *Geochimica et Cosmochimica Acta*, *70*(7), 1739–1752. https://doi.org/10.1016/j.gca.2005.12.002

Trotsenko, Y. A., & Khmelenina, V. N. (2005). Aerobic methanotrophic bacteria of cold ecosystems. *FEMS Microbiology Ecology*, *53*(1), 15–26. https://doi.org/10.1016/j.femsec.2005.02.010

Westcott, F., & Watson, L. (2007). End Pit Lakes Technical Guidance Document. Prepared by Clearwater Environmental Consultants Inc. for the Cumulative Environmental Management Association (CEMA) End Pit Lakes Subgroup., 51.

Whiticar, M. J. (1999). Carbon and hydrogen isotope systematics of bacterial formation and oxidation of methane. *Chem. Geol.*, *161*(1–3), 291–314. https://doi.org/10.1016/S0009-2541(99)00092-3

Whiticar, M. J., Faber, E., & Schoell, M. (1986). Biogenic methane formation in marine and freshwater environments: CO2 reduction vs. acetate fermentation-Isotope evidence. *Geochimica et Cosmochimica Acta*, *50*(5), 693–709. https://doi.org/10.1016/0016-7037(86)90346-7

Witherspoon, P. a., & Saraf, D. N. (1966). Diffusion of Methane, Ethane, Propane, and n-Butane.

Journal of Physical Chemistry, *510*(6), 3752–3755. https://doi.org/10.1021/j100895a017

Zhou, E., & Crawford, R. L. (1995). Effects of oxygen, nitrogen, and temperature on gasoline biodegradation in soil. *Biodegradation*, *6*(2), 127–140. https://doi.org/10.1007/BF00695343

3.6 Figures and Tables

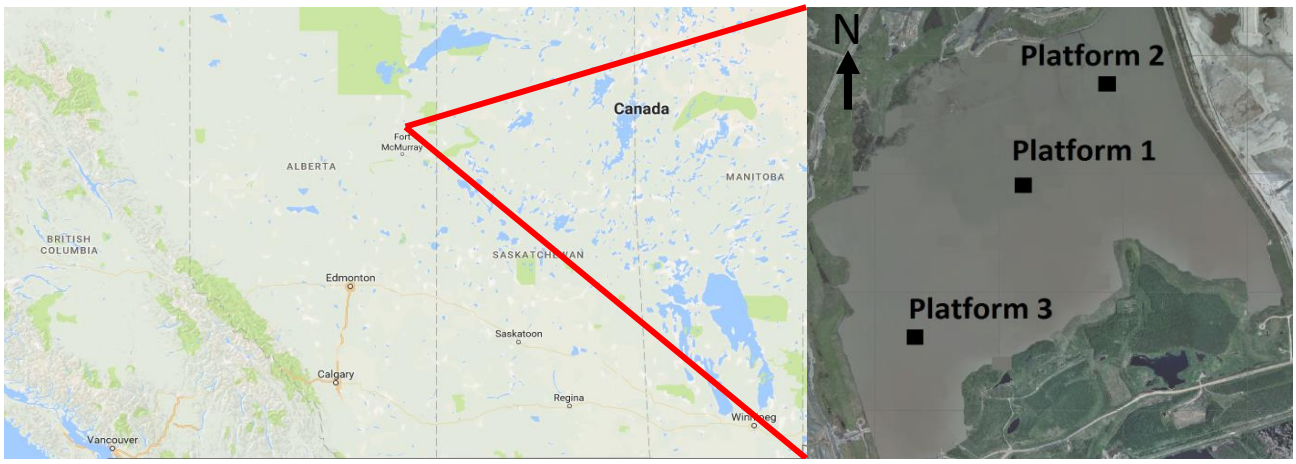

Figure 3.1**:** Location of BML in northern Alberta, Canada on the left. Satellite image of BML on the right, with sampling platforms labelled.

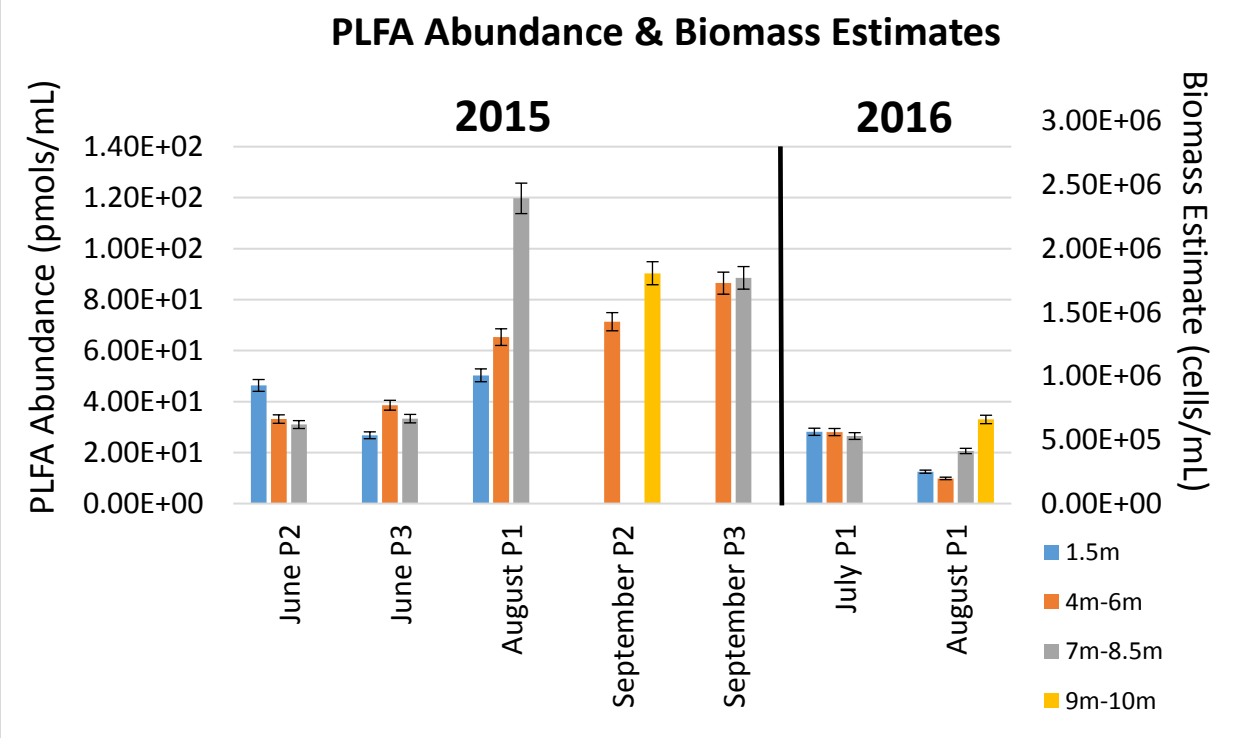

Figure 3.2: PLFA biomass estimates comprising each depth profile taken across 2015 and 2016.

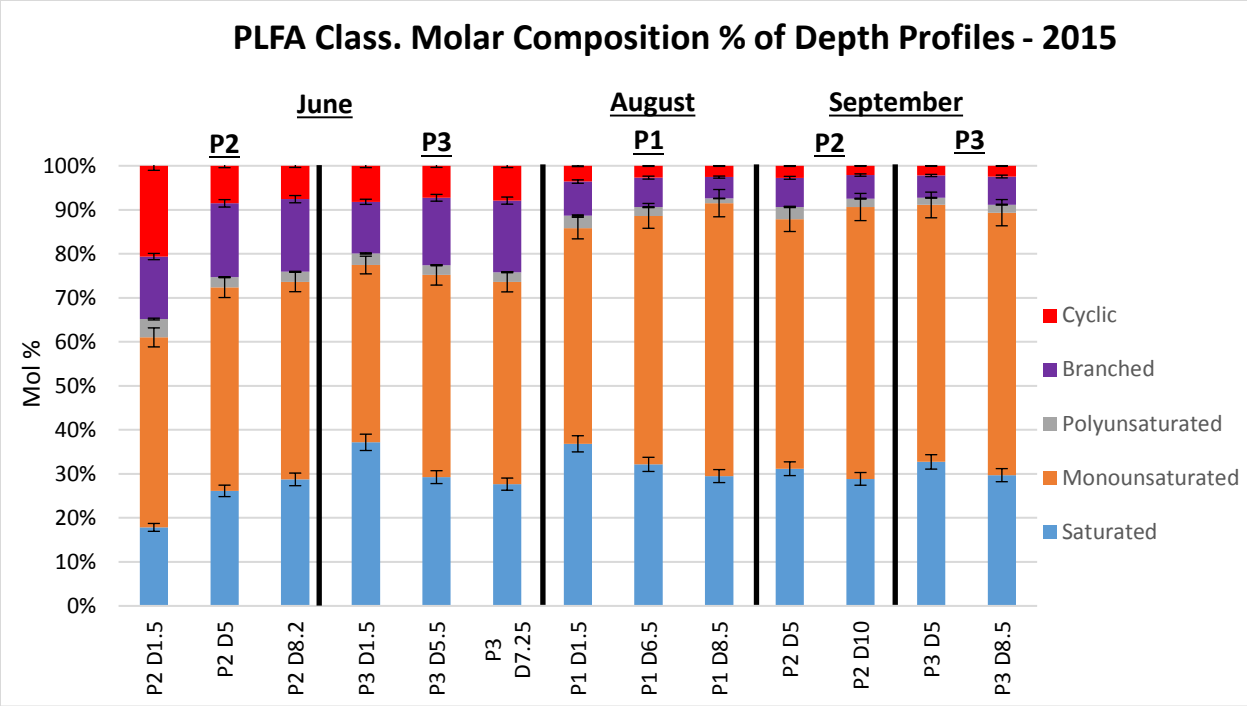

Figure 3.3: PLFA Profile breakdown by structural classification across sample depths and months in 2015.

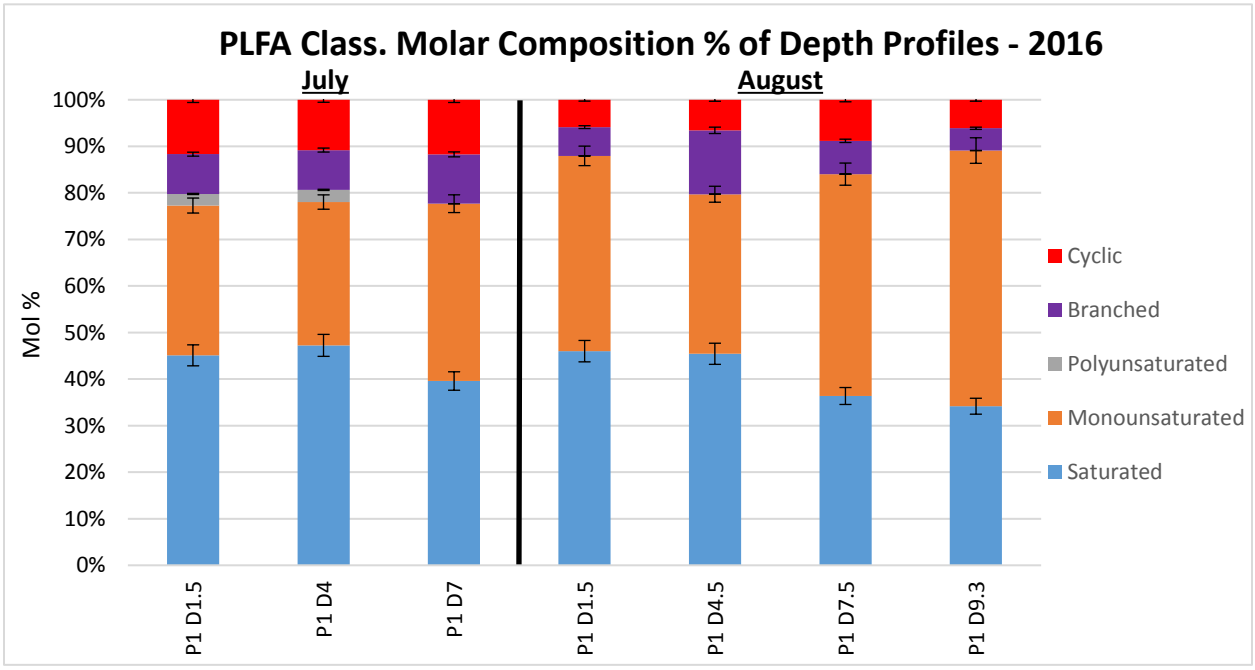

Figure 3.4: PLFA Profile breakdown by structural classification across sample depths and months in 2016.

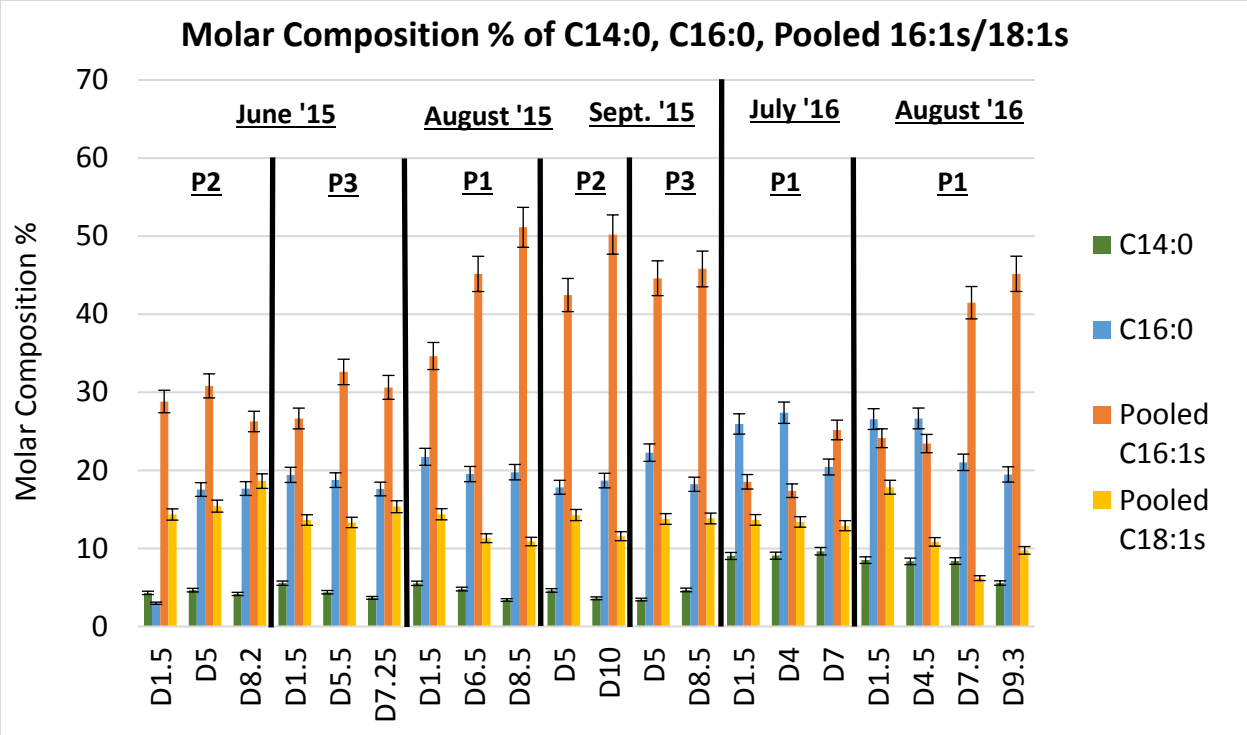

Figure 3.5: Comparison of molar composition % of C14:0, C16:0, and pooled C16:1 / C18:1 PLFAs containing methanotroph biomarkers across depth profiles of 2015 and 2016.

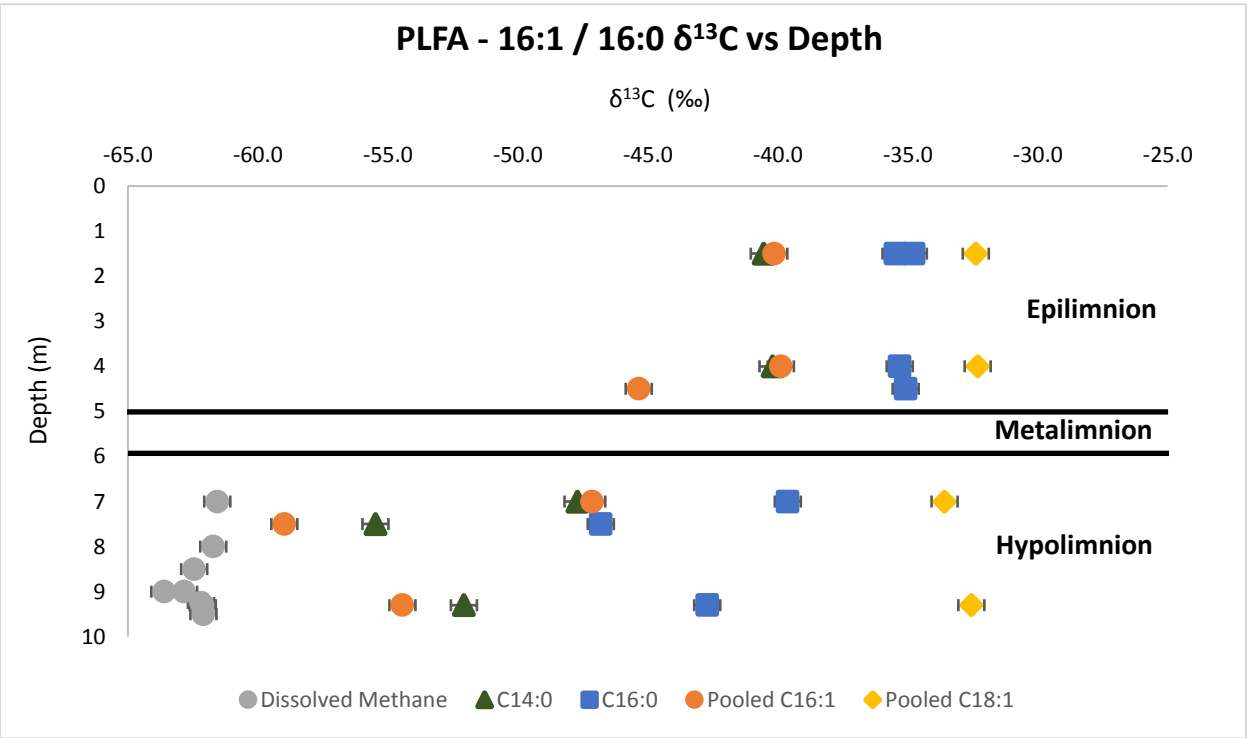

Figure 3.6: Distribution of $\delta^{13}C$ values for C14:0, C16:0, and pooled C16:1 / C18:1 PLFAs in August 2016 depth profiles.

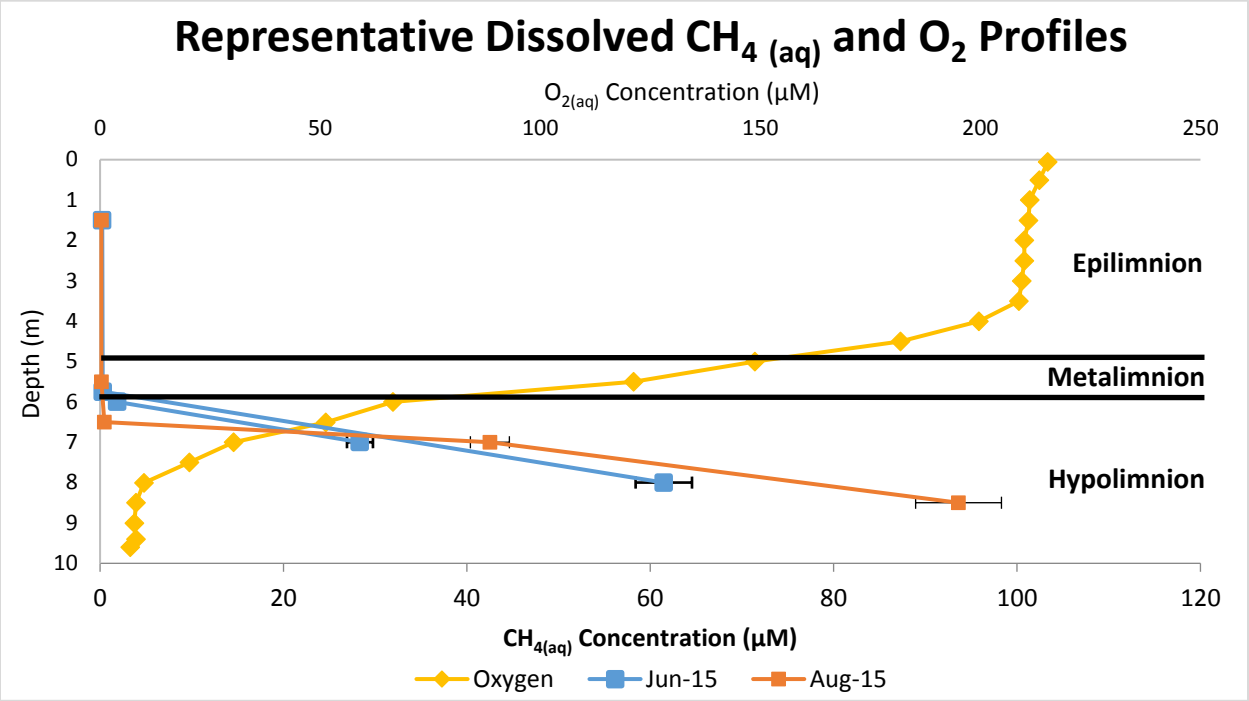

Figure 3.7: Representative dissolved methane and DO profiles for BML water column of 2015 and 2016.

Chapter 4: Summary

4.1 – Conclusions

4.1.1 – Project Summary

This Master's project focused on examining biogeochemical cycling of dissolved methane through identification of production and consumption metabolisms in Base Mine Lake (BML), the first full-scale demonstration of End Pit Lake (EPL) technology by Syncrude Canada Ltd. in Alberta, Canada. EPL technology is being developed in the Alberta Oil Sands Region (AOSR) to address the issue of long-term storage and management of Fluid Fine Tailings (FFT) inventories generated through the Clark Hot Water Extraction (CHWE) process that recovers bitumen from the crude oil sands mixture. BML's primary goal is to facilitate the de-watering of FFT over time, while remediating the landscape to a biologically productive state and facilitating the biodegradation of organic compounds present in the FFT. In order to demonstrate that BML is developing on a trajectory that will lead to these goals being met, extensive monitoring of water column biogeochemistry has been undertaken. Biogeochemical cycling of dissolved methane is of specific interest as FFT has been identified as a primary source zone of biogenic methane, which has a negative impact on dissolved oxygen concentrations when consumed by methanotrophic bacteria. Dissolved oxygen plays a critical role in water column development as a Terminal Electron Acceptor (TEA) and is required by many aerobic microbes to facilitate biodegradation of large organic compounds present in FFT. Understanding the occurrence, extent and impact of methanotrophy on BML water column dissolved oxygen concentrations is thus a key component of understanding the biogeochemistry and development of BML.

The goals of this project were to 1) identify if methanotrophic bacteria are present, if they're actively metabolizing dissolved methane and if so, where in the water column is this

occurring, and 2) assess development of the microbial community of the water column over time and depth profiles via Phospholipid Fatty Acid (PLFA) analysis and biomass estimates. These goals were addressed through concentration and stable carbon isotope analyses of the water columns dissolved methane alongside PLFA profiles compiled from the microbial community of the water column. Concentration profiling of dissolved methane and oxygen allowed for 1st order diffusive flux estimates, and general understanding of trends that enabled us to modify sampling protocols to target zones of interest with regards to potential methanotrophic activity. Stable carbon isotope analysis provided information in two separate ways; 1) As methanotrophic bacteria preferentially uptake ^{12}C carbon over ^{13}C carbon, an enrichment in the residual dissolved methane should be observed, and 2) bacteria partially incorporate the $\delta^{13}C$ signature of substrate utilized in their metabolism to their PLFA, meaning incorporation of a depleted dissolved methane signature should be observed in methanotrophs.

4.1.2 – Site Description and Sampling:

BML is a dimictic lake with a seasonally stratified water column that was commissioned in 2012. A 7.5m water column consisting of Oil Sands Process Water (OSPW) was established overtop a 48m deep FFT layer in 2013. The water column depth is increasing by circa 0.5 to 1.0/year as a result of FFT de-watering, with a depth of circa 10m in 2017. A zero-discharge practice is currently in place, meaning no water from BML is released to the natural environment. Samples were taken between May 2015 and February 2017, spread across three sampling platforms and the three stratified depth zones of the water column.

4.1.3 – Dissolved Methane Water Column Dynamics

The data presented in Chapter 2 of this study strongly supports the conclusion that methanotrophic bacteria are actively consuming dissolved methane and oxygen in the

hypolimnion layer of BML. In the FFT dissolved methane concentrations were at or near saturation for ambient conditions. The stable carbon and hydrogen isotope analyses of dissolved methane in the FFT indicates that it is being produced via fermentative methanogenesis. First order calculations of methane fluxes from the FFT to the water column indicate that transfer of this dissolved methane to the water column is primarily by advection via FFT porewater expression ($1.5x10^7$ moles/yr) over molecular diffusion ($2.8x10^6$ moles/yr). However, it must be noted that there are other potential mechanisms of methane transfer involved such as contributions from advection by interface mixing and dissolution from bubbles that should be addressed in future (see future work section 4.2). In the water column dissolved methane was always well below saturation and was primarily restricted to the hypolimnion which maintained sub-oxic conditions throughout both summers. In the epilimnion and metalimnion dissolved methane was detected at trace concentrations during both seasons. In the hypolimnion, dissolved methane concentrations decreased circa linearly from the FFT-water interface to trace concentrations at the bottom of the metalimnion, coinciding with a steeply increasing dissolved oxygen gradient. These concentrations built up over the summer months reaching maximums in late August before turnover. Methane diffusive fluxes decreased by four orders of magnitude over the hypolimnion, demonstrating mass loss was occurring. Removal of dissolved methane by methanotrophs in the hypolimnion would explain the change in flux rates observed. The observed decrease in concentration and flux rates coincided with a minor enrichment in dissolved methane $\delta^{13}C$ values of circa 3‰. If consumption via methanotrophic bacteria is the primary mechanism of removal, a larger fractionation was expected to be observed. This suggests other factors are influencing the profile, or that isotopic fractionation is being suppressed due to supply limitation to the reaction site as proposed by Templeton et al. (2006).

The same decreasing concentration trends were observed in the hypolimnion during winter stratification. In this case, a minor enrichment of ~5‰ was seen at the FFT-water interface, implying that the greatest consumption is occurring at this point, despite concentrations being the highest. Winter epilimnion methane concentrations were higher than summer hypolimnion maximums, potentially resulting from dissolution of gas bubbles trapped under the ice. Absence or decreased rates of methanotrophy in the epilimnion during the winter may have been due to low temperatures and their influence on metabolic rates, sinking of bacteria attached to particulate due to alum addition in the fall of 2016, or simply absence of methanotrophs. The results presented here provide evidence supporting removal of dissolved methane by methanotrophic bacteria in the hypolimnion, causing a decrease in dissolved oxygen availability.

4.1.4 – PLFA Distributions and $\delta^{13}C$ Incorporation

Chapter 3 presents data that further supports the presence of methanotrophic bacteria in the hypolimnion of BML through changes in the distribution of PLFAs and stable carbon isotope analysis. The trends in PLFA abundances, distributions and δ13C values confirm that type I methanotrophy is a significant metabolism occurring within the BML microbial community, mainly in the hypolimnion. The highly depleted δ13C values of C14:0 and C16:1 PLFAs in the hypolimnion in August both seasons support active metabolism by type I methanotrophs. The lack of depletion of C18:1 PLFA, indicates that type II methanotrophs were not active in the system. The depletion in $\delta^{13}C$ of the general bacterial biomarker C16:0 in the hypolimnion of BML indicates methanotrophy influenced the overall microbial community either by direct production of C16:0 PLFA by methanotrophs that make up an increase proportion of the community, or through partial incorporation of δ13C depleted carbon from methanotrophs to other organisms via heterotrophy. Observed increases in hypolimnion PLFA abundances later in

the summer coincided with increasing dissolved methane concentrations. In addition, the relative proportion of C16:1 PLFAs in the hypolimnion increased later in summer. These observations suggest that the increased concentrations of dissolved methane may have enabled increased growth rates of type I methanotrophs, though the fact that methane concentrations continued to increase indicates that their growth was outpaced by methane supply.

4.1.5 – Project Conclusions

The results of Chapter 2 & 3 provide strong evidence indicating the oxidation of dissolved methane by type I methanotrophs. This metabolism is a primary component of biogeochemical cycling and has a direct negative impact on dissolved oxygen concentrations through methanotrophy. Aerobic methanotrophs demonstrate a high affinity and efficiency in utilizing oxygen to metabolize methane, and in most lake systems consume the methane entirely at the oxic-anoxic interface. The diffusive flux calculations in Chapter 2 indicate this consumption occurring around the oxic-anoxic interface situated around the FFT-water interface. . Understanding this consumption and the resulting impact is important when considering the goals of EPL technology, specifically the development of a biologically productive ecosystem requiring constant oxic conditions. Oxic conditions are required to facilitate biodegradation of compounds introduced by FFT/OSPW as aerobic bacteria utilize it as a Terminal Electron Acceptor (TEA). Methanotrophic bacteria also have been demonstrated to facilitate biodegradation other organic compounds, which may have an important role in this EPL system. Due to the importance of dissolved oxygen and its persistence in this experimental reclamation system, it is important that monitoring of dissolved methane cycling processes continues and further work is done to understand factors influencing its concentration and distribution patterns.

4.2 – Future Work

As BML is the first demonstration of EPL technology in an oil sands environment, extensive monitoring is planned for many years to come. Continued monitoring of dissolved methane and oxygen trends within the water column of BML is recommended, similar to the work conducted in Chapter 2. If the BML water column continues developing and oxygen saturation increases in the hypolimnion down to the FFT-water interface, it is possible that the dissolved methane flux out of the FFT could be further reduced, and potentially one day be completely consumed across the interface. The difference in methane profile behavior and values between summer and winter seasons and the reverse trend in isotopic enrichment versus concentration is not well understood and must be further explored. As only one winter profile was obtained through this study, comparison and tracking of trends across winter seasons is missing. Addition of alum in fall 2016 may have influenced biogeochemical cycling of methane through sinking of particulate in the water column. This is poorly constrained as this was the first alum treatment throughout the course of this study, meaning further profile monitoring is required to understand the impact of this treatment on methane cycling within the water column. Preliminary 2017 results show elevated dissolved methane concentrations in the epilimnion in May that decrease in June and further in July suggesting something has changed, or unconstrained factors having an influence have changed, perhaps a result of the alum addition. The small isotopic fractionation of -3 ‰ in the summer and -5 ‰ in the winter observed for the dissolved methane needs to be further investigated, as a larger isotope fractionation should have been observed between the FFT and water column, as well as through the hypolimnion where the data supports methanotrophic consumption. Conducting stable carbon isotope analysis on the DIC in the water column would help refine the zones where methanotrophy is occurring. The

DIC pool in the areas containing methanotrophy should display increasingly depleted $\delta^{13}C$ values as more methane is oxidized, introducing more depleted carbon that originated from depleted sources present in the FFT.

The transfer mechanics that govern dissolved methane movement across the FFT-water interface must be further constrained, as all flux rate calculations were generated with a limited dataset for FFT methane concentrations. Utilization of the FIS sampling procedure directly across the FFT-water interface would improve diffusive flux estimates. Constraining advective loading is more challenging due to the complex interface mixing by waves, ebullition, and FFT consolidation. Modelling of wave interactions may help constrain this. Further constraining or getting a more accurate estimate of the FFT consolidation rate could have a significant impact, as advective and diffusive loading rates were only one order of magnitude different. Further constraint of these transfer mechanics will allow for refinement of our understanding of how much diffusion and advection are influencing this system, and their interaction with methanotrophy. Dissolution from ebullition is of interest in this system as well, as preliminary bubble modelling suggests a large percentage of the bubble's methane mass may diffuse out in the short travel time to the water surface.

While the evidence presented strongly indicates oxidation by type I methanotrophs is occurring, pairing this evidence with direct identification of biomarkers or genetic analysis would confirm all the trends observed. Genetic Analysis of the microbial community that is currently underway will offer more insight than specific biomarker analysis as it would provide information on other microbes in the community that may be of interest. Obtaining $\delta^{13}C$ values for DOC in the water column would strengthen interpretation of stable carbon isotope data and depletions seen in the PLFA, as a baseline value could be established for this particular system

rather than using a general guideline value. Monitoring this value over time would provide information on potential changes in contributions to DOC across seasons, as inputs to this pool may change with the shifting microbial community structure. Monitoring the species of compounds comprising the DOC pool will allow for continued understanding of what substrate are driving methanogenesis in the FFT, as well as what types of organic compounds are being biodegraded in the water column. This can be further paired with radiocarbon analysis, which would allow for determination of relative inputs of modern carbon via photosynthesis versus inputs from older carbon sources present in the OSPW/FFT generated from the crude oil sands mixture. This information would further understanding of carbon cycling in the system and may display changing trends over time as the water column develops further and biodegradation continues. With continued monitoring and further constraining these variables, accurate modeling can be carried out to fully understand the impact dissolved methane is having on oxygen availability in the BML water column, and thus the ability to develop into a functioning ecosystem facilitating biodegradation of organic compounds present in FFT and OSPW.